1) ***Jarid2 regulates mouse epidermal stem cell activation and differentiation***
2) ***Tumor heterogeneity and metastasis-initiation in human squamous cell carcinoma***

Stefania Mejetta

TESI DOCTORAL UPF / 2013

UNIVERSITAT POMPEU FABRA

Thesis director: Salvador Aznar-Benitah

Department of Gene Regulation, Stem Cells and Cancer a
Epithelial Homeostasis and Cancer Group
Centre of Genomic Regulation (CRG)

Questa tesi e' dedicata in special modo a
SB, non c'e' bisogno di altre parole.
Grazie per il sostegno che mi ha dato in
tutti questi anni, specialmente nell'ultimo.

ABSTRACT - RESUMEN

ABSTRACT PART 1

Jarid2 is required for the genomic recruitment of the polycomb repressive complex-2 (PRC2) in embryonic stem cells. However, its specific role during late development and adult tissues remains largely uncharacterized. In this first part of my thesis, we show that deletion of Jarid2 in mouse epidermis reduces the proliferation and potentiates the differentiation of postnatal epidermal progenitors, without affecting epidermal development. In neonatal epidermis, Jarid2 deficiency reduces H3K27 trimethylation, a chromatin repressive mark, in epidermal differentiation genes previously shown to be targets of the PRC2. However, in adult epidermis Jarid2 depletion does not affect interfollicular epidermal differentiation but results in delayed hair follicle (HF) cycling as a consequence of decreased proliferation of HF stem cells and their progeny. We conclude that Jarid2 is required for the scheduled proliferation of epidermal stem and progenitor cells necessary to maintain epidermal homeostasis.

RESUMEN PART 1

Jarid2 es necesario para la localización genómica del complejo represor polycomb repressive complex-2 (PRC2) en células stem embrionarias. Sin embargo, la función de Jarid2 en las últimas fases del desarrollo embrionario y su papel en la función de los tejidos adultos no ha sido aún caracterizada en profundidad. En esta primera parte de mi tesis doctoral, mostramos que la deleción de Jarid2 en la piel de ratón no afecta al desarrollo de la epidermis, pero reduce la proliferación y potencia la diferenciación de las células progenitoras epidermales en neonatos. La piel de los ratones neonatos Jarid2-KO muestra niveles reducidos de la marca represora de la cromatina, H3K27me3, en genes necesarios para la diferenciación de las células progenitoras. En cambio, en piel adulta la depleción de Jarid2 no afecta la diferenciación de la epidermis, pero sí que resulta en una reducción del número de células stem activas de los folículos pilosos, lo que desemboca en el retraso del crecimiento de los folículos. Por lo tanto, nuestros resultados demuestran que Jarid2 es necesario para la activación y diferenciación de diferentes células stem del compartimento queratinocítico de la piel necesarios para mantener la homeostasis epidermal.

ABSTRACT PART 2

Several human and mouse solid tumors, including squamous cell carcinomas (SCC), contain a population of Cancer Stem Cells (CSCs). CSCs are characterized by their unique ability to initiate and propagate the tumor; however, very little is known about their capacity to disseminate to distant organs and give rise to metastasis. CSCs display a great functional and molecular heterogeneity, and it has been proposed that different CSC subclones might exist to either maintain the primary tumor or to metastasize in distant sites. However, the identity of these heterogeneous populations of CSCs, as well as their molecular and functional characteristics for most type of tumors remains to be elucidated.

Using a novel xenograft system that we have developed to study human head and neck squamous cell carcinoma, we have identified a label-retaining (LRC) population inside the cancer stem cell pool defined by the high expression of CD44 and high activity of Aldh1. Unexpectedly, tumor LRC harbor poor initiating potential, and are more sensitive to chemotherapy than their proliferating counterparts.

Intriguingly, tumor LRCs are defined by a unique transcriptome signature previously linked with bone and lung identity, two major sites of SCC metastasis, suggesting they might be involved in the colonization of distant tissues by SCC tumors.

We have also identified surface molecules, including CD36 and CD37, that are uniquely expressed by tumor LRCs, that can be used as surrogate markers to isolate and characterize them from primary human SCCs.

Based on this signature, we could demonstrate that the presence or absence of this population in the primary tumor of a large cohort of

patients with cutaneous SCC is highly predictive of the metastatic occurrence. In addition, several markers exclusively expressed by tumor LRCs can be targeted with drugs currently in clinical trials for the treatment of other diseases. We are testing whether some of these therapeutical strategies are effective to preventing or reducing the metastatic potential of SCC tumors.

RESUMEN PART 2

Diversos tipos de tumores sólidos humanos y de ratón, incluyendo carcinomas de células escamosas (SCCs del inglés: Squamous Cell Carcinomas), contienen una población de células madre cancerosas (CSCs del inglés Cancer Stem Cells). Las CSCs se caracterizan porque pueden iniciar y propagar el tumor; sin embargo, se conoce muy poco sobre su capacidad de alcanzar órganos lejos del tumor primario y de formar metastasis. Las CSCs pueden ser muy heterogéneas tanto a nivel funcional como molecular, y se ha propuesto que podrían existir diferentes subclones sea para mantener el tumor primario, sea para formar metástasis. No obstante, no se conoce por ahora ni la identidad de estas poblaciones heterogéneas de CSCs, ni sus características a nivel funcional o molecular.

Usando un nuevo sistema de xenoinjerto que hemos desarrollado en nuestro laboratorio para estudiar SCC de cabeza y cuello, hemos identificado una población que es capaz de retener el marcaje con el tiempo (LRC de inglés: Label-retaining Cells), dentro de la población total de CSSs, definidas como células dentro del tumor que muestran alta expression de CD44 y alta actividad de Aldh1.

En contra de lo que esperábamos, las LRC del tumor tienen dificultad para iniciar tumores por sí solas y son más sensibles a tratamientos de quimioterapia cuando las comparamos con otras células más proliferativas.

Por otra parte, las LRC del tumor se pueden definir con un transcriptoma único que ha sido relacionado anteriormente con hueso y pulmón, que son dos de los órganos donde los SCC forman metástasis preferentemente. Esto sugiere que podrían estar involucradas en la colonización de órganos alejados del SCC primario.

Hemos identificado también moléculas de superficie, incluyendo CD36 y CD37, que se expresan exclusivamente en las LRC de tumor y que se pueden usar como marcadores para aislar y caracterizar las LRC de SCCs primarios humanos.

Basándonos en estos marcadores, hemos podido demostrar que la presencia o no de esta población en el tumor primario predice la formación de metástasis en pacientes con SCC cutáneos. Además, diversos marcadores que hemos identificado como únicos en LRC de tumor, son diana de fármacos ya usados en la actualidad en ensayos clínicos para tratamiento de otras enfermedades. En la actualidad estamos probando si alguno de estos tratamientos puede ser efectivo para prevenir o reducir el potencial de formar metástasis en SCC.

PREFACE

The work presented in this doctoral thesis was supported by La Caixa Foundation and was done in the Epithelial Homeostasis and Cancer Group at the Centre of Genomic Regulation (CRG), Barcelona, Spain, under the supervision of Dr. Salvador Aznar-Benitah (ICREA Research Professor).

The content of the first part of thesis contributes to our understanding of the complex epigenetic mechanisms regulating epidermal homeostasis during postnatal development, and was published in the EMBO J (2011), 30:3635-46, where I sign as the first author.

The second part of this thesis describes the discovery of a new subpopulation of cancer cells with potentially higher metastatic ability, and provides new insight that might be used to develop new prognostic tools and targeted therapeutic strategies for human squamous cell carcinoma.

TABLE OF CONTENTS

TABLE OF CONTENTS

ABSTRACT - RESUMEN **1**

ABSTRACT PART 1 ..... **3**

RESUMEN PART 1 ..... **4**

ABSTRACT PART 2 ..... **5**

RESUMEN PART 2 ..... **7**

PREFACE **9**

TABLE OF CONTENTS **11**

TABLE OF CONTENTS **13**

ABBREVIATION **17**

ABBREVIATIONS **19**

INTRODUCTION PART 1 ..... **23**

1 INTRODUCTION PART1 ..... **25**

1.1 The skin **25**

1.1.1 Interfollicular stem cells 27

1.1.2 Hair follicle stem cells 28

1.1.3 Stem cells markers 30

1.2 Epigenetic modifications **31**

1.2.1 Polycomb proteins: PRC1 and PRC2 complexes 32

1.2.2 Polycomb proteins in murine epidermis 33

1.3 The JMJ protein Jarid2 ..... **35**

1.3.1 Jarid2 during early development 36

1.3.2 Jarid2 as a regulator of PRC2 functions 37

OBJECTIVES PART 1 ..... **41**

2 OBJECTIVES **43**

RESULTS PART 1 ..... **45**

3 RESULTS PART 1 ..... **47**

3.1 Results **47**

3.1.1 Experimental strategy 47

3.1.2 Epidermal deletion of Jarid2 does not affect embryonic development of the epidermis 48

3.1.3 Deletion of Jarid2 results in enhanced postnatal epidermal differentiation 50

3.1.4 Deletion of Jarid2 results in inefficient entry of hair follicles in the second postnatal anagen 55
3.1.5 Jarid2 modulates PRC2 activity in mouse keratinocytes 60

DISCUSSION PART 1 ..... **67**

4 DISCUSSION **69**
4.1 Discussion **69**
4.1.1 Jarid2 in early postnatal epidermal development 69
4.1.2 Hair cycle is affected by Jarid2 loss 70
4.1.3 Jarid2-PRC2 interaction in the epidermis 71
4.1.4 Jarid2 and neoplastic transformation 72
4.1.5 Conclusions and future directions 73

SUMMARY PART 1 ..... **75**

5 SUMMARY OF SCIENTIFIC FINDINGS **77**

MATERIALS AND METHODS PART 1 ..... **79**

6 MATERIAL AND METHODS PART 1 ..... **81**
6.1 Material and methods **81**
6.1.1 Generation and handling of mice 81
6.1.2 Primary keratinocytes 81
6.1.3 Flow-citometry and cell sorting 82
6.1.4 Whole mount immunofluorescence 83
6.1.5 Immunoistochemistry 83
6.1.6 RNA isolation and qPCR 84
6.1.7 Chromatin immunoprecipation (ChIP) 84
6.1.8 Statistic 85

REFERENCES PART 1 ..... **89**

7 REFERENCES PART 1 ..... **91**

INTRODUCTION PART 2 ..... **97**

8 INTRODUCTION PART 2 ..... **99**
8.1 Squamous cell carcinomas **99**
8.2 Cancer stem cells **100**
8.2.1 Cancer stem cell markers in solid tumors 105
8.2.2 Cancer stem cell quiescence 106
8.3 Metastasis **108**
8.3.1 The metastatic niche 109
8.3.2 Metastasis-initiating cells 112
8.4 Tetraspanin receptor CD37 ..... **113**

OBJECTIVES PART 2 ..... **117**

9 OBJECTIVES PART 2 119

RESULTS PART 2 121

10 RESULTS SECOND PART 123

10.1 Results **123**

10.1.1 Experimental strategy 123

10.1.2 Identification of slow-cycling cancer cells 124

10.1.3 Tumor initiating-capacity of LRCs and active CSCs 127

10.1.4 Chemotherapy response in dormant versus active CSCs 130

10.1.5 Transcriptome analysis of Label-retaining cancer cells 131

10.1.6 Putative label-retaining cells in primary human SCC 135

10.1.7 Metastatic potential of Label-retaining CSCs 138

10.1.8 Functions of CD37 in SCC metastatic growth 140

DISCUSSION PART 2 143

11 DISCUSSION PART 2 145

11.1 Discussion **145**

11.1.1 Slow-cycling cancer stem cells in human SCCs 145

11.1.2 Gene expression signature of LRC cancer cells 147

11.1.3 The metastasis-initiating cells hypothesis 148

11.1.4 Selective targeting of LRC cancer cells in vivo 149

11.1.5 Possible clinical relevance of this work 150

MATERIAL AND METHODS PART 2 153

12 MATERIALS AND METHODS PART2 155

12.1 Materials and methods **155**

12.1.1 Clinical material 155

12.1.2 Plasmids and cloning 155

12.1.3 Cell culture and Vibram DID pulse 156

1.1.3 Immunostaining 157

12.1.4 Tumor xenografts 158

12.1.5 Tumor disaggregation from human biopsies and xenografts 160

12.1.6 Flow cytometry 161

12.1.7 MicroArray analysis and generation of CSC signatures 162

12.1.8 Real-Time qPCR 162

12.1.9 Statistical analysis 164

REFERENCES PART 2 165

13 REFERENCES PART 2 167
ACKNOWLEDGMENT 179
ACKNOWLEDGMENTS 181

ABBREVIATIONS

ABBREVIATIONS

BFP: Blue fluorescent protein

BMP: bone morphogenetic proteins

BrdU: 5-Bromo-2-deoxy-uridine

Ccnb1: Cyclin B1

Ccnd1: Cyclin D1

CD34: Cluster designation 34

CD31: Cluster designation 31

CD36: Cluster designation 36

CD37: Cluster designation 37

CD44: Cluster designation 44

CD71: Cluster designation 71

ChIP: Chromatin immunoprecipitation

CID: Inducer of dimerization

cKO: conditional knock out

c-Myc: v-myc myelocytomatosis viral oncogene homolog

CSCs: cancer stem cells

CSF1: colony stimulating factor 1

CTSK: cathepsin K

DAPI: 4',6-diamidin-2-fenilindolo

DDR: DNA-damage response

DMBA: 7,12-dimethyl-benzanthracene

DNA: deoxyribonucleic acid

ECM: extracellular matrix

EGF: epidermal growth factor

EGFR: epidermal growth factor receptor

EMEM: Eagle's minimum essential medium

epSC: epidermal stem cell

EPU: epidermal proliferative unit

EtOH: ethanol

ESC: embryonic stem cells

FACS: fluorescent activated cell sorting

FBS: fetal bovine serum

FGF: fibroblast growth factor

Flg2: Filaggrin family member 2

5-FU: 5-Fluor-Uracil

HAT: Histone deactheylases

H&E: hematoxil/heosin

GFP: Green fluorescent protein

HF:hair follicle

HGF: hepatocyte growth factor

HNCAF: Head and neck cancer associated fibroblast

HNSCC: Head and neck squamous cell carcinoma

IFE: interfollicular epidermis

iCaspase9: inducible Caspase9

i.f.: intrafemur

i.p.: intraperitnoeoum

i.v.: intravenous

Itga6: Integrin alpha-6

Jarid2: jumonji, AT-rich interactive domain 2

JMJ: jumonji

K14: keratin-14

K5: keratin-5

Ki67: antigen identified by monoclonal antibody Ki67

KO: knock-out

IVIS: in-vivo imaging system

Lce: Late cornified envelope

Lor: loricrin

LRC: Label retaining cells

MIC: Metastasis-initiating cells

PCR: polymerase chain reaction

PHK: primary human keratinocytes

PI3K: phosphatidylinositol-3-kinase

PRC1: polycomb repressive complex 1

PRC2: polycomb repressive complex 1

Pum-1: Pumilio 1

RFP: Red fluorescent protein

ROS: reactive oxygen species

rpm: rotation per minute

RUNX2: runt-related transcription factor-2

SC: stem cells

SCC: squamous cell carcinoma

SDS: sodium dodecyl sulfate

SEM: standard errors of the mean

TA: transit amplifying

TGF-b: transforming growth factor beta

TPA: 12-O-tetradecanoylphorbol-13-acteate

TSS: transcriptional start site

UTR: Untraslated region

UV: ultraviolet

YFP: yellow fluorescent protein

WT: wild type

INTRODUCTION PART 1

1 INTRODUCTION PART1

1.1 The skin

The skin is a multilayered tissue comprising the dermis, the epidermis (henceforth referred as interfollicular epidermis, IFE) and the related appendages, including hair follicles (HF), sebaceous glands and sweat glands (**Fig1.1**). The skin is the primary barrier that protects the body from dehydration, mechanical trauma, and microbial insults, and it is essential for temperature regulation, secretion and sensation.

Due to its constant exposure to the outer surface of the body, the epidermis has a high-turnover rate necessary to ensure long-term homeostasis and regenerate damaged areas. Since terminally differentiated cells are continuously shed away from the body surface, new cells have to replace the ones that are lost. In addition, hair follicles and sebaceous glands undergo re-occurring cycles of growth and regression.

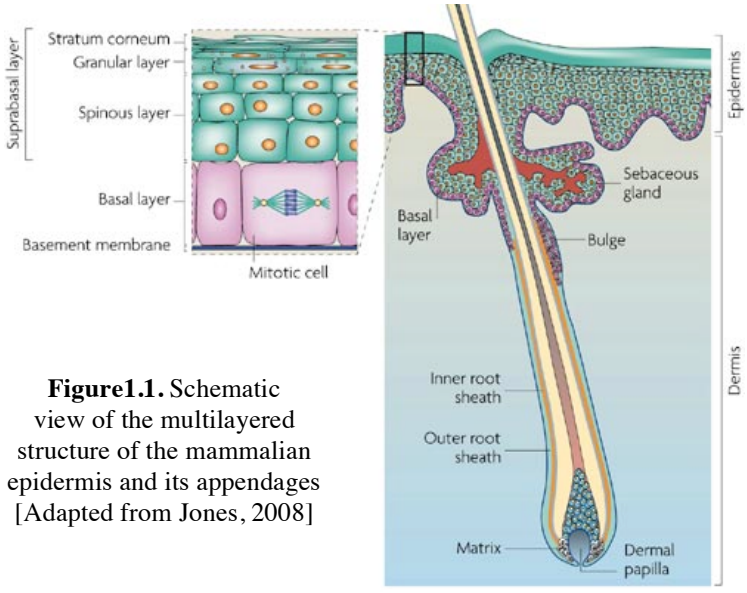

Figure1.1. Schematic view of the multilayered structure of the mammalian epidermis and its appendages [Adapted from Jones, 2008]

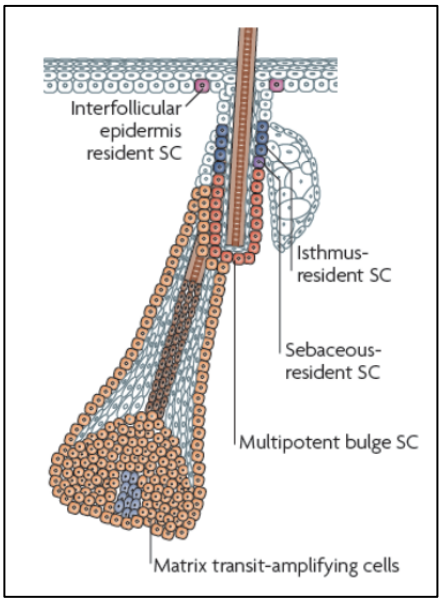

Figure1.2. Different locations of the epSCs in mammalian skin [adapted from Blanpain, et al, 2009].

Epidermal homeostasis, hair regeneration, and wound repair are maintained by several reservoirs of self-renewing stem cells located at distinct anatomical locations within the skin, that upon specific stimuli become activated, multiply and differentiate according to the needs of their particular compartment. Distinct pools of epidermal stem cells (epSC) have been found in the basal layer of the IFE, an area of the HF termed the bulge, and in the isthmus connecting hair follicles with the IFE (**Fig1.2**). Under normal homeostatic conditions, each subset of epSCs contributes uniquely to their compartment and responds to specific combinations of cues that regulate their periodic activation, and the onset of their differentiation (**Fig1.1**). However, in non-physiological condition, such as wounding, epSCs show their multipotent plasticity by leaving their niche to rapidly migrate to the damaged and differentiate into the new lineage thereby contributing to the repair of the compartment [Jones, et al, 2007; Horsley, et al, 2006].

1.1.1 Interfollicular stem cells

The murine interfollicular epidermis is organized in columns of geometric clonal units known as epidermal proliferative units (EPUs), consisting of a stack of hexagonally packed cells comprising around 10 cells in the basal layer, where they originate [Jones, et al, 2008].

IFE stem cells are located in the basal layer in tight contact with the basement membrane, and they express high levels of α1- and β1-integrins [Jones, et al, 1995]. Interestingly, whereas human epidermis contains populations of relatively quiescent and actively proliferating IFE stem cells, murine IFE is predominantly maintained by continuously dividing stem cells. Interestingly, the progeny of each basal murine IFE division can adopt different fates in a stochastic manner. In this sense, murine IFE division can either yield two daughter stem cells, two daughter differentiated cells, or one SC and one differentiated cell (in a 10:10:80 ratio). The stochastic nature of the SC divisions maintains homeostasis by a neutral competition mechanism, which has also been observed for other tissues with a very high turnover rate such as the intestinal epithelium [Snippert, 2010; Clayton, et al, 2007; Jones, et al, 2008].

Upon detachment from the basement membrane epidermal keratinocytes progress through several stages of differentiation that forms three consecutive suprabasal layers: the spinous layer, the granular layer and the outermost cornified layer. Each stage of differentiation is characterized by morphological and very complex biochemical changes corresponding to the expression of different structural proteins. For instance, spinous layer keratinocytes express high levels of Involucrin, granular cells express mainly Filaggrin and transglutaminase, whereas Loricrin and Cornifin mark the cornified layer. In addition, during this step-wise differentiation process,

keratinocytes undergo changes in the expression of keratins. They lose the basal markers Keratin5 and Keratin14, and start expressing suprabasal Keratin10 and Keratin1 [Candi, et al, 2005].

1.1.2 Hair follicle stem cells

Hair follicles (HFs) are epidermal appendages where the hair shaft is formed. Each HF is a complex mini-organ that undergoes periodic cycles of growth (anagen) and regression (catagen), followed by long periods of relative quiescence (telogen). Hair follicles are developed during the fetal skin morphogenesis through tightly regulated ectodermal-mesodermal interactions. During the development of murine skin, a group of dermal cells aggregate beneath the epidermis at embryonic day E14.5 to form dermal papillae (DP), a group of specialized fibroblasts that instruct the invagination of embryonic epidermal cells into the dermis to generate the primordium of the hair follicle, known as the hair placode [Fuchs, et al, 2007]. Later during development, the hair placodes extend downwards and enclose the dermal papilla to form the embryonic hair follicle (**Fig1.3**).

Hair follicles morphogenesis is fully completed 2 weeks after birth, when proliferating matrix cells located at the bottom of the follicles start to differentiate and generate the epidermal layers of the mature hair follicles: the outer root sheath, the companion layer, and the inner root sheath surrounding the central hair shaft [Fuchs, et al, 2007; Schneider, et al, 2009]. At this stage, HFs stem cells are located in the permanent area of the outer root sheath, in a region called bulge, where they will remain during the entire life of the mouse (**Fig1.3**).

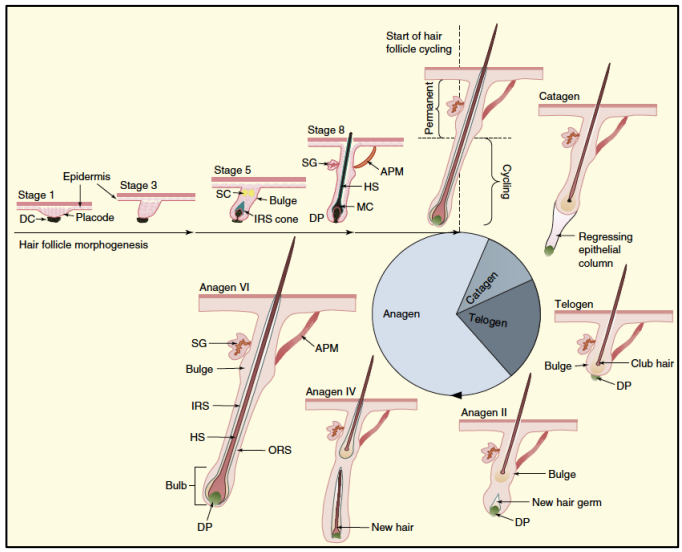

Figure1.3. Hair follicles morphogenesis and key steps of the hair cycle [Adapted from Schneider, et al, 2009].

Once the postnatal hair follicles have completed the first growth phase (anagen), HFs enter a destructive phase called catagen characterized by the loss of the lower part of the follicle due to apoptosis, but sparing the bulge stem cells. Catagen is followed by a 1-2 days long resting phase (telogen) and then all the HFs in the mouse enter synchronously a second growing phase (anagen), at P19-P21. This event marks the beginning of the repetitive cycles of hair follicle growth, which require the concerted actions of dermal papilla fibroblasts, secondary hair germ cells (the cells immediately below the bulge SCs), and bulge SCs. In this sense, DP cells signal to secondary hair germ cells to become active, and it is this population, rather than bulge SCs, that initiate anagen [Greco, et al, 2009]. One or two days later, intriguingly, bulge SCs egress the niche without any prior proliferation and feed into the secondary hair germ and the matrix, where transit-amplifying cells reside [Zhang, et al, 2009]. Subsequently (during P22-P28), bulge SCs

undergo a round of proliferation that replenishes the stem cells that were lost during the migration to the secondary hair germ at early anagen. In late anagen the proliferation of the bulge stem cells is subsequently reduced, resulting in full quiescence during the next catagen (P36-P42) and telogen (P43) phases [Greco, et al, 2009].

1.1.3 Stem cells markers

Two main approaches have been classically used to identify epSCs: label-retaining methods *in vivo*, or using stem cell markers [Blanpain, et al, 2006, Pincelli, et al, 2010]. Slow-cycling stem cells have been visualized through label-retaining assays that make use either of BrdU [Cotsarelis, et al, 1990; Morris, et al, 2004] or of the tetracyclin-inducible H2B-GFP system [Tumbar, et al, 2004]. However, these experiments have demonstrated that quiescence is not a defining trait of all epidermal stem cells. For instance, bulge stem cells can remain quiescent for very long periods of time, yet basal IFE progenitor/SCs are continuously cycling [Clayton, et al, 2007]. That said, the purification of long-term label retaining bulge cells has allowed identifying the bulge SC transcriptome signature, including most, if not all, of the stem cell markers defining this population of SCs [Tumbar et al, 2004; Morris et al., 2004].

Recent lineage tracing experiments have helped us visualize and characterize the behavior of the different populations of stem cells located in the skin. The evolving picture is very complex, and suggests that each compartment (bulge, IFE, sebaceous gland and sweat gland) might contain more than one population of SCs that exerts a specific spatiotemporal function. For instance, the bulge can now be subdivided in the upper part (identified by α6 integrin^{bright}/CD34+/Keratin-

15+/Gli2+ cells), middle part (α6 integrin^{bright}/CD34+/Keratin-15+/Sox9+/Lhx2+/NFATc1+/Lgr5+), and bottom bulge (α6 integrin^{bright}/CD34+/Keratin-15+/Sox9+/Gli2+/Lgr5^{bright}). In addition to this, the bulge contains two suprabasal layers that contain α6 integrin^{dim}/CD34+/Keratin-15+/Sox9+/Lhx2+/NFATc1+/Lgr5+ cells, with equal stem cell potential than basal bulge cells, and α6 integrin^{dim}/CD34+/K15+/Sox9+/Lhx2+/NFATc1+/Lgr5+/Keratin-6+ cells, which do not display stem cell potential but signal to basal bulge cells to remain quiescent [Hsu, et al, 2011; Blanpain, et al, 2004, Tumbar, et al, 2004]. The hair follicles contain two additional subsets of SCs both located at the isthmus region connecting the HFs with the epidermis. One of these is defined by the high expression of LRIG1, and they contribute to the maintenance of the isthmus and the sebaceous glands [Jensen, et al, 2008; Jensen, et al, 2009]. The second population of isthmus SCs expresses high levels of Lgr6 and MTS24 and also contributes to the isthmus, sebaceous glands, and possibly to the IFE, although this is still under intense debate [Snippert, et al, 2010]. It is not clear yet why both populations co-exist and what is their precise contribution to homeostasis and damage repair. At last, so far basal IFE progenitors have been identified as α6 integrin^{bright}/CD34-/deltaNp63+/Keratin-14+ cells [Frye and Benitah, 2012].

1.2 Epigenetic modifications

Large portions of the chromatin of SCs must be modulated to allow and promote the changes in gene expression required to mediate self-renewal or the onset of differentiation. Gene expression can be controlled by modulation of chromatin compaction, and several posttranslational changes, including methylation, acetylation,

phosphorylation, among others, of the histone tails correlate with a different chromatin state, permissive or not to transcription [Kouzarides, et al, 2007]. Not surprisingly, epigenetic modifications are necessary for the proper lineage specification into the three germ layers during embryonic development, and misregulation of pathways controlling chromatin compaction has been associated with early embryonic lethality and neoplasia [Sauvageau, et al, 2010].

1.2.1 Polycomb proteins: PRC1 and PRC2 complexes

Polycomb proteins are a group of epigenetic regulators of gene expression required for the earliest stages of embryonic lineage commitment [Sauvageau, 2010]. Polycomb proteins associate to form two major complexes, the Polycomb Repressive Complex-1 (PRC1) and -2 (PRC2) (**Fig1.4**).

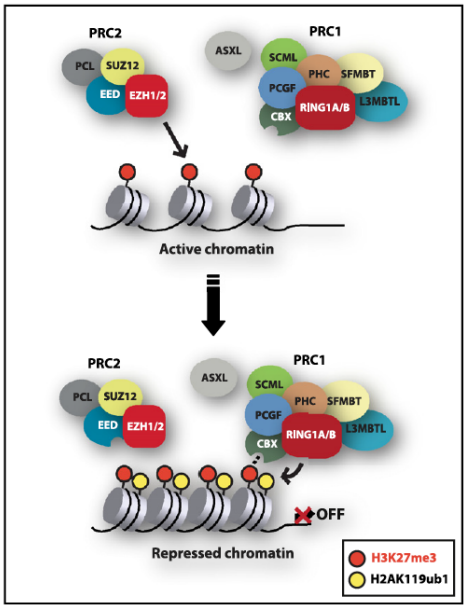

Figure 1.4. Chromatin compaction by sequential action of PRC-1 and PRC-2 [Adapted from Sauvageau, 2010].

The mammalian PRC1 complex consists of four main subunits: one of the Cbx proteins (Cbx2-4-6-7-8), Ring1 (Ring1A/B), PHC (PHC1-3) and PCGF (PCGF1-6) [Levine, et al, 2002]. Different combination of these various subunits and family members can generate a diverse array of PRC1 complexes with potentially distinct functions. On the other hand, PRC2 complex is formed by three core subunits Ezh2/Ezh1, Eed and Suz12.

Ezh2/Ezh1 mediates trimethylation of the histone H3 at the Lysine-27 (H3K27me3), a chromatin mark normally associated with gene repression [Sauvageau, et al, 2010]. The H3K27me3 mark is subsequently recognized by the Cbx proteins of the PRC1 and is thus important for the recruitment of this complex to chromatin (**Fig1.4**). Once PRC1 is bound, its Ring1 subunit ubyquitilates histone H2A at lysine 119 (H2AK119ub) through its E3-ligase activity, a mark that also correlates with gene repression.

Deletion of PRC2 subunits, or the PRC1 subunits Ring1b in ESCs causes profound changes in the expression of lineage commitment genes, resulting in early lethality [Surface, et al, 2010; Sauvageau and Sauvageau, 2010]. However, less is known about the function of PRC2 in adult tissues.

1.2.2 Polycomb proteins in murine epidermis

Three reports have highlighted the importance of polycomb proteins during mouse skin development [Ezhkova, et al, 2009; Ezhkova, et al, 2011; Mejetta, et al, 2011]. At the onset of epidermal stratification, the expression of the core PRC2 subunits Ezh2 and Eed is high in the basal proliferative cells, but it decreases as the cells enter the suprabasal compartment, and is restricted to the basal layer of the epidermis once

stratification is complete at E18.5. Although epidermal commitment is unaltered in Ezh2 conditional KO mice, its loss causes reduced proliferation and increased differentiation during late embryogenesis and in the first stages of postnatal development. As mice reach adulthood, the effect wanes due to decreased expression of Ezh2 [Ezhkova, et al, 2009]. Whereas Ezh2 deletion in mouse epidermis results in loss of H3K27me3 in the basal compartment, this repressive mark is maintained in the suprabasal layer, probably because of the activity of its ortholog Ezh1. Accordingly, single deletion of Ezh1 does not influence epidermal development, but double deletion of Ezh1 and Ezh2 is characterized by hyper-proliferation of the IFE, and an impaired cycling of adult hair follicle. In HFs this effect is due to the upregulation of Ink4b/Ink4a/Arf and subsequent overexpression of p16/p19 [Ezhkova, et al, 2011].

As mentioned before, adult hair follicles remain dormant for relatively long periods of time, and then undergo bouts of proliferation when hair growth is required. Bulge stem cells activation and differentiation are accompanied by global changes in the distribution of active and repressive marks. In bulge stem cells, H3K27me3 silences the genes required for hair follicle differentiation in a PRC2-dependent fashion [Ezhkova, et al, 2011; Lien, et al, 2011]. As bulge stem cells transit from a quiescent to an active state, H3K27me3 is lost at the promoter of cell cycle genes, whereas in transit amplifying progenitors H3K27me3 decorates stemness genes and is lost in epidermal differentiation genes. It is worth noting that the complete loss of PRC2 in bulge stem cells is not sufficient to change the fate of epidermal stem cells into non-ectodermal lineages, suggesting that additional chromatin remodelling factors are required for their epigenetic specification.

The important role of PRC2 in balancing proliferation and differentiation in mouse epidermis is conserved in human skin. Many differentiation genes are marked by the H3K27me3 repressive mark in basal human keratinocytes, but in this scenario PRC2 directly represses early differentiation genes, rather than genes expressed in later stage of the differentiation process [Sen, et al, 2009].

1.3 The JMJ protein Jarid2

The JMJ gene was first identified with a gene-trap technology approach as a gene important in mouse embryonic neural development [Takecuhi, et al, 1995; Tacheuchi et al, 2006]. JMJ (also known as Jumonji or Jarid2) belongs to the JmjC family of histone de-methylases, proteins containing a JmjC domain necessary for catalysing the removal of methyl groups from specific lysine residues on the histone tails. Despite the fact that JMJ was the first member identified for this class its catalytic domain is inactive due to naturally occurring aminoacid substitution. Jumonji also contains a Jumonji N AT-rich interaction domain (ARID domain), hence its name Jarid2. The ARID domain is highly conserved in fungi, plants and animals, and members of the ARID family play important roles in embryonic development, cell cycle regulation and chromatin remodelling [Jung, et al, 2005]. Some ARID proteins exhibit sequence specific DNA-binding, but nothing is known about preferential binding of Jarid2 to conserved motifs [Jung, et al, 2005]. (**Fig1.5**).

Figure1.5. Functional domains of Jarid2 [Adapted from Landeira, 2010].

Other functional domains found in Jarid2 are a Zn-finger domain that might mediate direct DNA binding, a nuclear localization signal and a trans-repression domain [Landeira, et al., Takeuchi, et al, 1995; Takeuchi, et al, 2006; Landeira, et al, 2010]. Human JMJ shares 90% of similarities with the mouse Jarid2 gene.

1.3.1 Jarid2 during early development

Jarid2 was identified as a key regulator of neural morphogenesis in mouse embryos and is expressed in a subpopulation of cells in the brain, heart, spinal cord and thymus of the developing embryos [Takeuchi, et al, 1995; Takeuchi, et al, 2006; Jung, et al, 2005]. Its expression is higher in neural ectoderm than in mesoderm at E7.5, whereas it starts to be detectable in the developing hearth at E8.5, where its expression is maintained in adult life. Jarid2 is expressed in other embryonic tissues, such as the spinal cord, dorsal root ganglia, thymus, brown fat and fetal liver. In later stages of mouse embryonic development, as well as in early postnatal development, Jarid2 becomes expressed in a variety of tissues, but its expression patterns seems to be tightly regulated in a temporal and spatial fashion [Takeuchi, et al, 1995; Takeuchi, et al, 2006; Mejetta, et al, 2011].

The complete KO of Jarid2 in mice results in embryonic lethality between E10.5 and E15.5 (depending on the genetic background) because of cardiac and neural development failure [Jung, et al, 2005]. At the molecular level, Jarid2 binds to the promoter of cyclinD1 and repress its expression to prevent cardiomyocite proliferation [Toyoda, et al, 2003]. Jarid2 also directly recruits the histone H3K9 dimethyltransferases G9a and GLP (H3K9me2), suggesting that this

process, rather than a PRC2-mediated mechanism, is responsible for the repression of the cyclinD1 promoter [Shirato, et al, 2009]. However, as shown below Jarid2 promotes IFE progenitor proliferation and inhibits their differentiation in a PRC2-dependent manner [Mejetta, et al, 2011]. These results suggest that Jarid2 is important for maintaining the balance between proliferation and differentiation, but it influences tissue homeostasis with different output depending on the cellular context.

1.3.2 Jarid2 as a regulator of PRC2 functions

Little is known about the mechanisms that mediate the recruitment of PRC2 to chromatin. Several publications have recently shown that Jarid2 associates with PRC2 in different cells types, such as ESCs, thymocytes, HeLa cells, and new-born mouse keratinocytes [Peng, et al, 2009; Shen, et al, 2009; Pasini, et al, 2010; Mejetta, et al, 2011]. In ESCs, Jarid2 is necessary for the recruitment of PRC2 to its promoters (**Fig1.6**), and the binding of Jarid2 and PRC2 to chromatin overlaps in more than 90% of genes [Shen, et al, 2010; Peng, et al, 2010; Li et al, 2010; Pasini et al, 2010].

However, whereas the role of Jarid2 in the genomic recruitment of PRC2 is well established, its impact on PRC2 activity is less clear [Landeira and Fisher, 2010; Herz and Shilatifard, 2010]. The interaction between Jarid2 and PRC2 has been reported by some to inhibit [Shen, et al., 2010; Peng, et al, 2010], and by others to promote [Li, et al, 2010; Pasini, et al, 2010], the H3K27me3 methyltransferase activity of PRC2.

In this sense, Jarid2 depleted ESCs consistently display reduced genomic recruitment of PRC2 on the DNA, but this effect is accompanied by either no, or only subtle, changes in H3K27me3 enrichment at their promoter regions.

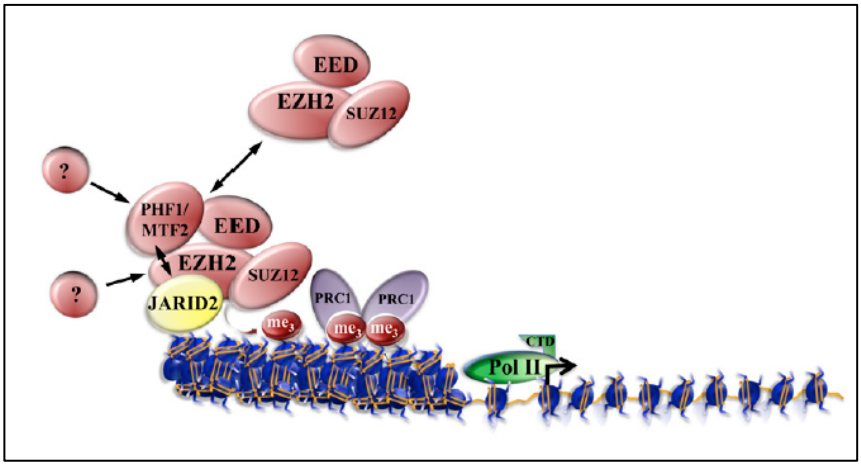

Figure1.6 Schematic view of the transcriptional regulation mediated by the Jarid2-PRC2 complexes. [Adapted from Herz and Shilatifard, 2011].

This controversy might be due the fact that Ezh2 recruitment is not completely abolished in Jarid2-depleted ESCs, or might involve compensatory mechanisms depending on Ezh1 [Landeira, et al., 2010; Shen, et al, 2009]. A clue to the role that Jarid2 might have in ESCs came from the discovery that bivalent domains (promoters containing both the repressive mark H3K27me3 and the active mark H3K4me3) in Jarid2 null ESCs lack RNApolII phosphorylated at Serine-5 (**Fig1.6**), which is important for the priming of genes for productive transcription [Peng, et al, 2009; Shen, et al, 2009; Pasini, et al, 2010; Li, et al, 2010]. Indeed, Jarid2 depleted ES are unable to initiate gene expression programs upon induction of differentiation [Landeira, et al, 2010].

OBJECTIVES PART 1

2 OBJECTIVES

Little is known about the mechanism by which PRC2 is recruited to specific loci in adult tissues, and which factors modulate its function. In addition, the role that Jarid2 plays in the genomic recruitment of PRC2 in adult tissues has not been described yet. Based on this, the objectives of this first part of my thesis were:

1. To determine the pattern of expression of Jarid2 in the mouse epidermis during development and adult homeostasis.
2. To determine the function, if any, of Jarid2 in the development and adult homeostasis of murine epidermis.
3. To determine if Jarid2 and PRC2 interact at the molecular and functional level in murine epidermis.
4. To determine whether Jarid2 has specific functions in epidermal stem cells.

RESULTS PART 1

3 RESULTS PART 1

3.1 Results

3.1.1 Experimental strategy

To study the role of Jarid2 in epidermal homeostasis during embryonic and postnatal development we generated mice carrying a conditional deletion of Jmj in all the keratin-14-expressing epidermal lineages. Jarid2 LoxP/LoxP mice [Mysliwiec, et al, 2006] were crossed with Keratin-14-Cre transgenic mice to achieve complete deletion of the gene in the epidermis starting from E12.5 (Jarid2cKO).

We verified that Cre expression was homogenous throughout the entire epidermal compartment by crossing Jarid2cKO mice with ROSA26-YFP transgenic mice (**Fig3.1A**). In addition, we verified by genomic PCR that Jarid2 was efficiently deleted in newborn epidermis of Jarid2cKO mice (**Fig3.1B**).

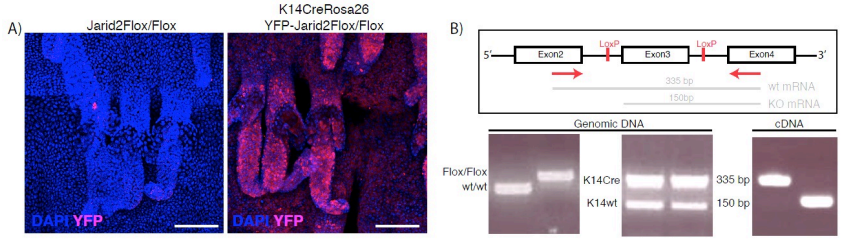

Figure 3.1. Jarid2 $^{Flox/Flox}$ mice were crossed with K14Cre/ROSA26-YFP mice to obtain specific deletion of the Floxed alleles in all the K14+ lineages. **A)** Immunofluorescence of whole-mount tail showing YFP expression in K14+ cells of the hair follicles. Scale bar: 100 μm. **B)** Schematic representation of the Jarid2$^{Flox/Flox}$ locus with the strategy used to visualize the wt and the Flox/Flox mRNA by PCR from cDNA. An example of the genotyping is reported.

3.1.2 Epidermal deletion of Jarid2 does not affect embryonic development of the epidermis

The Keratin14-Cre transgene drives Cre-recombinase expression during development of embryonic ectoderm at post-coitum day 12.5 (E12.5), coinciding with the onset of embryonic epidermal stratification. Therefore, our mouse model allowed us to study whether Jarid2 deletion had any effect on epidermal development. Histological analysis of the epidermis of E14.5-E19.5 Jarid2$^{wt/wt}$/K14Cre (WT mice), and Jarid2cKO littermate embryos, did not reveal any changes in epidermal stratification, thickness, and overall morphology (**Fig3.2A**). The expression of proliferation markers (Ki67), basal keratin14 (K14), and terminal differentiation genes (loricrin), was indistinguishable between WT and Jarid2cKO mice (**Fig3.2B**).

Embryonic hair follicles (HF) start to form from basal epidermal progenitors that invaginate around E14.5, to form hair placodes [Schneider, et al, 2009]. From E15.5 to birth, hair placodes grow inwards to give rise to embryonic hair follicle structures, which contain embryonic stem cells that remain present throughout the entire life of the organism. No changes in the number, spacing, or morphology of the HF placodes were observed in Jarid2cKO embryos, or in any of the subsequent HF embryonic morphogenesis stages from E15.5 until birth (**Fig3.2C**). Additionally, HF placodes from WT and Jarid2cKO embryos expressed similar levels of proliferation markers and basal keratin14 (**Fig3.2B**).

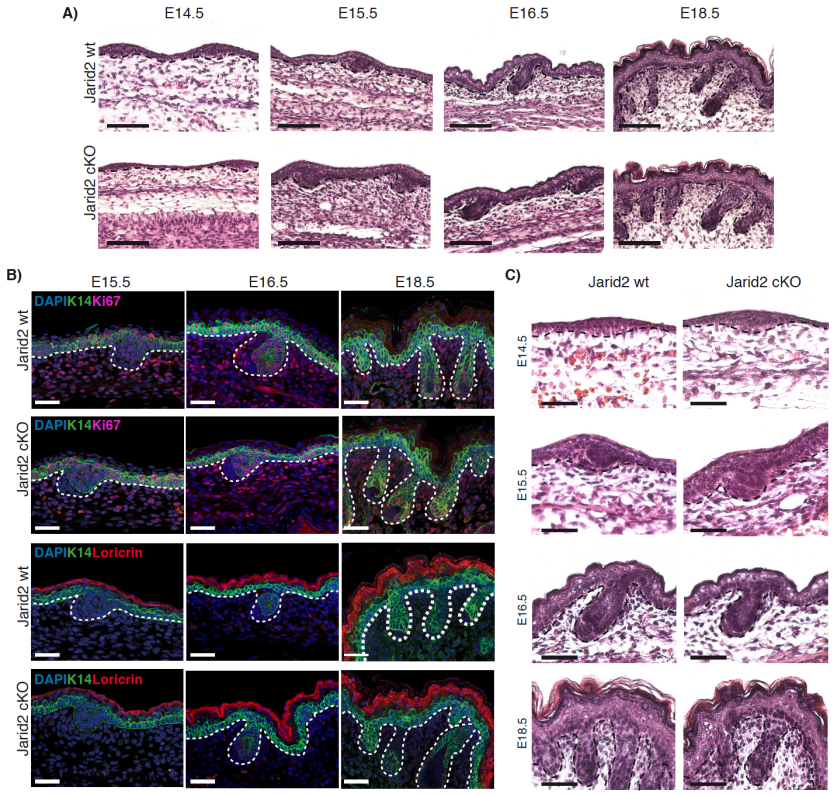

Figure 3.2. Epidermal deletion of Jarid2 does not affect embryonic development of the epidermis. **A)** Hematoxilin-eosin staining reveals no abnormalities in epidermal embryonic development of Jarid2 cKO mice. Different time points during the embryonic development of the skin are reported. At least three control (K14Cre/Jarid2$^{wt/wt}$) and cKO mice were analyzed per time-point. Scale bar 100 μm. **B)** Immunofluorescence of Ki67 and Loricrin indicates that proliferation and differentiation are not affected upon deletion of Jarid2. Scale bar 50μm. **C)** Higher magnification of skin sections to visualize the embryonic hair follicle structures shows a normal architecture in absence of Jarid2. Scale bar: 50 μm.

Therefore, Jarid2 is dispensable for late embryonic epidermal development and HF morphogenesis. Given that epidermal deletion of Ezh2 resulted in premature expression of terminal differentiation markers during embryonic epidermal development [Ezhkova, et el, 2009], it is likely that the Ezh2-containing PRC2 complex regulates this process independently of Jarid2.

3.1.3 Deletion of Jarid2 results in enhanced postnatal epidermal differentiation

We next studied whether deletion of Jarid2 affected epidermal neonatal morphogenesis. Expression of Jarid2 decreases as embryonic stem cells differentiate [Shen, et al, 2010; Peng, et al, 2010; Li, et al, 2010; Pasini, et al, 2010; Landeira, et al, 2010]. Likewise, FACS sorting of different mouse keratinocytes populations depending on α6-integrin expression revealed that basal epidermal progenitors ($\alpha6^{bright}$) had high Jarid2 transcript levels, while suprabasal differentiated cells ($\alpha6^{low}$) exhibited decreased Jarid2 transcript levels (**Fig3.3**).

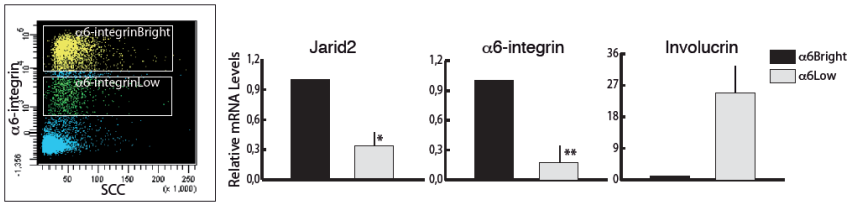

Figure3.3. Jarid2 is upregulated in basal epidermal progenitors in mouse and human postnatal skin**.** Differential expression of Jarid2 in basal and suprabasal interfollicular epidermal cells FACS sorted on the basis of their cell surface levels of α6-integrin from P1 wild type mice. Data shown represent the mean average, vertical bars represent the S.E.M. N=4. P*< 0,05; P**<0,01. A representative dot-plot of the sorting strategy used is shown on the left panel.

During the first two weeks after birth, strong proliferation is coupled with differentiation in the epidermis, to establish the definitive adult epidermal barrier. In addition, the first pelage emerges from the HF structures that formed during embryonic development [Schneider, et al, 2007]. A daily time-course analysis from postnatal days 0 (P0) to 7 (P7) indicated that Jarid2cKO mice had an expanded suprabasal granular layer and a thickened cornified envelope, compared to control littermates (**Fig3.4A**).

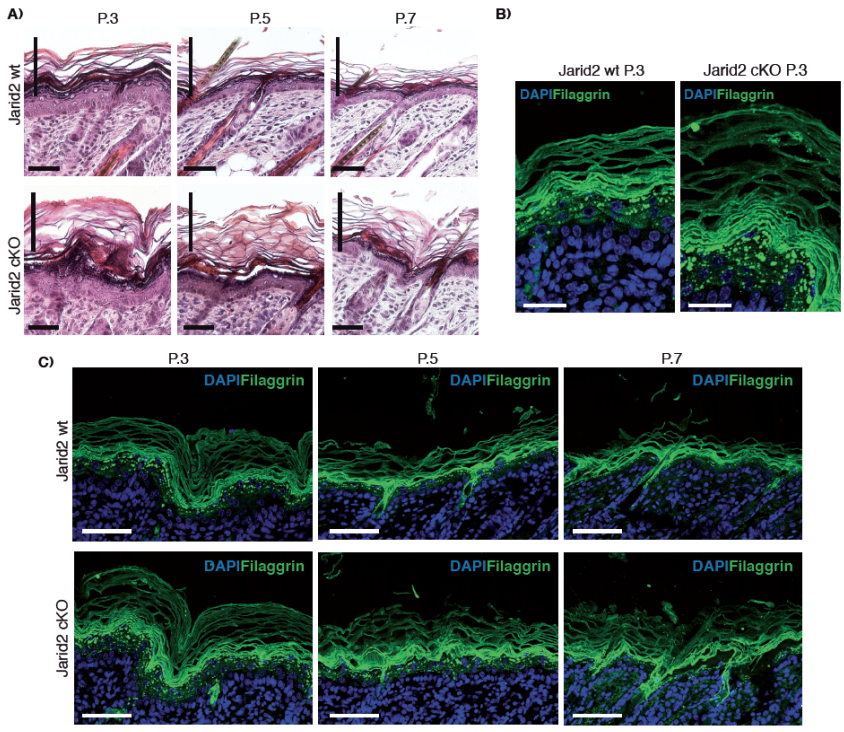

Figure3.4. Deletion of Jarid2 results in enhanced postnatal epidermal differentiation. **A)** Jarid2 cKO neonatal mice show increased differentiation and cornification. The analysis was performed from mice between P0-P9; only P3, P5 and P7 are shown. Differences between control and cKO mice are highlighted with a vertical bar. Scale bar: 50μm. **B)** High magnification of filaggrin staining in Jarid2 WT and Jarid2 cKO mouse skin. Scale bar: 25 μm. **C)** The IFE of Jarid2 cKO mice contains a thicker Filaggrin positive layer than control mice. Scale bar: 50 μm. N=2 for time points.

Expression of the interfollicular epidermis granular layer marker filaggrin was increased upon deletion of Jarid2, indicating an increased epidermal differentiation upon depletion of Jarid2 (**Fig3.4B-C**). Enhanced expression of filaggrin was also observed by immunofluorescence (**Fig3.5A**) and western immunoblotting (**Fig3.5B**) in cultured primary mouse keratinocytes isolated from Jarid2 cKO P0 epidermis compared with control littermates.

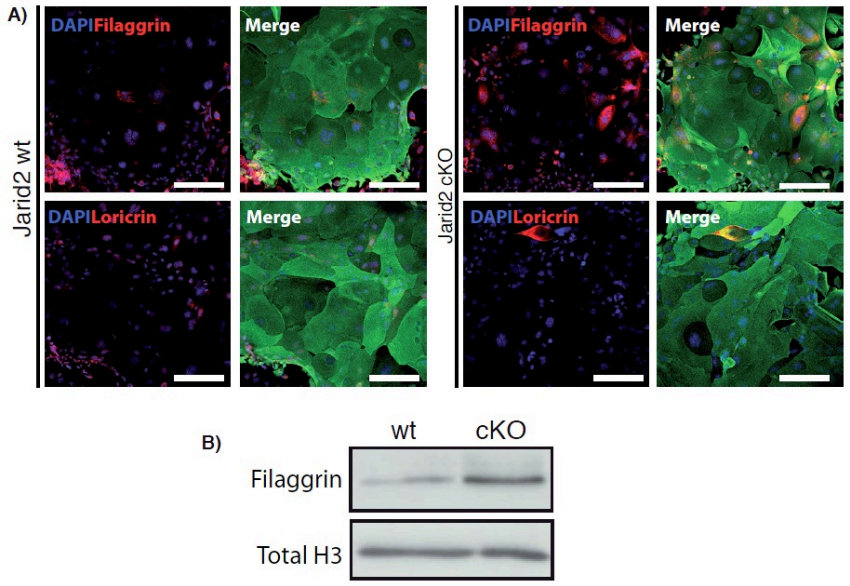

Figure3.5. **A)** Expression of filaggrin and loricrin is increased in newborn mouse keratinocytes isolated from Jarid2 cKO mice compared with control littermates. Keratin14 and DAPI are shown as counterstains. Pictures are representative of three independent experiments from three different litters of mice. Scale bar: 100 μm. **B)** Western blot showing increased filaggrin expression in Jarid2 cKO newborn keratinocytes. Total H3 is used for normalization.

The observed enhanced differentiation of the interfollicular epidermis was accompanied by a reduction in the proliferative potential of basal IFE progenitors. In this sense, both newborn and adult keratinocytes purified from Jarid2cKO epidermis formed fewer proliferative clones as compared to WT cells (**Fig3.6A**). Jarid2cKO cells not only formed fewer colonies but also displayed a morphology characteristic of terminally-differentiated abortive keratinocytes (**Fig3.6A**). Accordingly, we scored a statistically significant reduction in the number of proliferating basal interfollicular proliferative cells, as well as the transcript levels of the proliferation markers Ki67, in Jarid2cKO epidermis compared to WT epidermis (**Fig3.6B**).

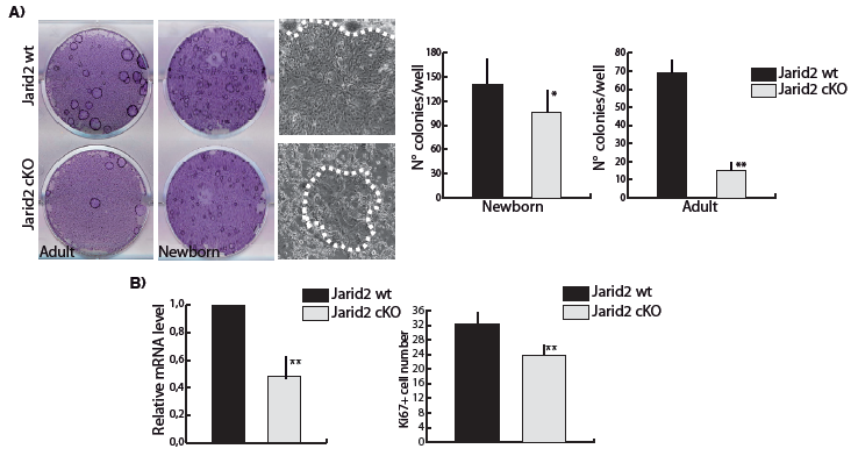

Figure3.6 A) Deletion of Jarid2 reduces the *in vitro* clonogenic potential of newborn (P0) and adult (8 weeks old) primary mouse keratinocytes. A magnified picture of a representative colony from control and Jarid2 cKO colonies is shown. Quantification of the number of colonies per well is reported on the right. Values are presented as mean + S.E.M., P*<0,05 and P**< 0,01; N=3. **B)** Basal interfollicular epidermal cells from P1 Jarid2 cKO mice express lower transcript levels of the proliferation marker Ki67 than their control littermates. Cells were FACS sorted on the basis of high cell surface levels of α6-integrin (N=4, vertical bar represent the S.E.M., P**<0,05).

Although the interfollicular epidermis of neonatal mice was less proliferative upon depletion of Jarid2, both postnatal hair follicle morphogenesis and pelage growth were unaffected in Jarid2cKO mice (**Fig3.7A**). Proliferation along the outer root sheath and the matrix of wild type and Jarid2cKO hair follicles was undistinguishable (**Fig3.7B**).

Altogether, these results indicate that loss of Jarid2 reduces the proliferative potential of basal epidermal progenitors while enhancing their differentiation, whereas it has no effect on the formation of the first wave of postnatal pelage formation.

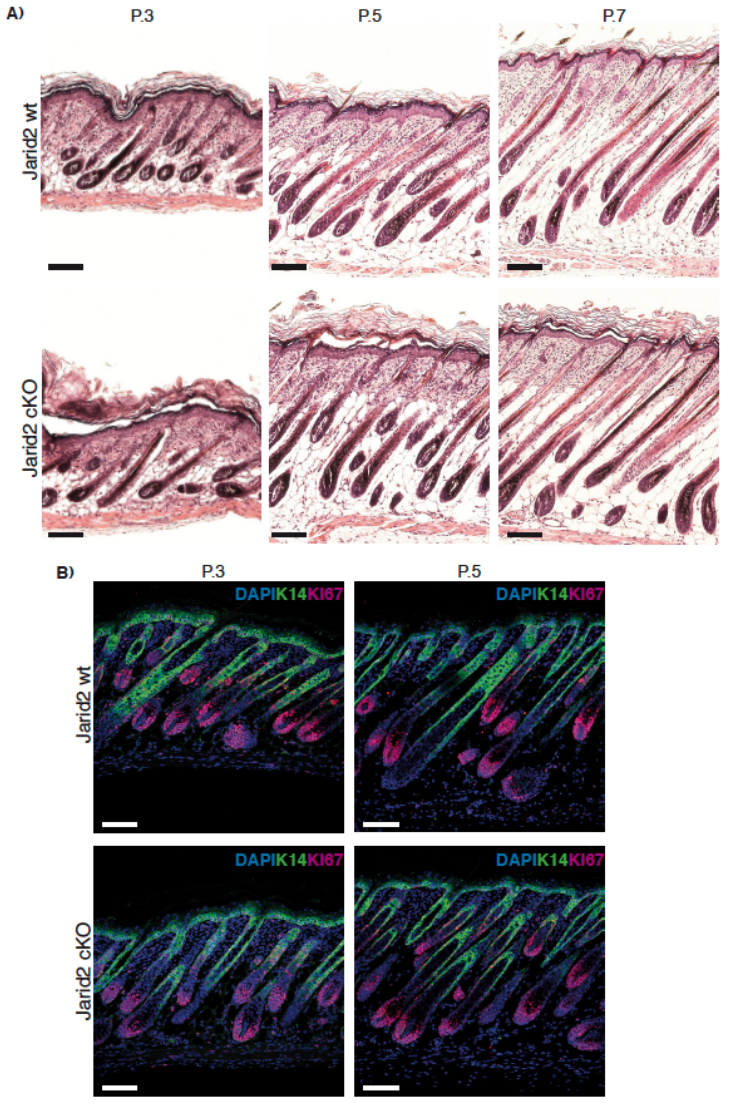

Figure3.7. A) Neonatal hair follicle morphogenesis is not altered upon the loss of Jarid2. Scale bar: 100 μm. **B)** Ki67 expression (red fluorescence) was unchanged in the HFs of neonatal Jarid2cKO mice compared with control mice, but was slightly reduced in the basal IFE. Keratin14 staining is shown as green fluorescence. Scale bar: 100 μm.

3.1.4 Deletion of Jarid2 results in inefficient entry of hair follicles in the second postnatal anagen

At postnatal days P8 to P10, a population of quiescent epidermal stem cells is stably established in the bulge [Nowak, et al, 2008]. Bulge cells remain slow cycling throughout the entire lifetime of the organism, and only undergo a reduced number of proliferative rounds during each cycle of adult hair morphogenesis [Tiede, et al, 2006]. After the first bout of postnatal pelage growth, all the hair follicles synchronously undergo a second phase of hair follicle growth (anagen) between P20 and P31, to establish the adult pelage [Morris, et al, 2004; Tumbar, et al, 2004; Blanpain, et al, 2004; Schneider, et al, 2009]. Continuous proliferation of basal epidermal cells is required from this stage onwards for the maintenance of the epidermis during adulthood [Clayton, et al, 2007]. We next studied whether deletion of Jarid2 had any impact on the maintenance of the quiescent bulge stem cell population, its activation during synchronous hair follicle growth, or basal epidermal progenitor homeostasis.

Similar to the situation in the neonatal epidermis, expression of Jarid2 in adult P19 mouse skin was highest in basal undifferentiated epidermal progenitors ($\alpha6^{bright}$/$CD34^{neg}$), and lower in the progressively differentiated keratinocytes ($\alpha6^{dim}$ and $\alpha6^{low}$ populations; **Fig3.8A**). Expression of Jarid2 was also gradually reduced upon differentiation (as measured by the cell surface levels of integrin $\alpha6$) of adult human epidermal keratinocytes, directly isolated from foreskin samples and maintained in culture (**Fig3.8B**).

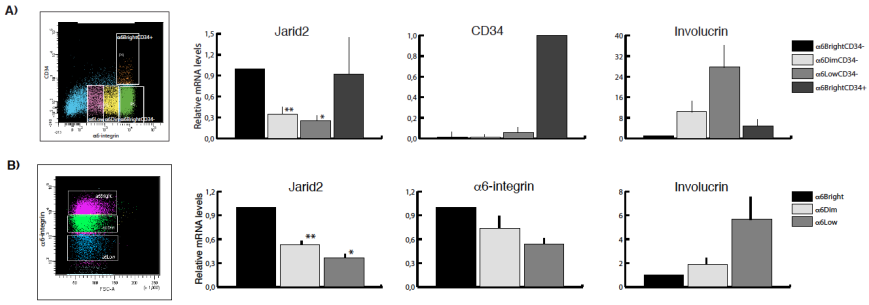

Figure3.8. mRNA levels of Jarid2 in basal and suprabasal interfollicular epidermal cells FACS sorted from P1 wild type mice **(A)** and primary human keratinocytes **(B)** depending of their cell surface levels of α6-integrin. Data shown represent the mean average, vertical bars represent the S.E.M. N=4. P*< 0,05; P**<0,01. A representative dot-plot of the sorting strategy used is shown on the left panel.

At adulthood, the percentage of bulge stem cells in the dorsal skin of Jarid2cKO mice, as determined by their high expression of α6 integrin and CD34 ($\alpha6^{bright}/CD34^{+}$), was virtually identical to that of control mice, indicating that Jarid2 is not necessary to establish or maintain hair follicle bulge stem cells (**Fig3.9A**). However, although the total number of bulge stem cells was unaffected in Jarid2cKO mice, the mice displayed a significant delay in the onset and the progression of hair follicles into anagen from postnatal days P21 to P31, with respect to control littermates (**Fig3.9B**). Accordingly, proliferation of hair germ cells, outer root sheath cells, and matrix cells, all of which are necessary to fuel hair follicle anagen [Itoh, et al, 2004; Greco, et al, 2009; Hsu, et al, 2011], was significantly delayed in Jarid2cKO mice between P21-31 as compared to control littermates (**Fig3.9B**, only P24 and P28 timepoints are shown as representative).

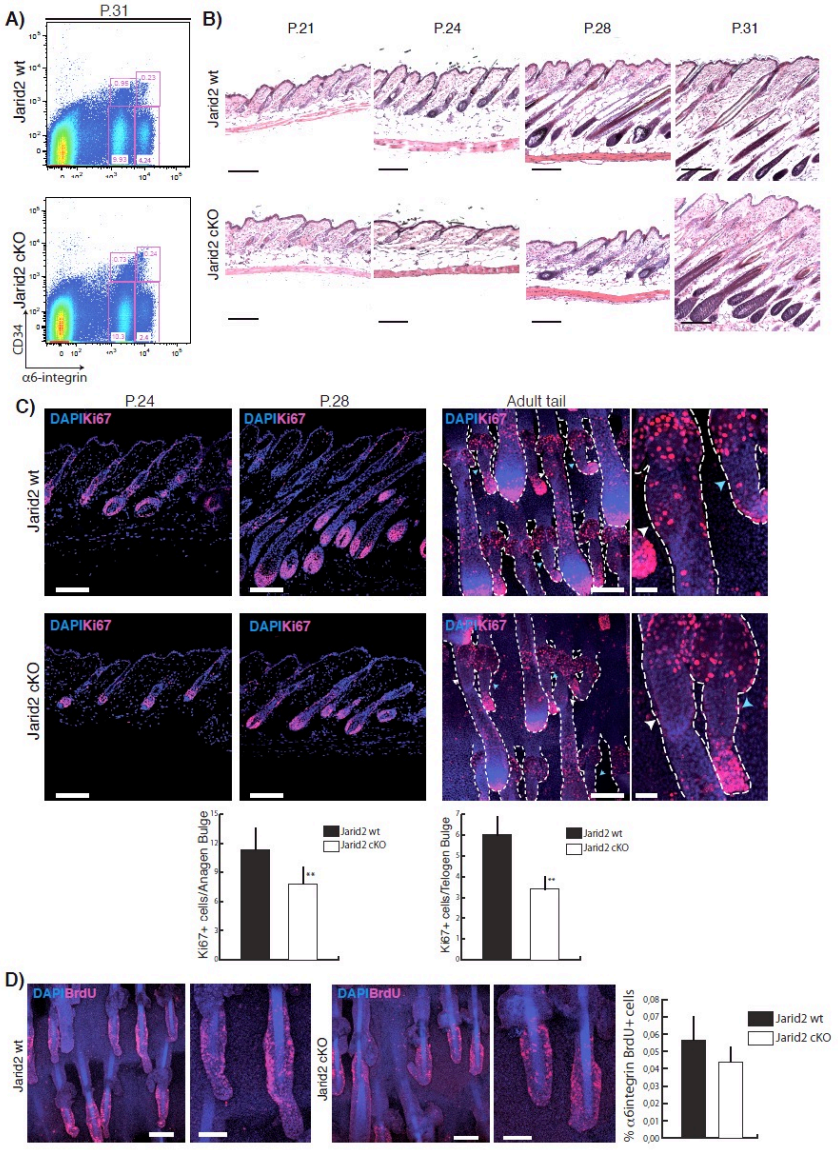

Figure3.9. A) Jarid2 cKO mice did not show significant changes in the proportion of bulge stem cells (α6bright/CD34+) with respect to control littermates. FACS profiles shown correspond to P31 mice. N=4 mice for time point. **B)** Deletion of Jarid2 resulted in a delay in the onset and progression of anagen between P21 and P31. Scale bar: 200 μm. N=8 for time point. **C)** Ki67 staining at P24 and P28, indicates reduced proliferation in matrix, bulge, and ORS in Jarid2 cKO HFs. Scale bar: 100 μm. The right panel shows whole-mount Ki67 immunostaining of tail epidermis of control and Jarid2 cKO P24 mice. Jarid2 cKO mice showed a significant reduction in the number of Ki67+

cells in the bulge, outer root sheath and matrix of late anagen (white arrow) and early anagen (light blue arrow) hair follicles. Scale bars: 100 and 25 μm, respectively. Quantification of the number of Ki67+ cells for either anagen (upper part) or telogen (lower graph) bulge is reported. Data are presented as average + S.E.M. P**<0.05; N=20 bulges. **D)** Jarid2 deletion does not affect the number of bulge label-retaining cells (LRCs) pulsed chased for 8 weeks. Scale bars: 100 and 50 μm. Right panel: measurement of the number of BrdU**.** bulge cells by FACS analysis in the epidermis of 8-week-old Jarid2 WT and Jarid2 cKO mice. Data are presented as average + S.E.M. Differences are non-statistically significant. N=4.

In addition, we observed a significant reduction in the number of Ki67+ proliferative cells in the bulge of hair follicles in full anagen (**Fig3.9C**). In spite of these changes in proliferation, the hair follicles of Jarid2cKO mice resumed their anagen cycle, resulting in normal, albeit delayed, hair growth. Although bulge proliferation was affected at late stages of anagen, a similar number of bulge cells were capable of stably accumulating BrdU, following an 8-weeks chase, in Jarid2cKO and WT mice (**Fig3.9D**).

Interestingly, Jarid2cKO bulge cells were more inefficient than WT ones in becoming active not only in physiological conditions, but also when ectopically stimulated to become hyperproliferative. In this sense, Jarid2cKO bulge cells were less efficient in responding to topical administration of the phorbol ester TPA, which causes bulge hyperproliferation and ectopic anagen entry. Jarid2 deletion resulted in a decrease in the number of TPA-induced proliferating bulge and hair matrix cells, as well as increased differentiation (**Fig3.10A**). Overall, Jarid2cKO mice did end up responding to TPA treatment, displaying hair follicles in full anagen (**Fig3.10B**). These results suggest that Jarid2 activity is essential in instances where strong proliferation is required (i.e., during postnatal morphogenesis, at the peak of anagen, and during TPA-induced hyperproliferation). However, deletion of Jarid2 does not

impair either normal, or ectopically induced, entry of hair follicles into the anagen state, indicating that Jarid2 is required for the scheduled activation of hair follicle bulge stem cells and their progeny, rather than being essential for their proliferation *per se*.

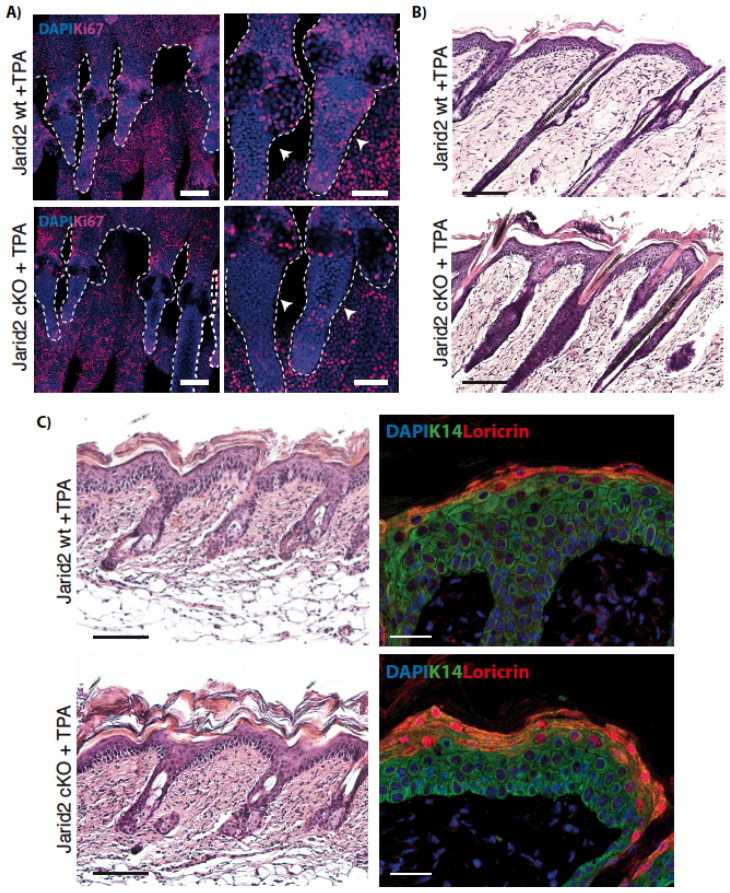

Figure3.10. A) Whole mount staining for Ki67 in TPA-treated tails reveals a reduction in the number of proliferative cells in the bulge and bulb. Scale bars: 100 μm and 25 μm, respectively. N=7. **B)** TPA-treatment in Jarid2 WT and cKO animals induces entry into anagen. **C)** The epidermis of TPA-treated Jarid2cKO animals displayed a thicker cornified layer than control littermates (left panel; scale bar: 100 μm) and increased expression of the loricrin marker (right panel, red fluorescence). Keratin14 is marked as green fluorescence. Scale bar: 25 μm.

At last, while the interfollicular epidermis of JaridKO mice was responsive to TPA, it displayed a thicker cornified layer than treated wild type littermates and a higher expression of the differentiation marker loricrin, similar to the effect observed in the interfollicular epidermis of neonatal Jarid2cKO mice (**Fig3.10C**).

Together, these results indicate that Jarid2 is required for the correct physiological timing of activating the cells required for the anagen phase of the hair cycle. In addition, robust hyper-activation of bulge stem cells depends on Jarid2 activity, which might be relevant for a possible role of Jarid2 during neoplastic transformation.

3.1.5 Jarid2 modulates PRC2 activity in mouse keratinocytes

Depletion of Jarid2 in embryonic stem cells significantly impairs binding of the PRC2 core complex subunits to their genomic targets [Herz and Shilatifard, 2010; Landeira and Fisher, 2011]. However, the effect of Jarid2 on the histone H3K27 methyltransferase activity of PRC2, and its consequences for the expression of polycomb targets in ES cells or adult stem cells, is still open to debate. We first confirmed that endogenous Jarid2 interacted with endogenous PRC2 (Suz12 and Ezh2) in primary mouse keratinocytes (**Fig3.11A).** We next tested whether epidermal deletion of Jarid2 affected genomic targeting of PRC2 and H3K27 trimethylation (H3K27me3) levels; and changed the expression of epidermal differentiation genes that have previously shown to be PRC2 targets in epidermal basal progenitors [Ezhkova, et al, 2009]. In newborn mouse keratinocytes, when cKO and control mice showed clear differences in interfollicular epidermal differentiation, Jarid2 localized to the proximal promoter region of several PRC2-target

genes (both epidermal and non-epidermal specific) [Ezhkova, et al, 2009], as determined by chromatin immunoprecipitation (ChIP) followed by quantitative PCR (**Fig3.11A-B**).

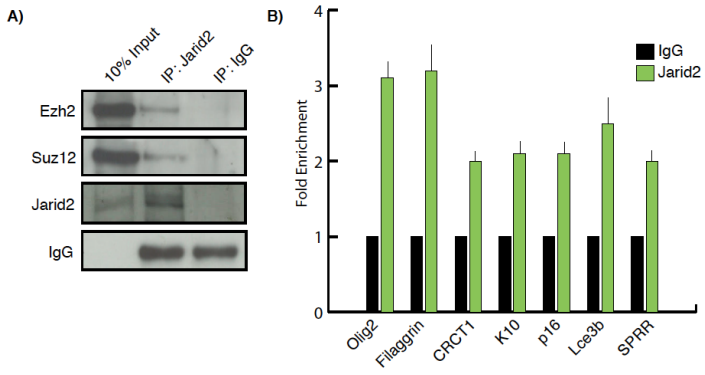

Figure3.11. A) Endogenous Jarid2 co-immunoprecipitates with endogenous Ezh2 and Suz12 PRC2 in newborn mouse keratinocytes. **B)** Jarid2 localizes to the promoters of PRC2 targets in newborn mouse keratinocytes, as shown by ChIP-qPCR. Data are presented as fold enrichment and are representative of three independent experiments.

In agreement with these results, Jarid2 cKO neonatal keratinocytes had reduced levels of Suz12 and H3K27me3 in both epidermal differentiation genes and non-epidermal specific PRC2 targets (note that p16, Olig2, Neurog1, and Neurog2 are representative of the non-epidermal PRC2 targets; **Fig3.12A-C**). The overall levels of H3K27me3 around the TSS of epidermal differentiation genes were considerably lower than in non-epidermal specific PRC2 targets, in agreement with previous findings [Ezhkova, et al, 2009] (**Fig3.12B**). In addition, Jarid2 cKO cells had lower levels of overall H3K27me3 than control cells (**Fig3.12E**). This slight reduction, albeit significant, was similar to that observed upon deletion of Jarid2 both in the levels of H3K27me3 in some lineage-commitment genes, and total level of H3K27me3, in ES cells [Peng, et al, 2009; Li, et al, 2010; Pasini, et al, 2010].

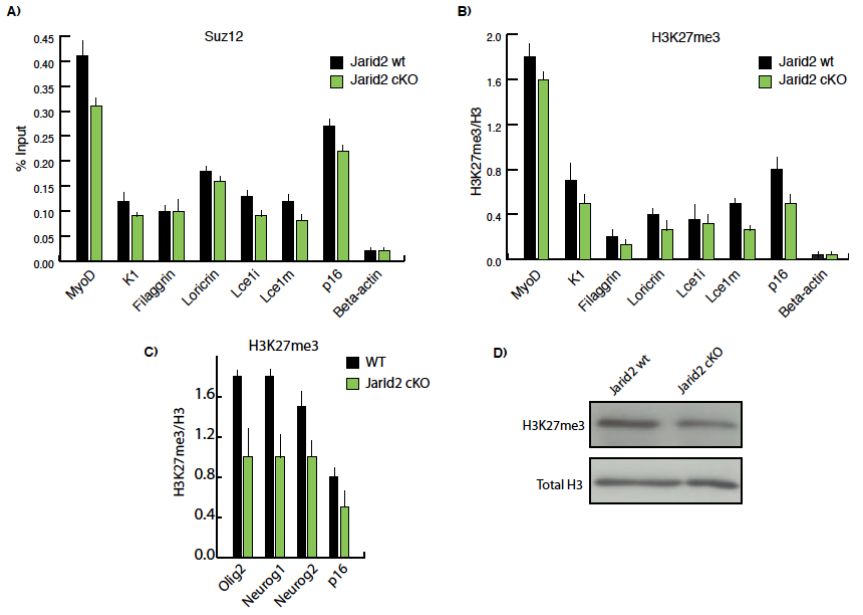

Figure3.12 A) ChIP analysis in newborn mouse keratinocytes isolated from Jarid2 cKO (N=15) and control mice (N=20) indicates that the occupancy of Suz12 in the promoters of epidermal differentiation and non-epidermal-specific PRC2 targets genes, is reduced in Jarid2 cKO mice. Data are presented as percentage of input. **B)** The levels of H3K27me3 are reduced in the promoters of the same cohort of genes in Jarid2 cKO cells. Data are presented as fold enrichment normalized to total histone H3. **C)** The levels of H3K27me3 in non-epidermal targets of PRC2 are reduced in Jarid2cKO cells. **D)** The global level of H3K27me3 is slightly reduced in Jarid2 cKO mouse keratinocytes compared with the control cells. Total H3 was used as a control of equal loading. All ChIP data shown is statistically significant ($P<0.05$).

As expected from our in vivo and ChIP analyses, loss of Jarid2 correlated with an increased transcription of this same group of genes involved in epidermal differentiation in purified basal (α6bright) cells isolated from newborn mice, as compared with WT littermates (**Fig3.13A**). The same pattern was observed in keratinocytes isolated from P8 mice, a time in which increased differentiation was still evident in the epidermis of Jarid2 cKO mice (not shown). The level of Cdkn2a/p16 (Ink4a locus) transcript and protein, a bona fide target of the PRC2 complex in all the tissues studied to date, including basal

interfollicular epidermal cells and HF stem cells [Sauvageau and Sauvageau, 2010; Ezhkova, et al, 2009, Ezhkova, et al, 2011], was also upregulated in Jarid2 cKO (**Fig3.13A-B**).

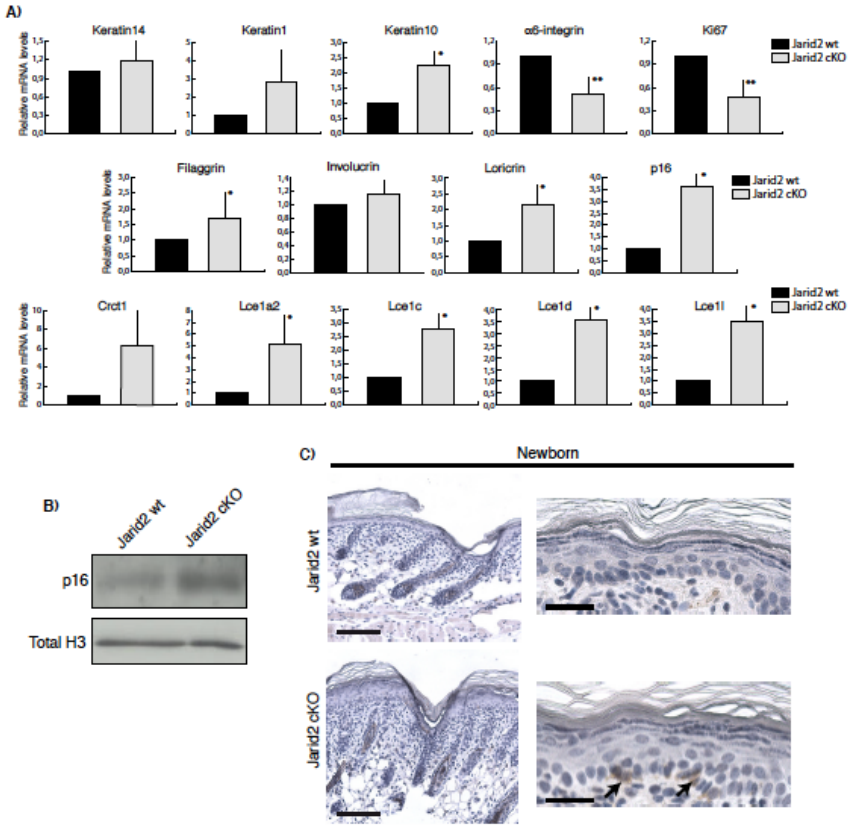

Figure3.13. A) The transcript levels (RT–qPCR) of epidermal specific and non-epidermal-specific targets of PRC2 are increased in basal interfollicular keratinocytes (α6bright/CD34- population) from Jarid2 cKO mice compared with the same WT control population. Data are mean + S.E.M. N=13; *P<0.09 and **P<0.05. **B)** Western blot showing p16 protein levels in Jarid2 WT and Jarid2 cKO newborn keratinocytes. Total H3 was used for normalization. **C)** Representative immunohistochemistry showing positive expression of p16 in the interfollicular epidermis of Jarid2 cKO newborn animals. (N=4 for WT and Jarid2 cKO mice). Scale bars: 100 μm and 20 μm.

In agreement with this, some basal cells of the interfollicular epidermis, but not HFs, of Jarid2 cKO newborn mice showed expression of p16,

compared with WT littermates (**Fig3.13C**; note that we did not detect any basal cell positive for p16 in the epidermis of any of the WT mice analysed). Cdkn2a/p16 inhibits G1/S transition and is a marker of senescent cells, and its repression by PRC2 is essential to maintain the proliferative state of undifferentiated ES and tumour cells [Sauvageau and Sauvageau, 2010] Accordingly, the transcript levels of the basal marker integrin α6 and the proliferation marker Ki67 were downregulated in Jarid2 cKO cells, as a further indication of their increased differentiation and higher levels of p16, and in agreement with the epidermal phenotype we observed in Jarid2 cKO mice (**Fig3.13B**).

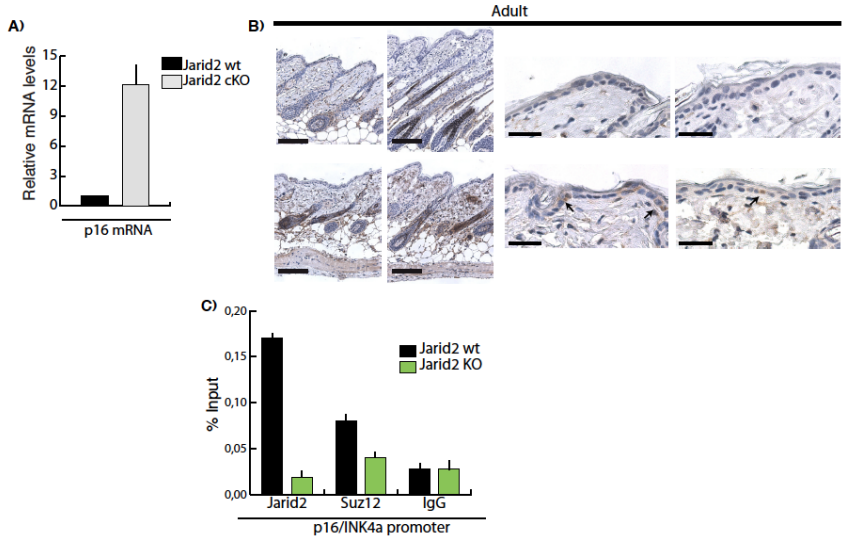

Figure3.14 A) The transcript level of Cdkn2a/p16 is elevated in basal epidermal keratinocytes isolated from 8-week-old mice compared with their WT counterparts. **B)** Immuno-histochemical analysis showing increased expression of p16 in the IFE and HF of Jarid2 cKO adult mice compared with their control littermates. Scale bars: 100 and 20 μm, respectively. **C)** Jarid2 and Suz12 colocalize on the promoter of the p16/INK4a locus. ChIP was performed on primary mouse keratinocytes isolated from 8-week-old Jarid2 cKO and control mice (N=5 for each). Data are presented as percentage of the input.

Enhanced transcription of the Ink4a locus resulted in positive immunostaining for p16 in the epidermis and HFs of adult Jarid2 cKO mice (**Fig3.14A-B**). Accordingly, both Jarid2 and Suz12 localized to the promoter region of p16, and this occupancy was significantly reduced in Jarid2 cKO keratinocytes (**Fig3.14C**).

DISCUSSION PART 1

4 DISCUSSION

4.1 Discussion

Our results show that Jarid2 is dispensable for the proper skin development in the embryos, in contrast to the phenotype developed in mice in which the PRC2 member Ezh2 has been deleted [Ezhkova, et al, 2009]. This indicates that at this stage of the epidermal morphogenesis Jarid2 is not functioning in a PRC2-dependant fashion. However, in the early postnatal development, the loss of Jarid2 results in increased differentiation and reduced proliferation in the IFE, similar to the phenotype seen in the embryonic epidermis of Ezh2cKO mice. Notably, at this stage Jarid2 expression is high in the proliferative, basal epidermal compartment, but decreases as cells differentiate, paralleling the expression pattern of Ezh2. Similarly to Ezh2, Jarid2 loss does not affect early hair follicle morphogenesis. These results suggest that the Ezh2-containing PRC2 complex regulates epidermal embryonic development independently of Jarid2, but its activity might become important after birth.

4.1.1 Jarid2 in early postnatal epidermal development

Although Jarid2-depleted hair follicles contain normal numbers of bulge stem cells, the entry of HFs into anagen is delayed, suggesting the impairment in the function of bulge stem cells. That said, Jarid2-depleted hair follicles resume the hair cycle and the hair growth is normal, albeit delayed. Together, these results indicate that Jarid2 is required for the correct physiological timing of activation of bulge SCs during the anagen phase of the hair cycle. In addition, robust hyper-activation of bulge stem cells depends on Jarid2 activity, pointing out a

possible relevant role of Jarid2 during neoplastic transformation. Our results therefore indicate that Jarid2 is required for instances when robust proliferation of interfollicular and hair follicle progenitor and stem cells is required.

4.1.2 Hair cycle is affected by Jarid2 loss

To understand whether Jarid2 deletion would affect the first postnatal hair cycle in adult mice, we analysed Jarid2 conditional KO mice and their control during the different hair follicles stages. We observed that whereas Jarid2-depleted hair follicles carry a normal bulge stem cell number, anagen entry is delayed, suggesting an impairment of the stem cells functions. Moreover, we showed that Jarid2 KO hair follicles are less proliferative than their controls, and they fail to proliferate when anagen entry is ectopically stimulated.

Although we observed reduced proliferation in the anagen bulges and matrix, with consequent delay in the occurrence of the hair cycle, Jarid2-depleted hair follicles resume the hair cycles and the hair growth is normal, albeit delayed.

Together, these results indicate that Jarid2 is required for the correct physiological timing of activating the cells required for the anagen phase of the hair cycle. In addition, robust hyper-activation of bulge stem cells depends on Jarid2 activity, pointing out a possible relevant role of Jarid2 during neoplastic transformation.

Our results indicate that Jarid2 is required for instances when robust proliferation of interfollicular and hair follicle progenitor and stem cells is required.

4.1.3 Jarid2-PRC2 interaction in the epidermis

Using primary newborn mouse keratinocytes we showed for the first time that Jarid2 is a PRC2 partners *in vivo* in the early postnatal epidermis. Whether the phenotype observed in Jarid2 KO epidermis is dependant or not on its interaction with PRC2 is still not clear, but our results suggest that Jarid2 regulates epidermal homeostasis through polycomb-dependant and independent mechanisms. In mouse keratinocytes, while loss of Jarid2 does not completely abolish PRC2 genomic occupancy and trimethylation of H3K27 at epidermal PRC2 targets, it does lead to a reduction in the level of both. These mild effects on PRC2 function are nevertheless casual, since deletion of Jarid2 results in enhanced differentiation and reduced proliferation of epidermal progenitors.

The epidermal consequences of deletion of Ezh2 [Ezhkova, et al, 2009] and Jarid2 are similar, (i.e., enhanced differentiation and reduced proliferation), but not identical. The two mouse models differ in the timing and the extent of their phenotypes, suggesting that the functional overlap between PRC2 and Jarid2 is limited, and that additional factors must be required for their epidermal activities. Several lines of evidence support this. First of all, whether Ezh2 deletion in the embryos causes a clear misregulation of epidermal differentiation [Ezhkova, et al, 2009], Jarid2 is dispensable for normal embryonic skin morphogenesis. Conversely, the premature differentiation defects of the Ezh2KO epidermis lessen as the mice are born, when these defects become visible in Jarid2cKO mice. Furthermore, Ezh2 deletion in the hair follicles does not affect the normal occurrence of the hair cycle, and only double Ezh1/Ezh2 loss have a deleterious effect on the hair

follicles physiology. Although Ezh1/Ezh2 double knockout and Jarid2cKO mice show a reduction in the proliferation of transit amplifying cells during hair follicle growth, the former undergoes a progressive loss of hair follicles [Ezhkova, et al, 2011], whereas the latter shows no gradual hair follicle deterioration in young adults. Furthermore, the fact that Jarid2 and Ezh1 have been reported to not interact [Landeira, et al, 2010], rules out any functional interaction among both. That Jarid2 and PRC2 may have non-dependent functions is underscored by the fact that several independently-generated, complete-knockout models of Jarid2 display various degrees of lethality as well as defects in heart, liver, neural tube closure, and hematopoietic development; this differs from the phenotypes of PRC2-subunit knockout mice [Takeuchi, et al, 1995; Lee, et al, 2000; Kim, et al, 2003; Toyoda, et al, 2003; Jung, et al, 2005a; Takeuchi, et al, 2006].

4.1.4 Jarid2 and neoplastic transformation

In our mouse model, Jarid2 deletion is associated with increased differentiation and reduced proliferation, and this phenotype suggests that Jarid2 might be important to balance these two complementary processes not only during physiological condition, but also in the context of neoplastic transformation. We have shown that Jarid2 depleted hair follicles respond less efficiently to the TPA-induced hyper-proliferation, suggesting that neoplastic cells might fail to enter cell-cycle in absence of this protein. In fact, through collaboration with the laboratory of Dr. Cedric Blanpain (University of Brussels) we have determined that Jarid2 is one of the most highly expressed genes in squamous cell carcinoma cancer stem cells, and that its loss of function induces a dramatic differentiation of squamous tumors *in vivo*

(unpublished data). Interestingly, a recent study [Walters, et al, 2013] shows that Jarid2 levels correlates with poor prognosis and metastatic development in human rabdosarcoma, and silencing of Jarid2 in these tumor cell lines promotes myogenic differentiation and reduce proliferation, paralleling the phenotype observed in our model. These results suggest that the effect of Jarid2 could be conserved in mouse and human.

4.1.5 Conclusions and future directions

Altogether, these results indicate that Jarid2 is necessary to maintain the correct level of epidermal differentiation and the efficient activation of hair follicle stem cells and their progeny after birth. Although Jarid2 is required for the robustness of PRC2 function in postnatal epidermal progenitors, other PRC2-independent interacting factors are likely required for Jarid2 to exert its epidermal function. It will be of interest to determine in future studies other partners of Jarid2 in epidermal progenitors, and whether Jarid2 plays a role in epidermal aging or neoplastic transformation.

SUMMARY PART 1

5 SUMMARY OF SCIENTIFIC FINDINGS

1) Jarid2 is a PRC2 component involved in the maintenance of epidermal stem cell homeostasis in early postnatal development.
2) Jarid2 is dispensable for skin embryonic development, pinpointing differences with the phenotype of its partner Ezh2.
3) Loss of Jarid2 causes unscheduled differentiation and restricts proliferation of basal IFE progenitors.
4) Proliferation defects observed upon Jarid2 loss results in delayed hair cycle, without affecting the number of bulge SCs.
5) Jarid2 interacts with PRC2 components in primary mouse keratinocytes and its loss results in H3K27me3 reduction in the promoter of PRC2 target genes.
6) Jarid2 might be important in maintaining the balance between proliferation and differentiation in non-physiological condition (i.e. hyper-proliferation, wounding, cancer).

MATERIALS AND METHODS PART 1

6 MATERIAL AND METHODS PART 1

6.1 Material and methods

6.1.1 Generation and handling of mice

To generate Jarid2 $^{flx/flx}$ /K14CreYFP-Rosa26 mice and their Jarid2$^{wt/wt}$ counterpart (referred to as Jarid2 cKO and WT, respectively), hemyzigous K14CreYFP-Rosa26 were mated with Jarid2 $^{flx/flx}$ mice. F1 Jarid2 $^{flx/wt}$ /K14CreYFP-Rosa26 mice were bred with other mice of the same genotype. All the mice were kept in the C57Bl6/FvBN mixed background. After standard isolation of the genomic DNA, mice were genotyped as described [Mysliwiec, et al, 2006], using primer reported in the **Tab6.1**. Mice were housed under 12 h light/12 h dark cycles and SPF conditions, and all procedures were evaluated and approved by the CEEA (Ethical Committee for Animal Experimentation) of the Government of Catalonia. For 5-Bromo-2-deoxyuridine (BrdU)-labelling experiments, 100 mg/g BrdU (Invitrogen) was injected intraperitoneally and chased for 2 months. To activate epidermal proliferation, backskin and tailskin of Jarid WT and Jarid2cKO mice were treated 3 times with 20 nM 12-O-tetradecanoylphorbol-13-acetate (TPA) (Sigma-Aldrich) during one week.

6.1.2 Primary keratinocytes

Primary mouse keratinocytes from either newborn mice or the tailskin of adult mice were isolated as described previously [Litchi, et al, 2008; Jensen, et al, 2010]. Cells were plated in EMEM (Lonza) containing 4% chelated FBS, 1% penicillin/ streptomycin, and 20 nM calcium, for 24 h; medium was then changed to growth medium (EMEM with 8%

chelated FBS, 1% penicillin/streptomycin, EGF (10 ng/ml) and 50 nM calcium). For clonogenic assays, keratinocytes were plated in E-medium on mitomycin (Sigma-Aldrich)-treated J2P 3T3 feeder cells [Nowak et al. 2009]. Primary human keratinocytes were isolated from neonatal or adult foreskin and cultured together with a feeder culture of fibroblasts (J2P-3T3) in FAD medium (1 part Ham's F12 medium with 3 parts Dulbecco Modified Eagle Medium (DMEM), containing penicillin, streptomycin and 18 mM adenine) supplemented with 10% Foetal Bovine Serum (FBS) and a cocktail of 0.5 μg/ml hydrocortisone, 5 μg/ml insulin, 100 pM cholera enterotoxin and 10 ng/ml EGF (all final concentrations), as described previously [Gandarillas, et al, 1997]. J2P feeder cells were cultured in DMEM with 10% FBS; they were treated with 4 μg/ml mitomycin prior to co-culturing them with primary keratinocytes.

6.1.3 Flow-cytometry and cell sorting

Primary mouse keratinocytes from either newborn mice or the tailskin of adult mice were isolated as described. Backskins of newborn or adult WT and Jarid2cKO mice were separated from the body with a scalpel. After enzymatic separation of the dermis from the epidermis, total keratinocytes were isolated, filtered through a 70 μm cell strainer (BDBioscience), and stained for 45 minutes in ice with primary antibodies. Primary antibodies used for FACS analysis and for cell sorting were α6-integrin (CD49f) coupled with PE (Serotech), and APC-coupled CD34 (BDBioscience). For cell sorting, total keratinocytes from newborn and adult mice, or primary human keratinocytes, were gated for single events and viability (DAPI incorporation), and sorted on the basis of α6-integrin expression, or

both α6-integrin and CD34 expression. FACS acquisitions were done with the FACS LSR-II system (BD), and cell sorting was performed with the FACS Aria system. Analysis was performed using FACS DiVa software (BDBioscience).

6.1.4 Whole mount immunofluorescence

Preparation of tailskin and whole mount stainings were performed as previously described [Braun, et al, 2003]. Primary and secondary antibodies were incubated overnight and used at the following concentrations: 1:1000 for anti-GFP (Invitrogen); 1:250 for anti-BrdU (Serotec) and anti-Ki67 (Abcam); and 1:500 for anti-rabbit and anti-rat conjugated to AlexaFluor488 or AlexaFluor594 (Molecular Probes). Nuclei were stained with DAPI (1:5000; Roche), and epidermal sheets were mounted in Mowiol. Pictures were acquired with a Leica TCS SP5 confocal microscope.

6.1.5 Immunoistochemistry

Samples were fixed in 4% NBF (Sigma-Aldrich) at 4C overnight, embedded in paraffin. Antigen retrieval was performed in boiling 0.01M tricitric acid (pH=6). Sections were permeabilized for 25 min in 0.25% Triton X-100/PBS and blocked for 90 min in 0.25% gelatin/PBS. Primary antibodies were incubated overnight at 4C, and secondary antibodies were incubated for 2 h at room temperature in 0.25% gelatin/PBS. Nuclei were stained with DAPI (1:5000; Roche), and the slides were mounted in Mowiol. The antibodies were against keratin14 (mouse, 1:200; Abcam), Ki67 (rabbit, 1:200; Abcam), filaggrin (rabbit, 1:200; Abcam), loricrin (rabbit, 1:200; Abcam), BrdU (rat, 1:100; Gibco), and GFP (rabbit, 1:100; Molecular Probes). Secondary

antibodies were conjugated with AlexaFluor 488 or 594 (Molecular Probes). Images were collected with a Leica SP5 confocal microscope. For immunohistochemistry for p16 (Santa Cruz M156 sc1207, 1:150 dilution), deparaffinized sections were incubated with H202 to block endogenous peroxidase and the staining was performed as described for immunofluorescence. The immune-complexes were stained using the ABC peroxidase method (Vector Laboratories).

6.1.6 RNA isolation and qPCR

Cells collected by FACS were directly lysed in RLT buffer (QIAGEN), and total RNA was extracted using the RNeasy Mini Kit (QIAGEN). mRNA was quantified with NanoDrop, and equal amounts of mRNA were retro-transcribed using oligo(dT) and SuperscriptIII (Invitrogen). cDNAs were normalized for the expression of two housekeeping genes, HPRT-1 and Pum-1. Samples were PCR-amplified using designed primers (**Tab6.2**). For real-time PCR, the same primers were employed using the LightCycler System (Roche), LightCycler 3.5 software and the LightCycler DNA Master SYBR Green I reagents. Differences between samples and controls were calculated based on the $2^{-\Delta\Delta CP}$ method.

6.1.7 Chromatin immunoprecipation (ChIP)

For co-immunoprecipitations, newborn mouse keratinocytes were lysed with 50 mM Tris-HCl pH 7,6; 300 mM NaCl; 10% Glycerol, 0,2%Igepal and total cell lysates were incubated with 10 μg of either Jarid2 or Suz12 antibody. The antibody-bound fraction was purified with protein A-agarose beads and then probed for immunoblotting.

For ChIP assays from intact epidermis, 2 month-old mice were sacrificed, and tails were incubated in 0.25% trypsin for 4 h at 37 °C, to

separate the dermis from the epidermis. Tail keratinocytes were extracted as described. Cells in suspension were cross-linked for 10 min at room temperature in 1% formaldehyde. Cross-linking reactions were stopped by addition of 1.25 M glycine to a final concentration of 125 mM. Cells were centrifuged for 10 min at 4 ºC and then washed in cold PBS. Cells were lysed with 1.3 ml of ChIP buffer (100 mM NaCl, 50 mM Tris-Cl, pH 8.1, 5 mM EDTA, pH 8.0, 0.2% NaN_3, 0.5% SDS, and 5% Triton X-100, in water) and sonicated for 10 minutes in a Bioruptor (Diagenode). The soluble fraction was quantified by Bradford, and 500 μg were used to immunoprecipitate transcription factors, while 100 μg were used to immunoprecipitate histones and specifically-modified histone. The chromatin and antibody mixtures were incubated overnight at 4 ºC in total volume of 500 μl. To recover the immunocomplexes, mixtures were incubated with 30 μl of protein A or G slurry for 1 h. The immunoprecipitated material was washed 3 times with a low salt buffer (50 mM HEPES, pH 7.5, 140 mM NaCl, 1% Triton X-100, and protease inhibitors), and once with a high salt buffer (50 mM HEPES, pH 7.5, 500 mM NaCl, 1% Triton X-100, and protease inhibitors). Samples were decrosslinked by incubation in 100 μl of 1% SDS and 100 mM $NaHCO_3$ at 65 ºC for 3 h. DNA was eluted in 200 μl of water using a PCR purification kit (Qiagen) and quantitated by real-time PCR. The specific primers used for ChIP are listed in **Tab6.3**.

6.1.8 Statistic

Results are presented as mean ± S.E.M. Statistical significance was determined by the Student's t-test.

Table6.1		
Genotyping PCR	Fw Primer	Rev Primer
Jarid2 Flox	GCGGTAAATGGTGAGTTGAAA	ACAGACTGACACACCTTCC
K14 wt	CAAATGTTGCTTGCTTGTCTGGTG	GTCAGTCGAGTGCACAGTTT
Cre Tg	GTCCATGTCCTTCCTGAAGC	TTCCTCAGGAGTGTTCTTCGC

Table6.2		
Mouse qPCR	Fw Primer	Rev Primer
K14	AGCGGCAAGAGTGAGATTTCT	CCTCCAGGTTATTCTCCAGGG
K1	GACACCACAACCCGGACCCAAAACTTAG	ATACTGGGCCTTGACTTCCGAGATGATG
K10	GGAGGGTAAAATCAAGGAGTGGTA	TCAATCTGCAGCAGCACGTT
Loricrin	TCACTCATCTTCCCTGGTGCTT	GTCTTTCCACAACCCACAGGA
Involucrin	GTCCGGTTCTCCAATTCGTGTTT	GCAATTGGAAGAGAAGCAGCATCAG
Lce1a2	GAGGTGCCCAAGGATCTTGTAC	CCAGGCTACAGCAGGAAGACAC
Lce1c	AGATCTCAAACATTCTATGCAGAGGAA	TCACAAAATACTGAAGAAGAAAGGGATT
Lce1d	GACTGCTGCTGATCTCAATGAGAA	TGCAGAAACTTTCCCTGAAGATTTC
Lce1l	CATGAAGGCTTCAGACAAGCAAT	TTGGAATCACAGAAGGAGATGAGAC
Lce1m	AGCATTGACTGAAGACCTGCAA	GCAAAGCCAATGCATCTCAGA
Crct1	ACTGCACTTTGATGTTCAGAAACTTC	CAGGAGGCCTGTTTTGAACACT
Filaggrin	GGAGGCATGGTGGAACTGA	TGTTTATCTTTTCCCTCACTTCTACATC
a6-integrin	TGCAGAGGGCGAACAGAAC	GCACACGTCACCACTTTGC
CD34	AAGGCTGGGTGAAGACCCTTA	TGAATGGCCGTTTCTGGAAGT
Ki67	AGGAGGAACCAACCAAGGACAGTT	TTTCTCTGTGCTGTGGGCTCTTCT
Jarid2	GGTGCAGGTACAAACAGTGCCAAA	GTGGTGGTTGGGTTTGGTTTCCTT
Jmj 150-387	AGGCCTTGCCGGGAGCCTGAA	AGCAAAGGCTCCACTATCTTC
Pum1	AGGCGTTAGCATGGTGGAGTA	TCCATCAAACGTACCCTTGTTC
HPRT-I	TCAGTCAACGGGGGACATAAA	GGGGCTGTACTGCTTAACCAG
Human qPCR	Fw Primer	Rev Primer
a6-integrin	CTAGTGGCTATTCTCGCTGGG	CGTTCCACTTTGTGATCCACTG
Involucrin	GACTGCTGTAAAGGGACTGCC	CATTCCCAGTTGCTCATCTCTC
Filaggrin	GAGAGGCGATCTGAGTCTGC	CTGCCACGTGACTGTATTCC
Jarid2	GGTCAGAAGAACGGGTGGTA	TTACCAAGGAGCCCATTCAC
Pum1	CGGTCGTCCTGAGGATAAAA	CGTACGTGAGGCGTGAGTAA
HPRT-I	TGGACAGGACTGAACGTCTTG	CCAGCAGGTCAGCAAAGAATT

Table6.3		
CHIp qPCR	Fw Primer	Rev Primer
Olig2	TGCTTATTACAGACCGAGCCAAC	CTAAATCCTAGCCACTTTGGAGAAGT
Neurg1	CCGGGTCGTACGGACAGTAA	TCGGTGAGGAAGCTGCACA
Neurog2	CAGATCTGATTGTTTTCTTGGTGGTATA	GCGTGGTTGTCTGTCAGTCAGT
HoxB13	TCTGGAAAGCAGCGTTTGC	CTTAGTGATAAACTTGTTGGCTGCA
Actin-B	CCGTAAAGACCTCTATGCCAACAC	GCTAGGAGCCAGAGCAGTAATCTC
p16 Promoter	GATGGAGCCCGGACTACAGAA	CTGTTTCAACGCCCAGCTCTC
K14	AGGAGGGATCTGATCGGGAGT	AGAGCTGCTCAGGTGTGTTAGAAAA
K1	CTCAGTATATAAGGGCACGGCACT	GACTCATGATGCCTTAGAGAGAGGT
K10	AGCAAAGCCTAGCACCTGTGA	GCTGCTGGAGCTGTATAGAACAGAC
Loricrin	CAGAGCAGGACAAGAGTATAAAACACA	GCCCACACTTACCTGAAGCAC
Lce1a2	GAGGTGCCCAAGGATCTTGTAC	CCTTCCCCCAACACTTCCAT
Lce1i	TCCTGGAGGTAAGGGCAGAGA	CAAGGCTGTGGCTAGTTATTGTCA
Lce1m	AGCATTGACTGAAGACCTGCAA	GCAAAGCCAATGCATCTCAGA
Lce3b	AAAGCATCCTCAGACACGGACTT	CCTATTGCACTTATGTCTGGATTTCTGT
Crct1	TCTGCCTAGCAGGTGTCAAGTTC	GCTACATTCTGGCTGCATCCTACT
Filaggrin	TCCCTTTTACAGGTGCATACACAC	CCTCCTTATCACTGGTTGAGTATTGTT
Sprr2f	TCTTTGAAAGGCCATATACCTCAGC	GTTCTGGTGCCCTGAGAAACC
Sprr2h	TGGTTCCAAACTCTGAGCAAGTGTA	CCTGTATATCAAGAGAGGGCATCAGAT

REFERENCES PART 1

7 REFERENCES PART 1

Blanpain C, Fuchs E. *Epidermal homeostasis: a balancing act of stem cells in the skin.* **Nat Rev Mol Cell Biol, 2009, 10(3):207-217**

Blanpain C, Lowry WE, Geoghegan A, Polak L, Fuchs E. *Self-renewal, multipotency, and the existence of two stem cells population in the epithelial stem cells niche.* **Cell, 2004, 118(5):635-48**

Beck B, and Blanpain C. *Mechanisms regulating epidermal stem cells.* **EMBO J, 2012, 31(9), 2067-75**

Candi E, Schmidt R, and Melino G. *The cornified envelope: a model of cell death in the skin.* **Nat Rev Mol Cell Biol, 2005, 6(4):328-340**

Clayton E, Doupe' DP, Klein AM, Winton DJ, Simons BD, and Jones PH. *A single type of progenitor cell maintain normal epidermis.* **Nature, 2007, 446(7132):185-189**

Horsley V, O'Carrol D, Tooze R, Ohinata Y. *Blimp1 defines a progenitor cell population that governs cellular inputs to the sebaceous glands.* **Cell, 2006, 126(3):597-609**

Cotsarelis G, Sun TT, Lavker *RM. Label-retaining cells reside in the bulge area of pilosebaceous unit: implications for follicular stem cells, hair cycle, and skin carcinogenesis.* **Cell, 1990, 61(7):1329-1337**

Ezhkova E, Pasolli HA, Parker JS, Stokes N, Su IH, Hannon G, Tarakhovsky A, Fuchs E. *Ezh2 orchestrates gene expression for the stepwise differentiation of tissue-specific stem cells.* **Cell, 2009, 136(6): 1122-1135**

Ezhkova E, Lien WH, Stokes N, Pasolli HA, Silva JM, Fuchs E. Ezh1 and *cogovern histon H3K27 trimethylation and are essential for hair follicle homeostasis and wound repair.* **Genes Dev, 2011, 25(5):485-498**

Frye M, Benitah SA. *Chromatin regulators in mammalian epidermis.* **Semin Cell Dev Biol. 2012, 23(8):897-905**

Gandarillas A, Watt FM. *c-Myc promotes differentiation of human epidermal cells.* **Genes Dev, 1997, 11(21):2869-82**

Greco V, Chen T, Rendl M, Schober M, Pasolli HA, Stokes N, Dela Cruz-Racelis J, Fuchs E. *A two-step mechanism for stem cell activation during hair regeneration.* **Cell Stem Cell, 2009, 4(2):155-69**

Herz HM, Shilatifard A. *The JARID2-PRC2 duality*. **Genes Dev, 2010, 24(9): 857-861**

Hsu YC, Pasolli A, Fuchs E. *Dynamics between stem cells, miche and progeny in the hair follicle.* **Cell, 2011, 144(1):92-105**

Jensen KB, Collins CA, Nascimento E, Tan DW, Frye M, Itami S, Watt FM. *Lrig1 expression defines a distinct multipotent stem cell population in mammalian epidermis.* **Cell Stem Cell, 2009, 4(5):427-429**

Jensen KB, Driskell RR, Watt FM. *Assaying proliferation and differentiation capacity of stem cells usingdisaggregated mouse epidermis.* **Nat Protoc, 2010, 5(5):898-911**

Jensen UB, Yan X, Woo SH, Christensen R, Owens DM. *A distinct population of clonogenic and multipotentmurine follicular keratnocytes residing in the upper histmus.* **J Cell Sci, 2008, 121(5):609-17**

Jones PH, and Simon BD. *Epidermal homeostasis: do committed progenitors work while stem cells sleep?* **Nat Rev Cell Biol, 2007, 9(1):82-87**

Jones PH, Simon BD, Fuchs E. *Sic transit gloria: farwell to the epidermal transit amplifying cells?* **Cell Stem Cell, 2007, 1(4):371-81**

Jung J, Mysliwiec MR, Lee Y. *Roles of Jumonji in mouse embryonic development.* **Dev Dyn, 2005;232(1):21-32**

Landeira D, Sauer S, Poot R, Dvorkina M, Mazzarella L, Jørgensen HF, Pereira CF, Leleu M, Piccolo FM, Spivakov M et al. *Inactive yet indispensable: the tale of Jarid2.* **Trends Cell Biol, 2011, 21: 74-80**

Landeira D, Sauer S, Poot R, Dvorkina M, Mazzarella L, Jorgensen HF, Pereira CF, Leleu M, Piccolo FM, Spivakov M et al. *Jarid2 is a PRC2 component in embryonic stem cells required for multi-lineage differentiation and recruitment of PRC1 and RNA Polymerase II to developmental regulators.* **Nat Cell Biol, 2010, 12(6): 618-624**

Levine SS, Weiss A, Erdjument-Bromage H, Shao Z, Tempst P, Kingston RE. *The core of the polycomb repressive complex is compositionally and functionally conserved in flies and humans.* **Mol Cell Biol, 2002, 22(17):6070-8**

Li G, Margueron R, Ku M, Chambon P, Bernstein BE, Reinberg D. *Jarid2 and PRC2, partners in regulating gene expression.* **Genes Dev, 2010, 24: 368-380**

Lichti U, Anders J, Yuspa SH. *Isolation and short-term culture of primary keratinocytes, hair follicle populations and dermal cells from newborn mice and keratinocytes from adult mice for in vitro analysis and for grafting to immunodeficient mice.* **Nat Protoc, 2008, 3(5):799-810**

Lien WH, Guo X, Polak L, Lawton LN, Young RA, Zheng D, Fuchs E. *Genome-wide maps of histone modifications unwind in vivo chromatin states of the hair follicle lineage.* **Cell Stem Cell, 2011, 9(3):219-32.**

Kouzarides T., *Chromatin modifications and their function.* **Cell, 2007, 128(4):693-705**

Mejetta S, Morey L, Pascual G, Kuebler B, Mysliwiec MR, Lee Y, Shiekhattar R, Di Croce L, Benitah SA. *Jarid2 regulates mouse epidermal stem cells activation and differentiation.* **EMBO J, 2011, 30(17):3635-46**

Mysliwiec MR, Chen J, Powers PA, Bartley CR, Schneider MD, Lee Y.*Generation of a conditional null allele of jumonji.* **Genesis, 2006, 44(9):407-11**

Müller-Röver S, Handjiski B, van der Veen C, Eichmüller S, Foitzik K, McKay IA, Stenn KS, Paus R. *A comprehensive guide for the accurate classification of murine hair follicles in distinct hair cycle stages.* **J Invest Dermatol, 2001, 117(1):3-15**

Nowak JA, Fuchs E. *Isolation and culture of epithelial stem cells.* **Methods Mol Biol, 2009, 482:215–232**

Nowak JA, Polak L, Pasolli HA, Fuchs E. *Hair follicle stem cells are specified and function in early skin morphogenesis.* **Cell Stem Cell, 2008 3(1):33–43**

Pasini D, Cloos PA, Walfridsson J, Olsson L, Bukowski JP, Johansen JV, Bak M, Tommerup N, Rappsilber J, Helin K. *JARID2 regulates binding of the Polycomb repressive complex 2 to target genes in ES cells.* **Nature, 2010, 464(7286): 306-310**

Peng JC, Valouev A, Swigut T, Zhang J, Zhao Y, Sidow A, Wysocka J. *Jarid2/Jumonji coordinates control of PRC2 enzymatic activity and target gene occupancy in pluripotent cells.* **Cell, 2009,139(7): 1290-1302**

Pincelli C., and Marconi A.*, Keratinocytes stem cells: friends and foe*. **J Cell Physiol. 2010, 225(2):310-5**

Sauvageau M, Sauvageau G., *Polycomb group proteins: multi-faceted regulators of somatic stem cells and cancer.* **Cell Stem Cell, 2010, 7(3): 299-313**

Sen GL, Webster DE, Barragan DI, Chang HY, and Khavari PA. *Control of differentiation in a self-renewing mammalian tissue by the histone demethylase JMJD3*. **Genes Dev, 2008, 22(14):1865-70**

Shen X, Kim W, Fujiwara Y, Simon MD, Liu Y, Mysliwiec MR, Yuan GC, Lee Y, Orkin SH. *Jumonji modulates polycomb activity and self-renewal versus differentiation of stem cells.* **Cell, 2009, 139(7): 1303-1314**

Shirato H, Ogawa S, Nakajima K, Inagawa M, Kojima M, Tachibana M, Shinkai Y, Takeuchi T. *A jumonji (Jarid2) protein complex represses cyclin D1 expression by methylation of histone H3-K9.* **J Biol Chem, 2009, 284(2): 733-739**

Snippert HJ, van der Flier LG, Sato T, van Es JH, can der Born M, Kroon-Veenboer C, Barker N, Klein AM, van Rheenen J, Simons BD, Clevers H. *Intestinal crypt homeostasis results from neutral competition between symmetrically dividing Lgr5 stem cells.* **Cell, 2010, 143(1):134-44**

Takeuchi T, Yamazaki Y, Katoh-Fukui Y, Tsuchiya R, Kondo S, Motoyama J, Higashinakagawa T. *Gene trap capture of a novel mouse gene, jumonji, required for neural tube formation.* **Genes Dev, 1995, 9(10): 1211-1222**

Takeuchi T, Watanabe Y, Takano-Shimizu T, Kondo S. *Roles of jumonji and jumonji family genes in chromatin regulation and development.* **Dev Dyn, 2006, 235(9): 2449-2459**

Toyoda M, Shirato H, Nakajima K, Kojima M, Takahashi M, Kubota M, Suzuki-Migishima R, Motegi Y, Yokoyama M, Takeuchi T. *Jumonji downregulates cardiac cell proliferation by repressing cyclinD1 expression.* **Dev Cell, 2003,5(1):85-97**

Tumbar T, Guasch G, Greco V, Blanpain C, Lowry WE, Rendl M, Fuchs E. *Defining the epithelial stem cell niche in skin.* **Science, 2004, 303(5656): 359-363**

Walters ZS, Villarejo-Balcells B, Olmos D, Buist TW, Missiaglia E, Allen R, Al-Lazikani B, garrett MD, Blagg J, Shipley J. *JARID2 is a direct target of the PAX3-FOXO1 fusion protein and inhibits myogenic differentiation of rhabdomyosarcoma cells.* **Oncogene, 2013**

Zhang YV, Cheong J, Ciapurin N, McDermitt DJ, Tumbar T. *Distinct self-renewal and differentiation phases in the niche of infrequently dividing hair follicles stem cells.* **Cell Stem Cell, 2009, 5(3):267-78**

INTRODUCTION PART 2

8 INTRODUCTION PART 2

8.1 Squamous cell carcinomas

Squamous cell carcinoma (SCC) is the sixth leading cancer by incidence worldwide, with 600,000 new cases every year [Leemans, et al, 2011]. The major risk factors of HNSCC are tobacco use, alcohol consumption, and HPV infection [Argiris, et al, 2008]. Despite advances in the epidemiology and pathogenesis of HNSCC, the survival rates for this cancer have improved little in the past 40 years, and only 50% of the patients will survive for more than 5 years.

Despite social awareness towards its prevention and early detection, a recent report by Cancer Research UK indicates that although the mortality rates for most common cancers is predicted to significantly diminish in the next 20 years, oral SCC-related mortality is expected to soar up to 20% (**Fig8.1**).

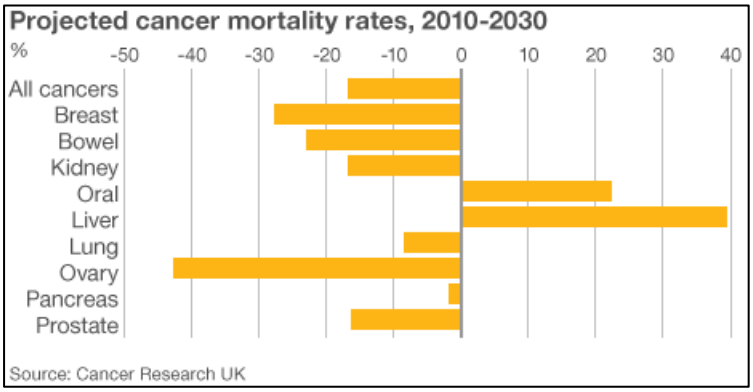

Figure8.1. Cancer mortality rate for the most common malignancies in the industrialized countries. Despite advances in basic and clinical cancer research, HNSCC mortality is increasing.

Early-stage patients with SCC are treated with surgery and radiotherapy, but the lack of efficient chemotherapy make this

combination the most common also for advanced tumors. Recently, drugs targeting signalling pathways aberrantly activated in HNSCC have been introduced, but the discovery of new molecules specifically targeting tumor-initiating cells is paramount [Price, et al, 2012].

Human SCCs are characterized by molecular heterogeneity, and many signalling pathway can contribute to the occurrence and development of the disease. Genes associated with cell cycle progression are often aberrantly regulated in HNSCC, and over-expression or amplification of CyclinD1, Cdk4 [Lazarov, et al, 2002] and TERT, as well as p53 [Van Houten, et al, 2002] or Rb deletion, contribute to the development of the disease. Other pathways that are aberrantly regulated in HNSCC are EGFR [Hynes, et al, 2005] and TGF-β [Li, et al, 2006].

Although the incidence of distant metastasis in cutaneous SCC is relatively small compared to other solid malignancies (less than 5%), the occurrence of secondary lesions is often deleterious. On the other hand, the prognosis of oral SCC is far worst, and approximately half of the patients develop distant metastasis. Pulmonary and lymph-nodes metastases are the most frequent in SCC, accounting for 66% of distant metastases. Other metastatic sites include bone (22%), liver (10%), skin, mediastinum and bone marrow [Ferlito, et al, 2001; Weinberg, et al, 2007].

8.2 Cancer stem cells

Tumors have long been recognized to consist of a heterogeneous population of cells with different proliferative capacity, histologic and immunophenotypic appearance, as well as tumorigenic potential

[Monroe, et al, 2010; Visvader, et al, 2011, Clevers, 2011]. Traditionally, this heterogeneity has been hypothesized to be the result of the stochastic accumulation of several individual mutations and micro-environmental signals that provide a selective advantage to certain tumor cells (Clonal Evolution model) [Nowell, et al, 1976]. However, over the last several years a new hypothesis has emerged suggesting the existence of tumor-initiating cells (TIC), or cancer stem cells (CSCs), that are able to continually sustain tumorigenesis [Reya, et al, 2001; Bonnet and Dick, 1997]. The central concept of the CSC hypothesis is the observation that not all the tumor cells are equal, and tumor growth is fuelled by its own stem cells, similar to the growth of a normal tissue [Clevers, 2011]. This implies a hierarchical organization of the tumor, with CSCs lying at the top of the hierarchy. However, the clonal evolution and the CSC model are not mutually exclusive, but rather interconnected, and recently it has become clear that a tumor comprises of multiple CSCs subtypes that compete with each other (**Fig8.2)**.

Cancer stem cells were first identified in leukemic cancers [Bonnet and Dick, 1997]; this discovery led Clarke and colleagues to apply the same concept to breast cancer where they first observed the existence of CSCs in solid tumor [Al-Hajj, et al, 2003]. After these landmark papers, CSCs have been discovered in many solid malignancies, such as colon cancer, pancreatic cancer, melanoma, and SCC [Ricci-Vitiani, et al, 2007; Dalerba, et al, 2007; Schatton, 2008; Prince, et al, 2007].

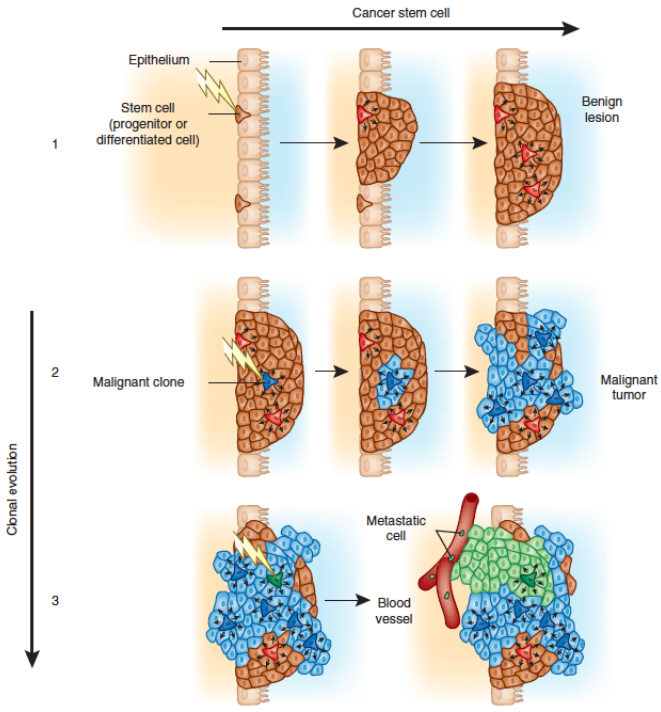

Figure8.2. Clonal evolution and CSC model. **1)** A first hit occurs in a stem cell or a progenitor, giving selective advantages with consequent grow of a benign lesion. **2)** A second hit targeting a cell of the benign lesion leads to the generation of a malignant neoplasia. **3)** A third hit provides invasive properties, with consequent extravasation and seeding at distant organs. Genetically independent clones can exist in the same tumor. At each step of this tumor evolution process there are clones that behave like cancer stem cells [Adapted from Clevers, 2011].

Experimentally, the existence of CSCs has been demonstrated by serial transplantation of different tumor subpopulation in immune-deficient mice; thus detection of CSCs is strongly assay-dependent [Ishizawa, et al, 2010]. Nevertheless, CSCs are not simply an artefact, since they have been identified in syngeneic mouse model [Malanchi, et al, 2008] and their existence has been recently proved using lineage-tracing experiments [Driessens, et al, 2012; Schepers, et al, 2012].

CSCs display features resembling those of normal stem cells: they are able to self-renew, are multipotent (they generate the different cellular subtypes of the tumor) and can reversibly enter quiescence [Visvader, et al, 2008; Visvader, 2011; Bacelli, et al, 2012]. Another feature that is shared by many, but not all, cancer stem cells is their relative resistance to conventional chemotherapy (**Fig8.3**). Whereas chemotherapeutic agents lead to tumor shrinkage, the treatments successfully eliminate the highly proliferating cells of the tumor bulk, but cancer stem cells remain mostly unaffected and are often responsible of tumor relapse [Loebinger, et al, 2008; Bertolini, et al, 2009]. CSCs might be chemo-resistant because of the expression of multidrug transporters, because of mutations conferring increased response upon DNA damage and ROS, and as a consequence of their slow-cycling nature [Baccelli, et al, 2012; Visvader, 2011; Clevers, 2011].

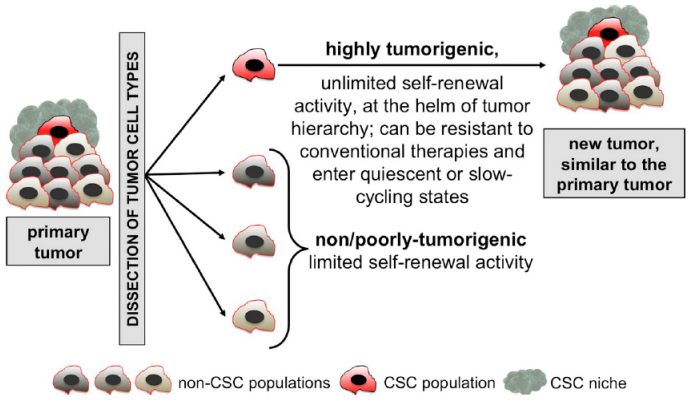

Figure8.3. Main features of CSCs [Adapted from Baccelli, et al, 2012]

CSCs are characterized by great plasticity and their dynamic traits might explain the great intra-tumoral heterogeneity. During cancer progression, tumor-initiating cells can acquire new mutations, with

consequent generation of several CSC clones inside the tumor. Moreover, micro-environmental cues can influences the traits of CSCs [Cabarcas, et al, 2011]. CSC plasticity is well-documented in glioblastoma: two recent papers have reported that tumor-initiating cells are able to strikingly trans-differentiate *in vivo* into pericytes and endothelial cells, demonstrating that CSCs can dynamically change to create a supportive niche permissive for tumor expansion [Ricci-Vitiani, et al, 2010; Cheng, et al, 2013; Wang, et al, 2013].

CSCs have also been reported to express many EMT factors, and the acquisition of an invasive phenotype normally correlates with disease progression and aggressiveness [Mani, et al, 2008; Biddle, et al, 2012]. During migration and invasion, both necessary for the first steps of metastatic colonization, CSCs acquire a mesenchymal phenotype with the consequent down-regulation of epithelial markers [Rhim, et al, 2012]. This implies that a CSC identified in an early stage tumor might have a completely different phenotype from those circulating in the blood or present at the metastatic site.

Another important aspect to consider in the CSC model is the tumor microenvironment. The idea that CSCs reside in a special niche that contributes to maintain the CSC traits is quickly evolving, and it is clear that cytokines and chemokines secreted by the stromal cells, vascular architecture, hypoxia and other niche clues can favours CSC survival [Cabarcas, et al, 2011; Malanchi, et al, 2012]. Moreover, CSC niche can provide CSCs traits to normal tumor cells [Li, et al, 2009; Grivennikov, et al, 2009].

8.2.1 Cancer stem cell markers in solid tumors

The most common method used to identify CSCs has relied on the expression of specific cell surface markers that enrich for cells with CSC properties. Many of these antigens were initially targeted because of their known expression on endogenous stem cells. A multitude of studies have identified CSC markers across a variety of solid malignancies, but none of them exclusively define the tumor-initiating population.

One of the most-common markers used to enrich for CSC in many solid malignancies is CD44, a surface glycoprotein involved in migration and cell adhesion. CD44 is a receptor for hyaluronic acid and other ECM components, first identified as a homing receptor in lymphocytes [Zoller, et al, 2011]. There is now great evidence for its role in the progression of many tumour types, as well as for its expression on cancer-initiating cells [Zoller, et al, 2011]. CD44 was first identified as a CSC marker in breast cancer [Al-Hajj, et al, 2003], and after this discovery CD44 started to be used as a common cancer stem cells marker for many malignancies, such as colon cancer, pancreatic cancer and HNSCC [Dalerba, et al, 2007; Prince, et al, 2007; Li, et al, 2007]. However, it has been later shown that a subpopulation of CD44-expressing cell in HSNCC are tumorigenic in a xenotransplantation assay [Prince, et al, 2007].

Aldehyde dehydrogenase (ALDH) is an intracellular enzyme involved in the retinoic acid and alcohol metabolism, whose activity is also known to enrich for stem/progenitor cells in normal tissues and in solid malignancies [Deng, et al, 2010, Chen, et al, 2009; Clay, et al, 2010]. In SCC and breast cancer, ALDH activity correlates with disease progression and resistance to cisplatin.

In addition, CD133, a surface glycoprotein expressed by stem cells in normal tissues is also used for purifying cancer stem cells from solid malignancies [Ricci-Vitiani, et al, 2007; Hermann, 2007]. However, the use of CD133 for the isolation of squamous cell carcinoma CSCs is controversial [Monroe, et al, 2010].

With regards to human SCCs, recent data have shown that SCC tumor cells enriched in TICs are often characterized by the expression of the surfaces molecules CD44 and Met (HGF-R) and by high ALDH activity [Sun, et al, 2011; Monroe, et al, 2010; Prince, et al, 2007; Ginestier, et al, 2007], features used also to purify CSCs from other solid tumors.

8.2.2 Cancer stem cell quiescence

Certain types of adult stem cells can transit between actively proliferating and quiescent states [Fuchs, et al, 2009; Tian, et al, 2011]. Slow-cycling stem cells are often identified by their propensity to retain DNA labels much longer than their rapidly proliferating offspring, and BrdU (or inducible H2B-GFP) pulse-chase experiments have been used to characterize quiescent population in adult stem cells [Braun, et al, 2003; Cotsarelis, et al, 1990; Tumbar, et al, 2004].

CSCs are able to initiate and sustain malignant growth, and high proliferative capacity is necessary for the expansion of the tumor at the primary site. However, CSCs have to sustain tumor growth over the time and to self-renew, thus infrequent division is suggested to be important for maintenance of a subset of CSCs. Evidence suggests that quiescence might play an important role in protecting stem cells from exhausting their proliferative capacity, inhibiting differentiation, and

limiting accumulation of mutations during frequent rounds of DNA synthesis [Moore, et al, 2011; Viale, et al, 2009]. The slow-cycling nature of some CSCs might also explain chemotherapy resistance, as well as relapse and metastatic occurrence [Moore, et al, 2010; Aguirre-Ghiso, et al, 2007; Baccelli, et al, 2012].

Indeed, conventional chemotherapy and radiotherapy are effective on proliferative cells and require active cycling to induce apoptosis, thus the treatment might lead to tumor shrinkage without affecting the few slow-cycling CSCs [Pece, et al, 2010; Parada, et al, 2012].

Moreover, slow-cycling cells can survive hypoxia and avoid the immune-surveillance because they are not dividing and metabolically inactive, but they can reactivate after many years giving rise to aggressive secondary tumor and metastasis [Klein, et al, 2011; Aguirre-Ghiso, et al, 2007].

Different pieces of evidence have proved that slow-cycling CSCs are responsible of tumor and metastasis initiation, and some of these studies have shown that quiescent cancer cells are invasive and undergo EMT [Pece, et al, 2010; Roesch, et al, 2010; Dembinski, et al, 2009; Qin, et al, 2012], but little is known about the molecular pathways that governs CSCs quiescence and the functional differences between slow-cycling and proliferative TICs.

It has been proposed by several groups that the dormant nature of a subset of CSCs enhances their ability to migrate at distant sites and generate secondary tumors.

Most likely because of technical challenges, the existence of dormant CSCs in human cancers has not been extensively explored.

8.3 Metastasis

Metastatic growth in distant organs is the major cause of cancer mortality. The development of metastasis is a multistage process with several rate-limiting steps.

The basic steps of metastasis include the progression of the primary tumor towards invasive carcinoma and dispersion of cancer cells through the lymphatic or blood vessels, thus the epithelial–mesenchymal transition (EMT) is a necessary requirement in the case of solid malignanices [Rhim, et al, 2012; Biddle, et al, 2012].

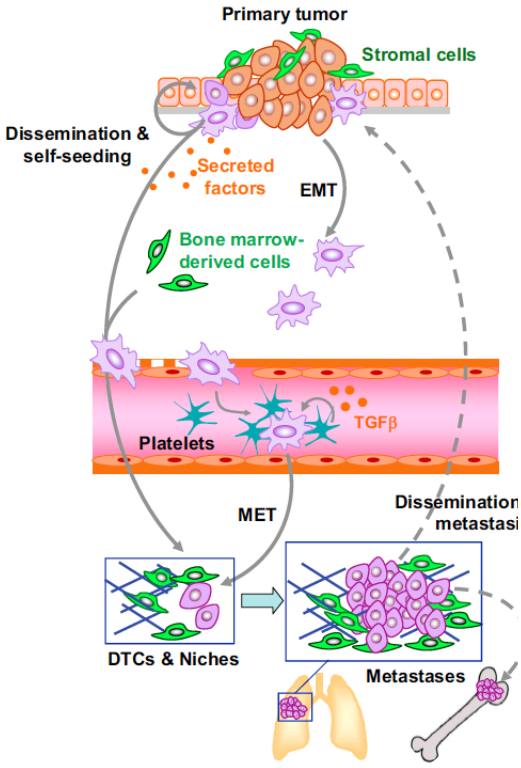

Figure8.4. The key steps of dissemination, survival, and expansion of metastatic tumor cells.
Tumor cells at the primary site undergo EMT or use other means of invasion to escape from the primary tumor. Platelets might be involved in extravasation processes. Tumor-derived factors promote the seeding and expansion of metastasis. Stromal component of the metastatic niches enhances tumor survival, stemness, and immune evasion.
[Adapted from Kang and Pantel, 2013]

Although dissemination of tumor cells seems to be an early and frequent event, the successful initiation of metastatic colonization and growth is inefficient for many cancer types and is accomplished only by a minority of cancer cells that reach distant sites [Chambers, et al, 2002].
Circulating cancer cells that survive could infiltrate distant organs after extra-vasation, and once in the new microenvironment they might generate overt metastasis with or without an intervening period of latency. Several lines of evidence indicate that the initiation of metastasis begins early during tumorigenesis [Rhim, et al, 2012], and rare tumor circulating cells (CTCs) can be detected in the patient before the occurrence of overt metastasis, that could require several years, depending on the nature of the primary tumor [Baccelli, et al, 2013].

It has been proposed that circulating cancer cells that do not have metastatic potential may prepare sites for engraftment by more invasive cells; alternatively, fully transformed cancer cells can acquire mutation that favours the spreading to metastatic sites [Bidard, et al, 2008; Psaila, et al, 2009].

8.3.1 The metastatic niche

The metastatic growth strongly depend on functions acquired by the cancer cells, but the surrounding stroma play an important role in recruiting tumor cells at distant sites and in creating a pre-metastatic niche. In addition to the tumor-initiating events that produce an incipient carcinoma, metastasis requires functionally distinct classes of genes mediating initiation and progression in the distant site [Nguyen, et al, 2009; Li, et al, 2007].

It has been shown in several kind of cancer that molecules expressed by CSCs promote colonization or survival at distant sites. For example, metastatic cancer cells express factors that recruit tumor associated macrophages or that induce the surrounding fibroblasts to release pro-survival signals or ECM remodeling factors [Chen, et al, 2011; Sethi, et al, 2011; Malanchi, et al, 2011; Gao, et al, 2012].

One component in this evolving process that remains particularly perplexing is the tissue-specific pattern of metastatic progression in cancer. Both 'seed' (the cancer cell) and 'soil' (factors in the organ environment) contribute to this organ specificity [Kaplan, et al, 2006]. A considerable amount of evidence indicates that molecular factors that are present in specific organs can influence whether or not various types of cancer cell will grow there [Chambers, et al, 2002; Nguyen, et al, 2009]. These studies indicate that tumor cells will respond quite differently (gene expression, growth ability, chemotherapy response) depending on the environment they encounter in the new organ (**Fig8.5**). Moreover, the primary tumor cells produce a unique array of tumor chemokines that orchestrates formation of the pre-metastatic niche and specifically dictates the pattern of tumor spread [Kaplan, et al, 2006; Chen, et al, 2011; Sethi, et al, 2011].

Recent elegant studies have shown that tumour cells express patterns of chemokine receptors that match chemokines that are specifically expressed in organs to which these cancers commonly metastasize [Chambers, et al, 2002; Li, et al, 2007]. However, Massague' and coworkers have shown that specific gene signature present in subpopulation of cancer cells confer the ability to growth in a particular tissue instead of another [Minn, et al, 2005; Kang, 2003], thus it seems

that both the cancer cells themselves and the microenvironment present at the metastatic site contribute to the colonization of a specific organ.

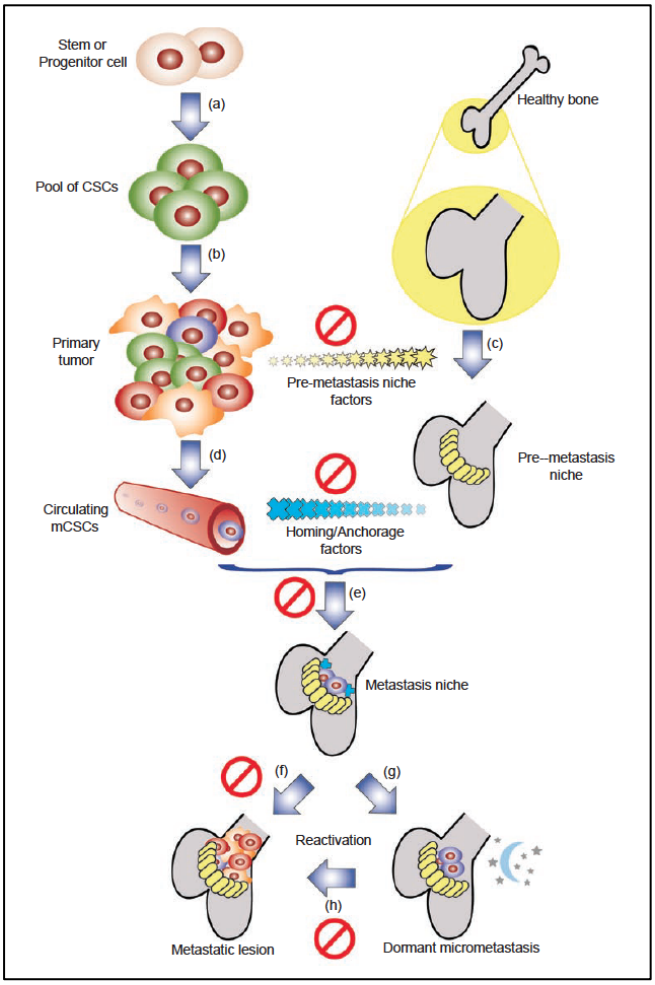

Figure8.5. Model for tissue-specific metastasis. **A-B)** Transformation events lead to the expansion of the CSC pool, with consequent tumor formation. **C)** The secretion of pre-metastastic niche forming factors plays a crucial role in determining the tissue tropism of the future metastatic lesion. **D)** Circulating metastatic CSCs are guided by the homing/prosurvival factors produced by the niche. **E)** After seeding, the local microenvironment will determine whether the metastatic CSC will enter a period of queiscence with consequent reactivation **(G)** or will give rise to an overt macrometastasis **(F)**. [Adapted from Li, et al, 2007].

8.3.2 Metastasis-initiating cells

To date, human metastatic initiating cell (MIC) have not yet been identified, but several lines of evidence indicate that MICs might be found within subpopulations of CSCs.

Specifically, recent reports suggest that MICs might be found within CSC populations: CD44+ breast cancer cells are enriched in metastatic-initiating cells [Malanchi, et al, 2012], and CSCs subpopulation were proposed to give rise to metastasis in pancreatic and colon cancer [Hermann, et al, 2007; Pang, et al, 2010]. However, only a subset of cancer stem cells that possess a specific gene signature and is able to adapt in the foreign environment might be endowed with metastasis-initiating properties.

It has been recently proposed that the ability of a tumor to metastasize is an inherent property of a subset of CSCs, named metastatic CSCs (mCSCs) (**Fig8.5**). This capacity seems to be modulated through the interactions of the mCSCs with the local microenvironment [Li, 2007].

CSCs possess many traits that render them more suitable to initiate metastasis. First of all, CSCs display tumor-initiating capacity, which is mandatory for the establishment of secondary tumors in distant organs. Given the high number of tumor cells present in the circulation, it is feasible that many normal tumor cells seed in a distant site, but they lack the tumor-initiating ability to generate an overt metastasis [Liu, et al, 2007].

Second, CSCs express EMT markers, which suggests that they are able to migrate and which makes them likely candidates for metastasis initiating activities.

The inherent CSCs plasticity makes them more adaptable to a foreign microenvironment, and genetic instability of this subpopulation of

tumor-initiating cells contribute to the increased adaptation. Once in the distant organs, metastatic CSCs can either enter a period of dormancy and then reactivate in presence of specific niche components [Gao, et al, 2012], or can immediately undergo proliferation and generate a metastatic lesion [Aguirre-Ghiso, 2007]. Moreover, CSCs that seed into distant organ might not survive in the new microenvironment, but genetic and epigenetic changes might generate new CSC clones with selective advantages in the new sites [Hermann, et al, 2007]. It has been recently proposed that the CSC clones present in the primary tumor differs from the ones identified at the metastatic sites, and additional driver mutations in primary CSC clones are necessary to generate metastasis-initiating cells [Baccelli, et al, 2012].

CSCs may be necessary to re-initiate the tumor in the new environment, but they might be insufficient to maintain metastatic growth if their progeny cannot survive owing to a lack of organ-specific adaptability [Malanchi, et al, 2012; Chen, et al, 2011].

8.4 Tetraspanin receptor CD37

Tetraspanin are small transmembrane proteins that are expressed in a wide variety of cells and are highly conserved among species [Zoller, 2009]. These molecules interact with several surface proteins, such as other tetraspanin receptor, integrins, CD44 and growth factor receptors. Moreover, they are often found in exosomes and participate to cell-cell communication, an important process during tumor invasion and migration. The specific function of tetraspanins in cancer has not been addressed completely, but it is known that some of these receptors are metastasis-suppressor (CD9, CD82), whereas others promotes metastatic outgrowth (CD151, Tetraspanin-8) [Zoller, 2009; Zijlstra, 2008].

CD37 is a member of the transmembrane 4 superfamily (TM4SF) of tetraspanin proteins, which have four potential membrane-spanning regions [LaPalombella, et al, 2012], and it is expressed in developing B cells from pre-B to peripheral mature B cell stages, but not plasma cells. T cells, monocytes, and natural killer (NK) cells express very low levels of CD37, and it is absent on platelets and erythrocytes [La Palombella, et al, 2012].

Although the precise function of CD37 and its ligand remains unknown, it has been proposed to have a role in signal transduction pathways that affects cell development, activation, and motility [Gartlan, et al, 2013]. Moreover, CD37 is expressed in B cell endosomes and exosomes, reflecting possible involvement in intracellular trafficking or antigen presentation. Recently, it has been shown that CD37 has a unique function as a death receptor in B cells, since its N-terminal domain mediates SHP1-dependent cell death, whereas the C-terminal activates PI3K-mediated survival (**Fig8.6**) [La Palombella, et al, 2012].
Given its B cell-selective expression, CD37 represents a candidate therapeutic target for B cell malignancies, such as chronic lymphocytic leukemia (CLL) [Heider, et al, 2011]. Several peptides, including anti-CD37 SMIP (SMIP-016), have been shown to induce rapid and potent *in vitro* direct tumoricidal activity in lymphoma/leukemia cells. TRU-016, a humanized SMIP-016, is currently in a phase 2 clinical trial for relapsed CLL and small lymphocytic lymphoma (SLL) [Zhang, et al, 2009]. Other CD37 targeted antibodies are currently in early clinical development [La Palombella, et al, 2012; Heider, et al, 2011].

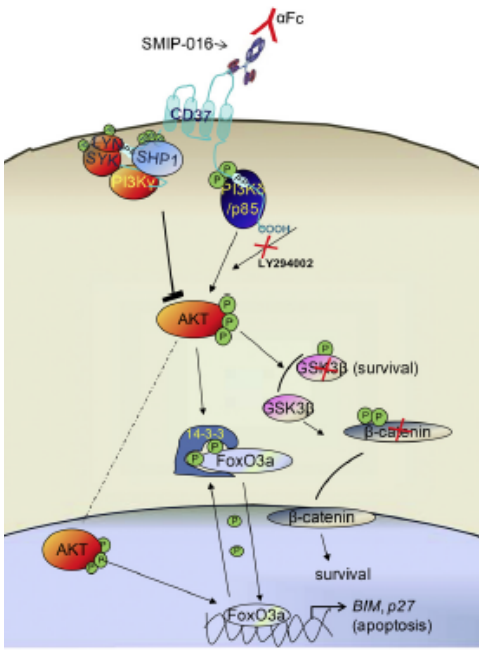

Figure8.6. SMIP-016-induced cytotoxicity. Upon ligation of CD37, two signaling pathways are generated, one acting through phosphorylation of the N-terminal motif of CD37, leads to cell death. A second pathway acts through tyrosine phosphorylation of the C-terminal domain and promotes cell survival [Adapted from La Palombella, et al, 2012].

OBJECTIVES PART 2

9 OBJECTIVES PART 2

The concept of cancer stem cell (CSCs) heterogeneity has emerged recently, and it states that different clones possess different tumor-initiating abilities and coexist in the tumor. Some of these CSC populations might be endowed with the ability to metastasize, whereas others lack of this capacity. Thus, the understanding of cancer stem cells heterogeneity has great clinical significance. This second part of my thesis will focus on two unknown aspects of the behaviour of CSCs: the *in vivo* relevance of CSC cell-cycle heterogeneity, and whether CSCs are the cell of origin of metastasis.
Our aims are the following:

1. To identify a population of slow-cycling, label-retaining cancer stem cells in human skin and oral squamous cell carcinomas using novel xenografts assay.

2. To functionally characterize label-retaining cancer stem cells with respect to their tumor-initiating capacity and response to chemotherapy.

3. To identify a slow-cycling cancer stem cells signature from human squamous cell carcinomas xenografts.

4. To determine whether slow-cycling CSCs display higher metastatic potential *in vivo*.

5. To use surrogate markers of slow-cycling CSCs to isolate and characterize a putative label-retaining population from human sample.

6. To analyse the power of slow-cycling cancer cells markers to predict tumor relapse/metastatic occurrence.

RESULTS PART 2

10 RESULTS SECOND PART

10.1 Results

10.1.1 Experimental strategy

With the purpose to study cancer stem cell heterogeneity and to identify metastasis-initiating cells in human squamous cell carcinoma (SCC), we have developed a novel xenotransplantation system to recapitulate the growth of human SCCs in mouse. This method is based on the skin reconstitution assay that we have previously used in our lab to grow normal human epidermis [Lichti, et al, 2008; Luis, et al, 2012]. We hypothesized that co-transplanting human squamous cell carcinoma cells (of cutaneous and oral origin) would mimic the natural cellular interactions that occur during the development of real human SCCs.

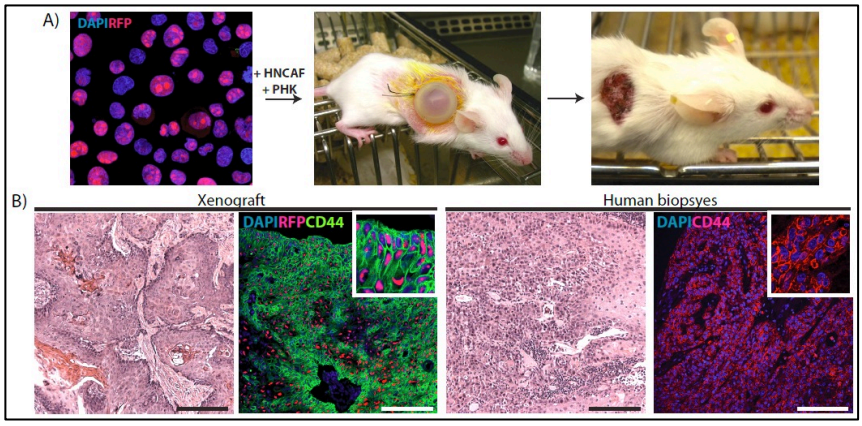

Figure10.1. Experimental strategy used to grow human SCC in immunocompromised mice. **A)** SCC-RFP cells are co-injected with HNCAFs and PHKs in the back of the recipient mice. After removal of the silicon chamber, tumors grow from the skin and invaginate in the surrounding dermis. **B)** Histology and immunofluorescence of the basal stem cell markers CD44 in xenografts and in primary human SCCs. Scale bar: 200 μm.

Cultured SCC cell lines (either SCC13 or SCC25) were infected with a lentiviral vector driving the constitutive expression of a fluorescent tag (RFP, BFP or Luciferase-GFP) to distinguish the transplanted human cells from the mouse host cells after transplantation. These cells were transplanted in combination with tumor associated fibroblasts (HNCAFs) and primary human keratinocytes (PHKs) in the back of immune-compromised mice using a silicon chambers (see Materials and Methods). The orthotopically-transplanted mice develop SCC tumors that are histologically very similar to those of patients, since they invaginate and extensively migrate into the stroma (**Fig10.1A-B**), as opposed to the encapsulated tumors that grow when SCC cells are injected subcutaneously.

10.1.2 Identification of slow-cycling cancer cells

As mentioned above, the aim of this project is to study CSC cell-cycle heterogeneity, and identify the population responsible for generating metastasis in human SCCs *in vivo*.

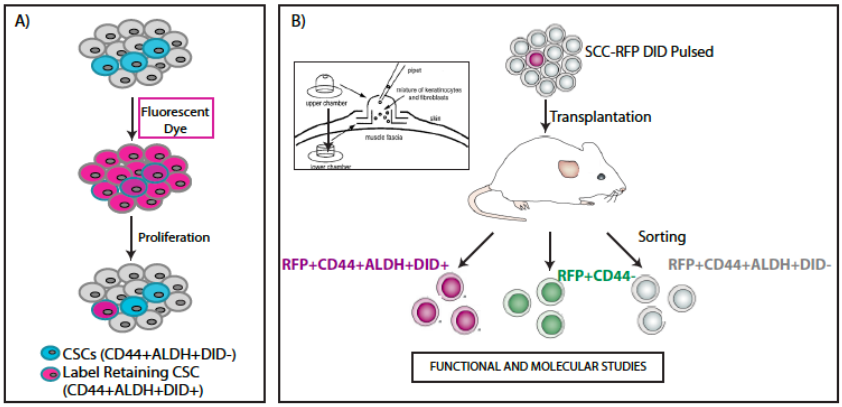

Figure10.2. Strategy used to characterize slow-cycling and active CSCs from human SCC. **A)** Label-retaining method to mark slow-cycling cells. **B)** Scheme of the *in vivo* strategy used to purify slow-cycling CSCs.

To test whether slow-cycling and proliferative CSCs co-exist *in vivo* we used a label-retaining technique based on hydrophobic fluorescent dyes (**Fig10.2**). These dyes bind to cell membranes, are non-toxic and do not leak between cells (data not shown), are very stable, and are only diluted upon cell division [Li, et al, 2008]. Using squamous cell carcinoma lines SCC13 or SCC25, we observed that the dye is no longer detectable by FACS or confocal microscopy after 8-10 cellular divisions (**Fig10.3A-B**). Label-retaining cancer cells are detected inside the CD44+ population in 3D-spheres. These cells are no proliferative (they stain negative for Ki67) and are undifferentiated (**Fig10.3C**).

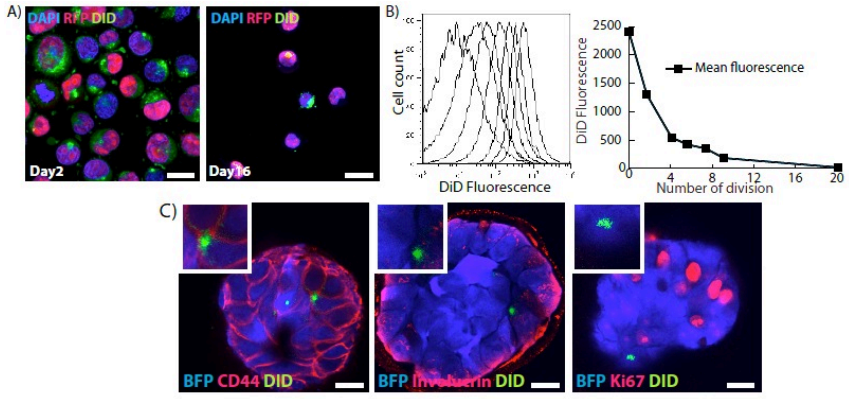

Figure10.3. **A)** SCC-RFP cells are pulsed with DID and grown in 2D for 16 days. Whereas all the cells are homogenously labelled after the pulse, DID is retained only in not proliferative cells after division. **B)** FACS analysis of cultured SCC cell lines showing the kinetic of dilution of the fluorescent DID *in vitro*. DID is no longer detected after 10-12 cell divisions. **C)** SCC-BFP cells were cultured at limited dilution in 3D-matrigel, and full-grown spheres were stained to detect DID direct fluorescence (in green), CD44 (red, left panel), Involucrin (red, middle panel) and Ki67 staining (in red, right panel). Scale bar: 25 μm.

Previous studies have shown that human squamous cell carcinoma CSCs can be purified on the basis of their high expression of CD44 and

high activity of aldehyde dehydrogenase 1a (ALDH). Interestingly, when we pulsed the SCC lines with the dye and orthotopically-transplanted them into SCID mice (**Fig10.2B**), we could detect by FACS analysis a population of CD44+ALDH+ cells that have retained the label in tumors grown for approximately 2-3 months (**Fig10.4A**). Thus, we can subdivide the CSC population into CD44+ALDH+DID- (proliferative), and CD44+ALDH+DID+ cells (slow-cycling/quiescent), hereafter referred as DID+ and DID- cells. DID+ cancer cells can be detected by direct fluorescence in histological sections (**Fig10.4B**).

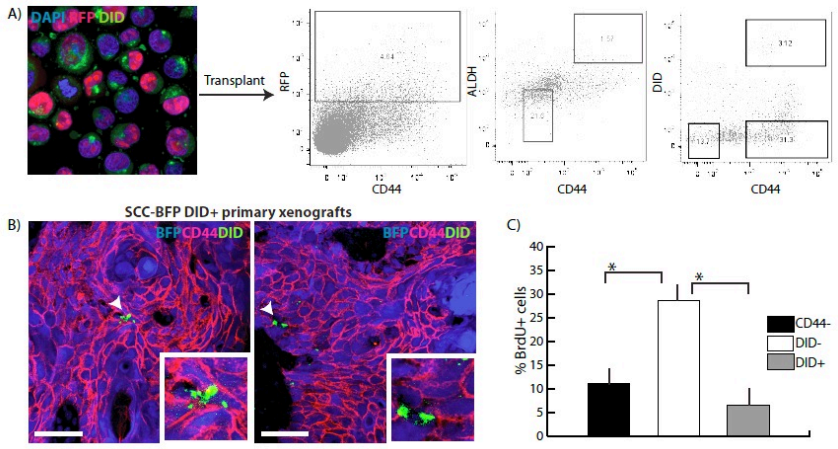

Figure10.4. **A)** SCC13-RFP or SCC25-RFP cells are pulsed with DID and orthotopically transplanted. FACS analysis of the full-grown tumors shows that RFP+ cancer cells contain a CD44+ALDH+ CSCs population that can be further subdivided in DID+ and DID- cells, depending on their different label-retention. **B)** Immunofluorescence of SCC13-BFP or SCC25-BFP xenografts shows the existence of rare DID+ label-retaining cancer cells found in the CD44+ area. Scale bar: 100 μm. **C)** Transplanted mice were injected with BrdU for 72h before collecting the tumors to mark cells actively replicating their DNA. FACS analysis of BrdU incorporation in CD44+DID+, CD44+DID- and CD44- cells shows that label-retaining cancer cells are less proliferative than their active counterpart. (Data are shown as average +/- S.E.M. P*<0.05, N=4 pools, 6 mice per pool).

DID- cells are much more abundant that DID+ cells, the former constituting a 1-5% of the tumor, whereas the latter represent a 3-5% of the CD44+ALDH+ population (approx. 100 cells/1cm^3 tumors). That is, 95% of all CD44+ALDH+ cells are proliferative, whereas 5% are label-retaining. Administration of pulses of BrdU to the mice 72 hours prior tumors collection confirmed that in average 50-80% of CD44-DID- cells are proliferative, whereas only 10-20% of CD44+DID+ have undergone DNA synthesis (**Fig10.4C**)

10.1.3 Tumor initiating-capacity of LRCs and active CSCs

Although serial orthotopic transplantation is the best method to study functional properties of CSCs, non-adherent sphere assays are increasingly being used to evaluate stem cell activity of putative CSCs *in vitro*. Thus, we analysed the sphere-forming potential of the different population of CSCs sorted from primary xenografts,

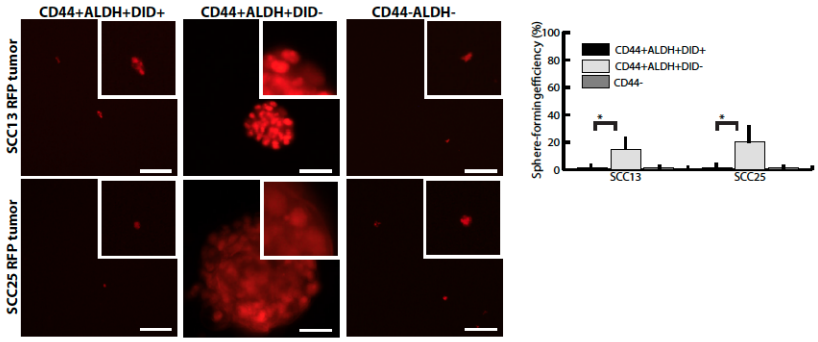

Figure10.5. RFP+CD44+DID+, RFP+CD44+DID- and CD44- cells were sorted from SCC13-RFP or SCC25-RFP primary tumors and seeded in matrigel. Active CSCs are able to grow as spheres in these conditions, whereas CD44+ALDH+DID+ and CD44- cancer cells divide a few times and give rise to abortive colonies. Sphere-forming efficiency is reported in the right chart (N=4, $P_{SCC13}<0.02$; $P_{SCC25}<0.01$, data are presented as average +S.E.M, n=3).

Equal numbers of active (DID-), slow-cycling (DID+) CSCs and bulk CD44- tumor cells were sorted from 2-3 month-old SCC xenografts and immediately plated in 3D-matrigel in sphere-forming conditions. Unexpectedly, whereas CD44+ALDH+DID- cells grew as spheroids (despite the low efficiency), their label-retaining counterpart failed to give rise to spheres (**Fig10.5**).

To better evaluate the biological significance of slow-cycling CSCs *in vivo*, we tested their tumor-initiating ability following serial transplantation. Equal number of CD44+ALDH+DID+, CD44+ALDH+DID- and RFP+CD44-ALDH- cells (non-tumorigenic control) were sorted from primary xenografts, mixed with tumor associated fibroblasts and matrigel, and subcutaneously injected in recipient mice (**Fig10.6A**). Due to the small percentage of slow-cycling RFP+CD44+ALDH+DID+ cells in the primary tumors, only 600-1000 cells can be isolated from each pool of mice and serially re-transplanted, posing some limits to the functional assay.
We could detect tumor development after injection of 800 active DID- CSCs with a latency of around 3 months, but the same number of slow-cycling DID+ CSCs failed to generate tumors in 88% of the cases. None of the mice transplanted with CD44- cells had developed subcutaneous SCCs (**Fig10.6B**), in agreement with what has been previously published [Prince, et al, 2007]. Notably, as few as 150 CD44+ALDH+DID- cells were able to give rise to secondary and tertiary tumors when serially re-transplanted. Tumors originated with serial transplants with DID- cells contained DID+ and DID- cells, as well as CD44- bulk tumor cells (**Fig10.6C**), indicating that DID- cells behave as *bona fide* CSCs. The ability of CD44+ALDH+DID- CSCs to give rise to CD44+ALDH+DID+ cancer cells in secondary transplants

suggests that the DID- cells are hierarchically positioned on top of the LRC population.

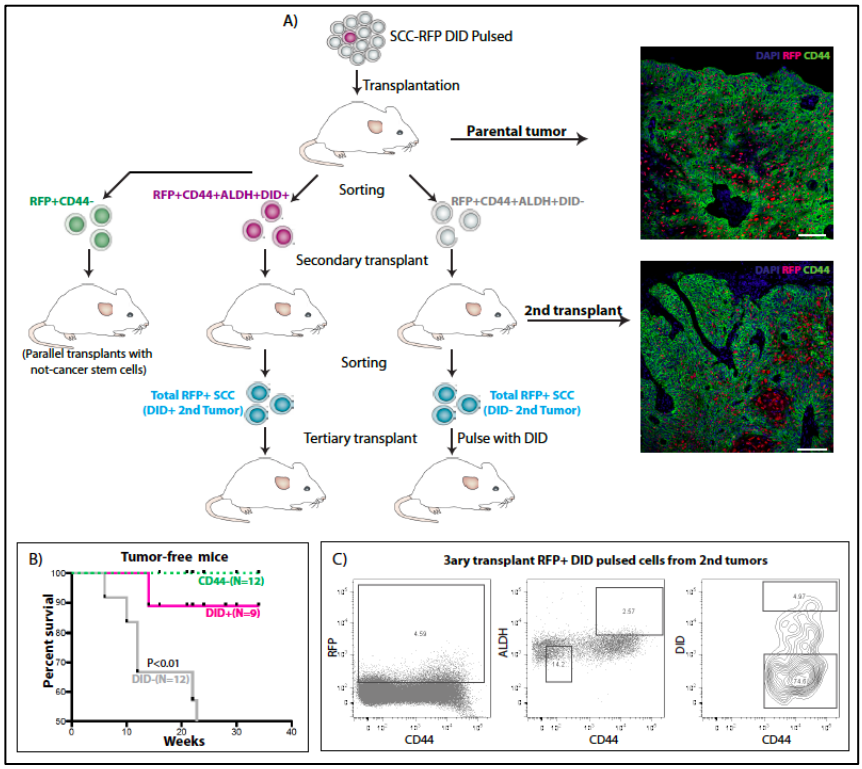

Figure10.6. A) SCC13-RFP or SCC25-RFP were pulsed with DID and orthotopically transplanted. Once full-grown tumors appeared, CD44+ALDH+DID+, CD44+ALDH+DID- and CD44- cells were sorted from primary xenografts and injected subcutaneously. Bulk tumor cells from secondary transplants were sorted depending on RFP fluorescence, pulsed with DID and re-transplanted. The morphology of the tumors and the expression of CD44 are unchanged in the primary and in the secondary xenografts. Scale bar: 100 μm. **B)** Kaplan-Meyer curve reporting tumor free survival of mice serially transplanted with the different subpopulation (N=9-12, $P^{**}_{DID+/DID-}<0.01$, $P^{**}_{CD44+/CD44-}<0.01$). **C)** Total RFP+ cells from the secondary transplants are pulsed with DID before injection in the recipient mice. As shown in the FACS plot, tumors generated with DID- active CSCs are able to give rise to slow-cycling DID+ CSCs.

10.1.4 Chemotherapy response in dormant versus active CSCs

It has been recently reported that slow-cycling CSCs that reside in the primary tumor can display increased resistance to chemotherapy, and might therefore constitute the tumor population responsible of cancer relapse [Pang, et al, 2010; Pece, et al, 2010]. We therefore tested whether tumor LRCs and proliferative CSCs display different sensitivity to front-line chemotherapeutic agents used for the treatment of patients with aggressive forms of SCC. One of the most commonly used drugs for human SCC is Cisplatin, together with 5-FU and Doxorubicin [Price, et al, 2012]. Transplanted mice were treated with Cisplatin and the percentage of early and late apoptotic cells was analysed by FACS using AnnexinV and DAPI. In contrast to what has been previously reported, tumor LRCs were more sensitive to these chemotherapeutic agents than the proliferative CSCs (**Fig10.7**).

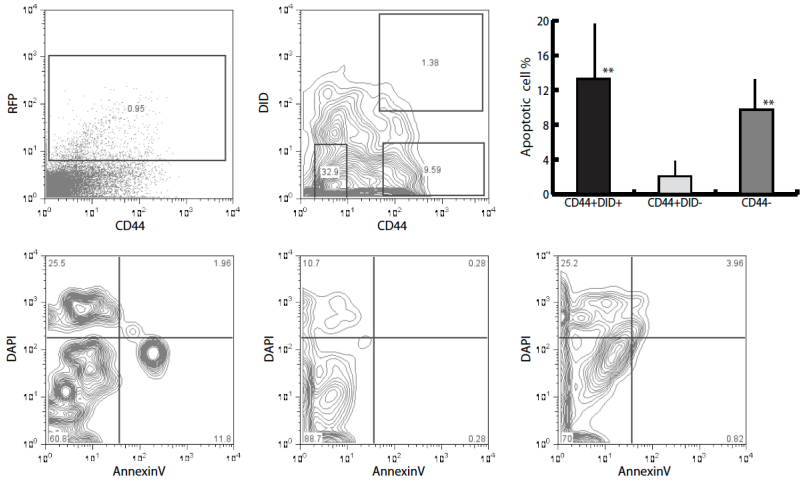

Figure10.7. SCID mice were transplanted with SCC-RFP DID-pulsed cells and Cisplatin was administered for 4 days before collecting the tumors. Percentages of apoptotic cells were analyzed by FACS in the different tumor populations using AnnexinV and DAPI. CD44+DID+ cells have a higher apoptotic index that the DID- counterparts. DID- were also more resistant to Cisplatin-induced cell death than CD44- cells (n=4 pool of 5 mice; $P_{DID+/DID-}$ <0.05; $P_{CD44+DID+/CD44-}$<0.01, data are presented as average +S.E.M.).

Notably, CD44+ALDH+DID- cells were the most resistant to Cisplatin-mediated cell death compared to DID+ and CD44- cells, indicating that these treatments result in overall tumor shrinkage but increase the relative percentage of CSCs. The high resistance of the CD44+ALDH+DID- population to Cisplatin might be explained with the fact that this population overexpress many genes involved in the DNA damage response (DDR, as shown in **Paragraph 10.1.5**). Indeed it is known that Cisplatin initially induces the activation of such DDR, causing cell death. The same results were observed after 5-FU treatment (data not shown).

10.1.5 Transcriptome analysis of Label-retaining cancer cells

These intriguing results prompted us to characterize molecularly DID+ and DID- cells, to better understand their biological significance *in vivo*. To this end, we isolated DID+, DID- and CD44- cells from primary tumors generated from SCC13 and SCC25 cells, and compared their transcriptome by microarrays (The full list of gene differentially expressed is reported in **Supplementary File1** and **File2**). We used a new method recently developed at the Institute for Biomedical Research in Barcelona (IRB) that allows obtaining microarray data from RNA isolated from as few as 100 cells [Gonzalez-Roca, et al, 2010]. This technology is being crucial for our studies, since in average we can isolate at most 100 DID+ cells from $1cm^3$ tumors. By performing gene expression analysis in parallel with tumors originated from two different cell lines we obtained a more consistent signature that could be used to predict CSCs genes also in other kind of SCC, and we eliminated differences that might be cell-line specific.

Several conclusions can be extracted from this data. First, unsupervised clustering indicates that DID+ and DID- cells share a common transcriptome compared to CD44- cells, yet DID+ cells express a unique set of genes compared to DID- cells (**Fig10.8**). Second, Gene Ontology (GO) analysis indicates that active CSCs are primarily proliferative, evade the immune system, and are drug resistant. They are recognized as being of keratinocyte origin, and classified as "aggressive squamous cell carcinomas".

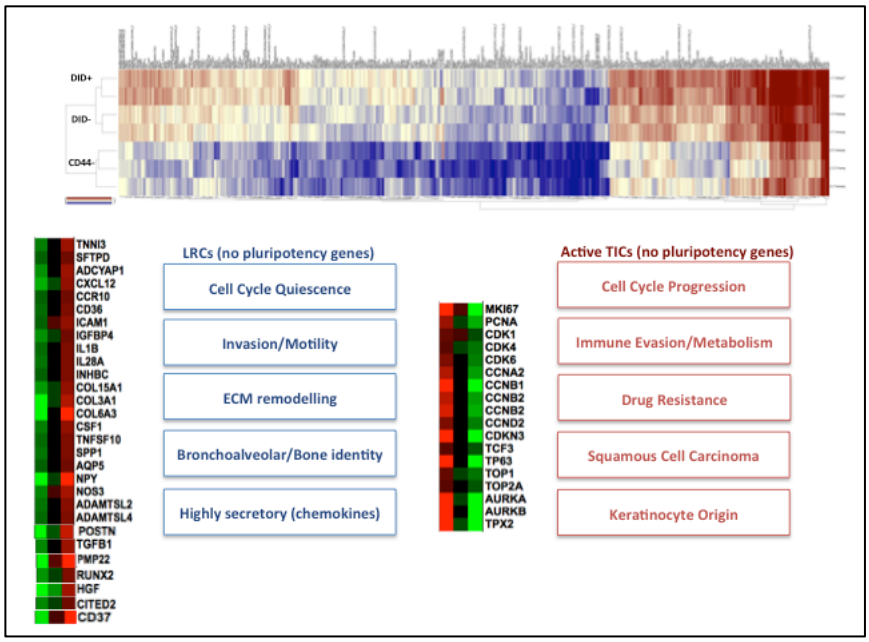

Figure10.8. Heat-map showing genes differentially expressed in CD44+ALDH+DID+ and CD44+ALDH+DID- cells sorted from primary SCC xenografts. CD44- cells were also analysed as a control of not-CSCs. DID+ and DID- cells share a common signature, but each express a unique set of transcripts. Categories of genes more represented in slow-cycling and active cancer stem cells are reported in the bottom panel.

In contrast, GO analysis of the transcriptome of DID+ cells indicates that they are non-proliferative, and express a large number of cytokines as well as genes conferring motility and invasiveness. Intriguingly, they

are no longer identified as ¨keratinocytes¨ or ¨squamous cell carcinoma¨ but rather as bone-, lung- (bronchoalveolar) and pericyte-like cells (**Fig10.8**). For instance, SCC LRCs display a signature similar to breast cancer cells that metastasize to the bone and lungs, and many genes overexpressed in DID+ CSCs are involved in bone remodelling and were previously associated with bone metastasis, such as CTSK and Runx2 [Akech, et al, 2010; Weilbaecher, et al, 2011; Guise, et al, 2006; Kang, et al, 2003, Pratap, et al, 2006; Yee, 2011], suggesting that they might be prone to colonize these organs.

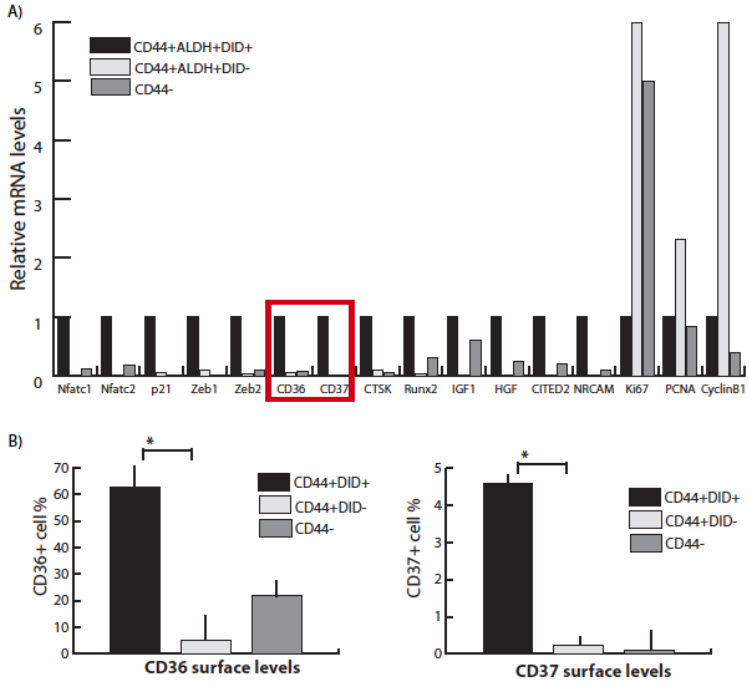

Figure10.9. **A)** Representative RT-qPCR analysis of genes found differentially expressed by microarray in CD44+ALDH+DID+ and DID- CSCs and CD44- not cancer stem cells sorted from SCC25-RFP+ xenografts. Similar results are obtained with cDNA from SCC13-RFP tumors. **B)** CD36 and CD37 surface levels were analyzed by FACS in SCC25-RFP and SCC13-RFP xenografts. As suggested by the transcriptome analysis, CD36 and CD37 were highly expressed in Label-retaining cancer stem cells. (N=4 pool of 3 mice each. $P_{DID+/DID-}$*<0.01, data are presented as average +S.E.M.).

Other genes involved in bone identity were osteopontin (SPP1), CXCL12, IL1B, Colony stimulating factor-1 (CSF1), TGFβ1, HGF, and TNFSF10. In addition, DID+ cells expressed high levels of ADCYAP1, Surfactant proteins (SFTPD), NPY, TNNI3, AQP5 and NOS3, all of which are associated with a broncho-alveolar identity.

DID+ cells also expressed several cell surface markers not expressed in DID- cells that could be used as their surrogate markers in primary human SCC samples. Among the genes differentially expressed in the 3 populations, we selected several to validate by qPCR and by protein levels (**Fig10.9A-B)**.

Surface markers specifically expressed in this slow-cycling population include CD177, a marker associated with bone marrow homed neuroblastoma cells [Morandi, et al, 2012] CD248 (also known as Endosyalin), which is enriched in pericytes and its expression highly associated with lymph-node metastasis of breast cancer cells, and CD274 (also known as PDL1) which is involved in immune evasion of cancer cells [Aerts, et al, 2013]. In addition, DID+ cells express very high levels of CD36, the thrombospondin receptor, that was previously associated with reduced proliferation and increased invasion [Firlej, et al, 2011], and CD37, a membrane receptor with pro-survival and pro-apoptotic functions in B-cell (as referred in **Section8.4**), for which monoclonal blocking antibodies are available [Heider, et al, 2011; Lapalombella, et al, 2012]. We could validate by FACS analysis from xenotransplanted tumors that CD44+DID+ cells are enriched for both CD37 and CD36, whereas only a negligible fraction of CD44+DID- cells is positive for these markers (**Fig10.9A-B**).

10.1.6 Putative label-retaining cells in primary human SCC

After characterization of the Label-retaining CSC population using a novel SCC xenografts system, we aimed at determining whether this population is detectable and presents the same functional and molecular traits in primary human SCCs.

To do so, we used CD36 and CD37 that we had previously validated as surrogate markers of DID+ cells in tumor xenografts. Thus we analysed by FACS whether a subset of the CD44+Lineage- population in primary human SCCs (both of cutaneous and oral origin) contained cells that expressed CD36 and CD37. Interestingly, we could detect 4 populations: a majority of CD36-CD37-cells, a small CD36+CD37+ population, CD36+CD37- cells and CD36-CD37+ cells (**Fig10.10A**). We could also visualize these populations by immunofluorescence staining of paraffin sections of oral and cutaneous SCC tumors (**Fig10.10B**). In this analysis we also included Runx2 (**Fig10.10B**).

At the moment we are sorting these four populations directly from human tumor biopsies to obtain gene expression analysis through microarrays. These studies will allow us to identify the common signature of CD36/CD37+ primary tumor cells with the one we identified in label-retaining cells in our xenograft models. These studies will also allow us to determine whether the presence of CD37+ cells, or their percentage, is predictive of the propensity of the patients analyzed to develop metastasis (in the case or oral SCCs, patients typically develop metastasis 7-12 months after the appearance and resection of the primary tumor).

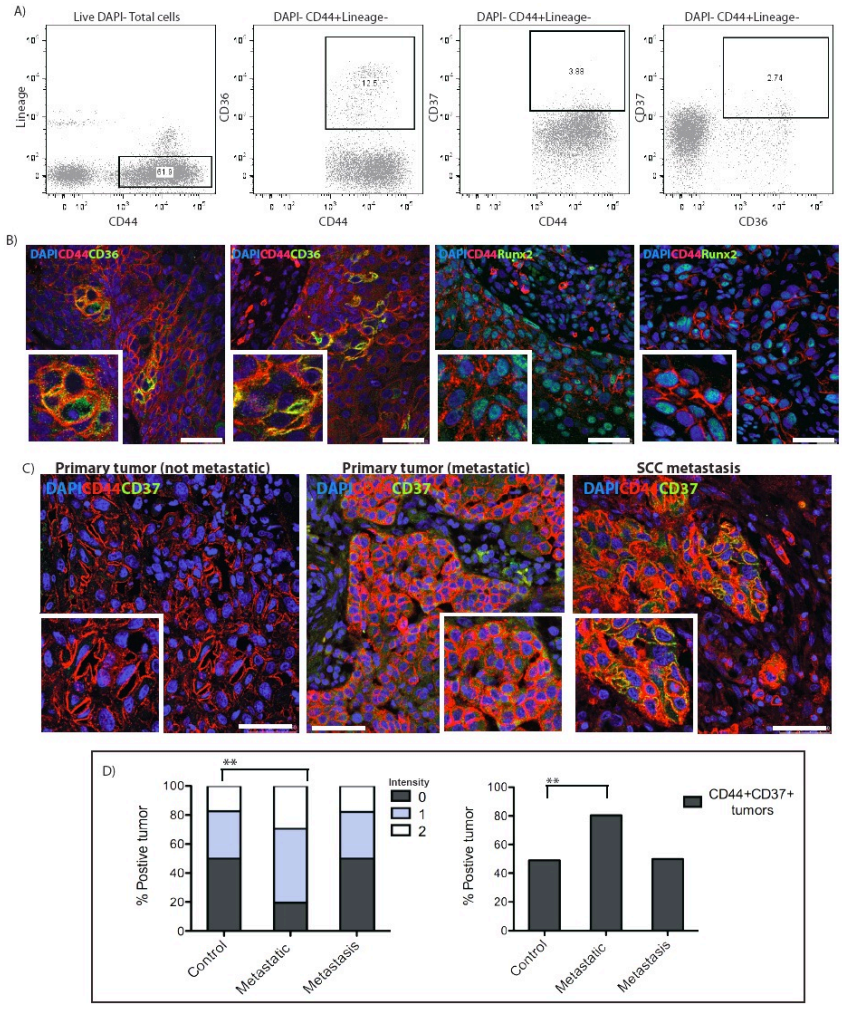

Figure10.10. **A)** Representative FACS analysis of CD36 and CD37 in the CD44+Lineage- cancer cell of primary human SCC. **B)** Immunofluorescence of CD44, CD36 (left, green fluorescence) and Runx2 (right, green fluorescence) in cutaneous and oral primary SCCs. **C)** Representative images showing CD44 and CD37 expression in not-metastatic and metastatic SCCs, as well as in their relative metastasis. D) TMA of a cohort of 96 cutaneous SCC patients shows a significant correlation between the percentage of CD44+CD37+ cancer cells and metastatic occurrence (N=96, P**<0.05). Scale bar=50μm.

However, since we could detect the expression of CD44/CD37+ cells in paraffin sections of human SCCs, we are studying the presence and

percentages of this population in tissue microarrays (TMAs; these have been generated in collaboration with the Hospital del Mar and Hospital Vall D´Hebron in Barcelona) containing a large cohort of tumor samples from patients with cutaneous, oral or penis SCC (**Fig10.10B-C**; only cutaneous TMA results are shown. The analysis of oral and penis SCC are being performed). Since we have all the clinical data from these patients, these studies are allowing us to determine whether the presence and/or % of CD44/CD37+ cells correlates with any clinical parameter, including metastasis.

The cutaneous SCC TMA (Hospital del Mar) contain samples of primary tumors from 120 patients, with 50% of patients not developing and 50% of patients developing metastasis (for these the TMA also include sections of their lymph-node metastasis). Notably, the results of these TMAs show that the presence of CD44+CD37+ cells in the primary cutaneous SCCs highly correlates with the propensity of these tumors to form metastasis. More specifically, approximately 80% of the patients whose primary tumor contained CD44/CD37+ cells developed metastasis, whereas 80% of those whose primary tumor did not contain CD44/CD37+ cells, never showed any metastatic spread (**Fig10.10B-C)**. Of note, primary tumors that metastasized and their corresponding metastasis did not show a statistically significant difference in the % of CD37+ cells, or the intensity of CD37 expression, indicating that these cells are not enriched in the tumors that grow at distant sites (not shown). Thus, these exciting results suggest that the presence of CD44/CD37+ cells could be used in the future as a prognostic factor for metastasis. As mentioned above, we are extending this analysis with a large cohort of oral (120 patients) and penis (80 patients) SCCs.

10.1.7 Metastatic potential of Label-retaining CSCs

Our results suggest that CD44+ALDH+CD37+ cells might be cells already present in the primary tumor that are poised to metastasize to distant organs. The unique slow-cycling CSC signature that we have discovered suggests that this population might be able to recognize the lung and bone (and perhaps lymph-nodes) as self, and therefore survive there. However, there are several possibilities regarding their mode of action: (i) first, they might reach the distant sites and revert to a proliferative state; (ii) they might reach the distant sites and secret chemo-attractant and pro-survival factors towards proliferative CSCs (as a reminder, the transcriptome of CD37+ cells indicates that they produce a large number of cytokines); and (iii), third, proliferative CSCs reach the distant site, they generate CD37+ cells that support their growth in these foreign environments.

To address these questions, we decided to use imaging technology based on firefly luciferase to localize metastatic cancer cells in our xenografts. To this purpose we infected cultured SCC cell lines with the retroviral vector pLuc-GFP-Neo [Zuber, et al, 2009], that was previously reported as one of the most sensitive to detect few number of cells clustered together in a micro-metastasis (although reported to detect as few as 100 cells, the detection limit *in vivo* in our setting is 10.000 cells). SCCpLUC-GFP SCC cell were pulsed with DID and immediately transplanted as described. Primary xenografts were used for sorting of tumor LRCs (pLucGFP+CD44+DID+) and active (pLucGFP+CD44+DID-) CSCs, as well as CD44- bulk tumor cells, and these populations were then assayed for their ability to colonize the lung and the bone. Equal numbers of sorted cells were therefore injected in the tail vein or in the femur of recipient mice, and metastatic occurrence

was monitored weekly by bioluminescence assay up to one year after injection (**Fig10.11**). These mice have been transplanted and we are currently waiting for the results of these experiments. We will therefore be able to accurately determine which tumor subpopulation (DID+ or DID-) is capable of homing into the lung and the bone. In addition, if DID- cells can generate metastasis, we will be able to determine if co-transplanting them with DID+ cells enhances their metastatic potential (i.e. DID+ cells generate a pro-metastatic supportive niche for DID- cells). However, since the number of DID+ cells we can sort from tumors is quite low, these assays might not be informative due to the very low cell survival observed when less than 1000 cells are injected intravenously or into the femur.

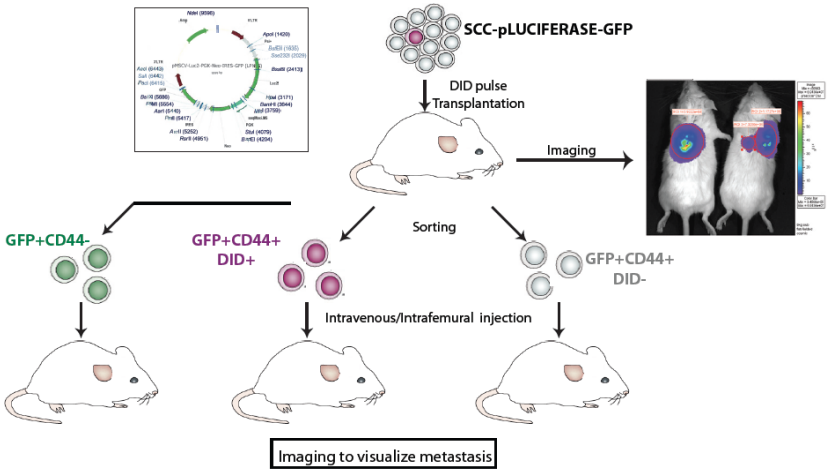

Figure10.11. SCC cell lines are infected with pLUC-GFP vector (left upper inset) to achieve expression of the dual Luciferase-GFP cassette. Cells are pulsed with DID and transplanted as described. Primary tumors are imaged with the IVIS system and used for sorting of the slow-cycling and active CSCs. Equal numbers of cells are directly injected in the femur or in the tail vein of recipient mice to test their ability to metastasize.

10.1.8 Functions of CD37 in SCC metastatic growth

To circumvent the probable problems regarding the low number of cells we can use for the metastatic assays, we have decided to perform in parallel a different approach to determine the putative pro-metastatic activity of CD37+ SCC cells. So far, we have used CD37 as a surrogate marker of LRC cells in human SCC. However, CD37 is highly expressed in Chronic Lymphocytic Leukemia (CLL) cells, and monoclonal blocking antibodies targeting CD37 are now in clinical trial for treating patients with recurrent CLL which has become refractory to anti-CD20 treatment [Zhao, et al, 2007; Heider, et al, 2011]. These antibodies specifically induce a Natural Killer-dependent antibody dependent cell death (ADCC) when coupled to a CD37-expressing cell [Zhao, et al, 2007; Heider, et al, 2011]. Since CD37+ cells are the only ones within the tumor that express this marker, we surmised that if targeting them affects the metastatic potential of SCC tumor cells then they must be pro-metastatic. We are using three approaches to target CD37+ cells via CD37: (i) knockdown of CD37 in SCC cell lines; and (ii) a lentiviral mediated suicide strategy.

For the first strategy, we have knocked-down SCC25-pLucGFP using a lentiviral expressing an shRNA targeting CD37 and have inoculated these cells through intravenous and intrafemural injections. We are monitoring metastatic occurrence in the lung and in the bone weekly by Bioluminescence to seek for differences between the controls versus the knock-down cells (**Fig10.12A**). These experiments are ongoing. In parallel, SCC25pLUCGFP are infected with the pMSCV-empty or with the pMSCV-CD37 vector to analyse the effect of CD37 overexpression during the process of metastatic development (**Fig10.12A**).

For the second strategy, we have cloned a 3Kb fragment of the human CD37 promoter (spanning from -3000bp to the +1 position, including the 5-UTR region) upstream of the cDNA encoding for and inducible iCaspase9 cassette (**Fig10.12B**). iCaspase9 is an engineered constitutively active Caspase9 fused to a human FK506 binding protein (FKBP) to allow conditional dimerization using a small molecule pharmaceutical [Straathof, et al, 2005]. A single dose of synthetic dimerizer drug induces apoptosis in 99% of transduced cells selected for high transgene expression *in vitro* and *in vivo*. SCC25pLUCGFP CD37-iCaspase9 will be inoculated in the tail vein or in the femur of recipient mice, and the inducer of dimerization (CID) will be injected i.p. to induce cell death in the engineered cells. Mice will be then monitored weekly by Bioluminescence to assess the effect of the selective killing on metastatic growth (**Fig10.12B**).

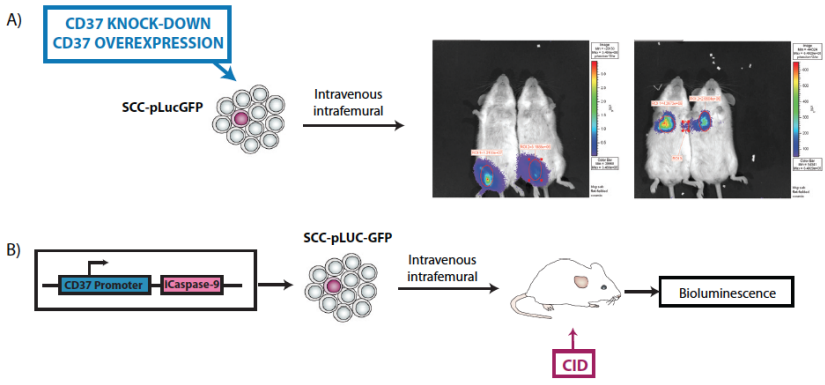

Figure10.12. A) SCCpLucGFP cell lines are infected with vectors to achieve efficient knock-down or over-expression of CD37, and infected cells are injected in the femur or in the tail vein of recipient mice to analyse different metastatic potential in presence/absence of CD37. B) The inducible-Caspase9 cassette is cloned under the promoter of CD37, thus to obtain its expression only in CD37-expressing cells. SCC25pLucGFP are infected with this vector and injected in the tail vein or in the femur of immune-compromised mice. After injection, mice are treated with the inducer of dimerization CID (resulting in Caspase9 activation) and metastatic outgrowth is monitored over the time.

DISCUSSION PART 2

11 DISCUSSION PART 2

11.1 Discussion

In this second part of my PhD we proposed to study the relevance of human cutaneous and oral SCC cancer stem cell heterogeneity, and to identify and characterize the population of cells responsible for initiating or promoting metastasis *in vivo*. In particular, we were able to show that CSCs from human SCCs are heterogeneous regarding their cycling property *in vivo*, and we could identify a small population of slow-cycling cancer stem cells with a label-retaining technique. By gene expression analysis of label-retaining cancer stem cells we could identify a set of genes preferentially expressed by this population that are associated with a bone- and lung-like identity. Furthermore, we have identified surface markers that can be used as predictors of metastatic occurrence in human SCCs.

11.1.1 Slow-cycling cancer stem cells in human SCCs

Regarding CSC cell-cycle heterogeneity, recent evidence in breast and prostate carcinomas and in melanomas grown in culture suggest that tumors might contain co-existing subsets of actively proliferating and slow-cycling CSCs [Roesch, et al, 2010; Qin, et al, 2012; Pece, et al, 2010]. In these studies, the authors have elegantly shown that slow-cycling cancer cells are a more aggressive CSCs population that is resistant to conventional chemotherapy, which is normally targeting actively proliferating cells. However, these studies have been performed with tumor cells grown in 3D as spheres, or in 2D cultures, and therefore the *in vivo* significance of tumor LRCs in these cancer models has not been confirmed yet.

By means of a novel transplantation system combined with the use of a label-retaining method, we could study cell-cycle heterogeneity in human SCC *in vivo*, and we were able to identify and isolate a slow-cycling population inside the cancer stem cell subset. Our results suggests that slow-cycling cancer stem cells might be a population with specific functional properties that can be found in all the kind of solid cancer.

However, our functional studies suggest that Label-retaining cancer cells in human SCCs display different properties compared to breast, prostate, and melanoma tumor LRCs. Whereas in the previously published work the quiescent cancer stem cells are highly tumorigenic, in our experimental setting LRCs fail to efficiently give rise to tumor growth when serially transplanted. This difference can be due to several reasons. First, in the previous studies the slow-cycling and active CSCs populations were isolated from cancer cells grown *in vitro* as spheroids, and not from xenografts, thus, tumor LRCs isolated from cells in culture might constitute a different population of tumor LRCs isolated directly from tumors. Second, the small number of quiescent CSCs that we are able to isolate from engrafted SCCs is very small (only 100 cells for each tumor), thus the injection of these cells might result in their cell death, whereas their active counterpart might have been selected to survive in a foreign environment. However, the fact that as few as 150 active CSCs can give rise to tumors when serially transplanted indicates that small number of tumor cells are capable of surviving such harsh experimental conditions.

Another difference between the tumor LRCs we have identified compared to those in breast cancer is their different response to front-

line chemotherapy. Pece and coworkers reported that quiescent cancer stem cells in breast cancer are resistant to chemotherapy, whereas we observed a higher apoptotic index in slow-cycling cancer cells from SCCs than in active CSCs. Of note, the transcriptome signature of DID+ and DID- cells indicates that the latter expresses many genes involved in the DNA damage response (DDR), the typical response the cells have to Cisplatin treatment. That said, although approximately 50% of tumor LRCs undergoes apoptosis upon cisplatin or 5-FU treatment, the remaining cells that survive after Cisplatin administration might indeed be responsible for tumor re-growth. This last hypothesis is difficult to test since DID+ cells become undetectable after some months, but future lineage-tracing experiments to mark LRCs might help us in clarifying this point.

11.1.2 Gene expression signature of LRC cancer cells

Gene expression profiling of DID+ and DID- cancer cells isolated from engrafted SCCs have shown that slow-cycling tumor LRCs are enriched for many genes that are normally associated with metastatic disease and display a strong bone and lung identity. Conversely, DID- CSCs are identified as cells of keratinocytes lineage with aggressive squamous cell carcinoma traits, and display over-representation of genes related with cell-cycle progression, DDR, and immune evasion. Among the genes exclusively expressed in LRC cancer cells we were particularly interested in some previously linked with bone and lung identity, since their expression might render them more prone to survive in these different environments during the metastatic process. In particular, we decided to focus on CTSK and Runx2, previously linked with the propensity of breast and prostate cancers to form bone metastatic

lesions [Pratap, et al, 2010; le Gall, et al, 2007]. We hypothesize that the expression of these genes in LRCs cancer cells might promote the colonization of the bone, thus the selective target of these molecules could be used in the clinic. Of note, CTSK inhibitors are now being used for the treatment of patients with osteoporosis, and are commercially available [Stoch, et al, 2012]. Other genes expressed in DID+ cancer stem cells that are linked with metastatic occurrence and can favour the survival of this population in distant organs are Surfactant Protein D and C and NPY (lung identity), osteopontin, IL1B, POSTN, CSF1 and IGF1 (bone/lung metastasis). Thus, this signature suggests that primary SCC tumors already contain a population of cells (i.e. DID+) that might be primed for metastatic colonization, opening the possibility that their detection and targeting could be of prognostic and therapeutic value.

11.1.3 The metastasis-initiating cells hypothesis

The results obtained so far suggest that CD44+ALDH+DID+ Label-retaining cells might be primed to survive in the bone and lung, two major sites of SCC metastasis. Specifically we are testing several hypotheses:

- Label-retaining cancer cells (DID+) secrete factors supporting the growth and promoting invasion of DID- active CSCs.

- The lung and bone signature of DID+ cells allows them to home and survive in these tissues where they generate a supportive niche for proliferative CSCs (DID-).

- DID- cells reach the lung and bone and either upon division they generate DID+ cells that support their growth, or by being in contact with DID+ cells in the primary tumor they have been already ¨educated¨ to survive in these distant sites.

- DID+ cells reach the metastatic sites where they convert into DID- cells. This hypothesis is based on studies showing that SCC cells can reversibly transit in culture between an epithelial, proliferative state, and a mesenchymal state.

11.1.4 Selective targeting of LRC cancer cells in vivo

The results obtained from the transcriptome analysis of DID+ and DID- CSCs suggest that slow-cycling cancer cells might be metastasis-initiating cells (MICs), thus it become paramount to find a strategy to test this hypothesis. For this reason, we decided to take advantage of the unique expression of some surface molecule in DID+ cells.

CD37 is a tetraspanin membrane receptor that satisfies all our requirements: it is uniquely expressed by tumor LRCs in xenografts and in primary as well as metastatic SCC tumor samples, it is interestingly not expressed *in vitro* in cultured SCCs (thus it is probably important for the cross-talk between the tumor and its microenvironment), and it can be detected by FACS and immunofluorescence. Importantly, it can be targeted by a monoclonal antibody now in Phase II clinical trial for the treatment of Burkitt lymphomas and Chronic Lymphocytic Leukemia (CLL) [La Palombella, et al, 2012; Heider, et al, 2011].

We are testing several strategies to target slow-cycling CD37+ SCC cells. One is based on a selective suicide strategy via a killing cassette driven by CD37 promoter. In this way we will be able to analyse whether CD37+ cells are necessary for homing into the lung and bone, and for the expansion of the tumor at these sites (two essential steps of the metastatic process). Furthermore, the easy detection of CD37 by FACS analysis and immunofluorescence is allowing us to analyse its prognostic significance. At present, the analysis of CD37 expression in a large cohort of human SCCs patients has revealed that the presence of this marker highly correlates with metastatic occurrence.

It is now important to clarify some aspects of our approach. It is true that CD37 is exclusively expressed in DID+ cancer stem cells in the xenografts, but not all the DID+ cells are CD37+. That is, it is possible that CD37+ cells are metastasis-initiating cells, but we do not know whether the tetraspanin receptor by itself mediates the pro-metastatic behaviour (thus rendering its targeting innocuous to the tumor). However, as mentioned above, the pro-apoptotic effect of anti-CD37 monoclonal antibodies currently in clinical trials primarily depends on the NK-mediated death of cells coupled to the antibody. Thus, irrespective of the signalling cascades triggered by CD37 in human SCC cells, this approach might be therapeutically valid.

11.1.5 Possible clinical relevance of this work

Our results suggest that SCC tumors might contain cells primed to metastasize. Although the concept that tumors already express a pro-metastatic signature has been previously described [Ricci-Vitiani, et al, 2009, Bos, et al, 2010], the identity of the pro-metastatic cells *in vivo* is

not known. That a subset of SCC cells appears to have trans-differentiated to acquire a lung and bone identity is, in our opinion, quite intriguing. It has been recently shown that glioblastoma cells can convert into endothelial- and pericyte-like cells to provide blood supply and enhance survival to the tumors, indicating that loss of cell identity might be a common event in carcinomas [Wang, et al, 2013]. Understanding the molecular basis underlying these changes in identity will be challenging, but might help us to better understand the biology of the tumor. Nonetheless, irrespective of the mechanisms involved, our observations could have future clinical implications regarding prognosis and therapy. We are therefore putting much effort to repeat every experiment with 1^{ary} human samples obtained from resected tumors. This will be crucial to validate or refute the clinical relevance of our observations.

MATERIAL AND METHODS PART 2

12 MATERIALS AND METHODS PART2

12.1 Materials and methods

12.1.1 Clinical material

Biological samples were obtained from individuals treated at the Hospital del Mar (Barcelona, Spain) or Hospital Vall d'Hebron (Barcelona, Spain) under informed consent and approval of the Bank of Tumor Committees of each hospital according to Spanish Ethical regulations (CEIC). The study followed the guidelines of the declaration of Helsinki and patient's identity and pathological specimens remained anonymous in the context of the study. TMAs containing primary cutaneous SCC and their metastasis were generated by the Department of Pathology in Hospital del Mar after the patients gave their informed consent. CD44 and CD37 immunoreactivity was evaluated independently by 2 different observers.

12.1.2 Plasmids and cloning

Lenti-RFP vector was obtained after cloning the RFP-NLS sequence between Nhe-I and Brsg-I restriction sites of the LentiLox3.7 vector. To obtain a Lenti-BFP vector, BFP coding sequence was cut from the pEBFP2-Nuc vector and introduced between Nhe-I and Brsg-I of the Lenti-Lox3.7. MSCV-IRES-Luciferase-GFP retrovirus was kindly given from J. Zuber [Zuber J, et al, 2009]. Knockdown experiments were conducted using lentiviral shRNA targeting the selected gene (Sigma Aldrich). Non-targeting shRNA sequence was used as control (Sigma Aldrich).

12.1.3 Cell culture and Vibram DID pulse

SCC13 cells were cultured in FAD (1 part Ham's F12 medium, 3 parts Dulbecco Modified Eagle Medium (DMEM), penicillin, streptomycin and $1,8x10^{-4}$M adenine) supplemented with 10% Foetal Bovine Serum (FBS) and a cocktail of 0,5μg/ml hydrocortisone, 5 μg/ml insulin, 10^{-10} M cholera enterotoxin and 10 ng/ml EGF (all final concentrations), as described previously [Gandarillas, et al, 1997].

SCC25 cells were grown in keratinocytes serum free media (KSFM, GIBCO) supplemented with penicillin, streptomycin, 5 mg/mL bovine pituitary extract and 0,2 ng/mL of hEGF. Tumor associated fibroblasts (HNCAF) were cultured in DMEM supplemented with FBS 10% and Insulin-Transferrin-Selenium 1X (GIBCO).

Primary human keratinocytes were isolated from neonatal or adult foreskin and cultured together with a feeder culture of fibroblasts (J2P-3T3) in FAD medium as reported [Gandarillas, et al, 1997].

J2P feeder cells were cultured in DMEM + 10% BS and treated with 4 μg/ml mitomycin, prior to co-culture with primary keratinocytes to irreversibly stop their proliferation. All the cells were grown at 37 ºC with 5% CO_2.

Retrovirus and lentivirus were produced in PhoenixA and 293T cells, respectively, after transfection with Calcium Phosphate. The selection of the infected cells was carried out with either Puromycin 2 μg/mL or Neomycin 0.4 mg/mL.

For Label retaining experiment, SCC lines or single cell suspension from tumors were collected, washed twice in PBS 1X and incubated with Vibram DID (Invitrogen, V-22887) or Vibram DIO (Invitrogen, V-22886) 1:200 (Invitrogen) for 20 min at 37 C. After the incubation, the excess of dye was removed by washing the cells twice with PBS 1X.

Tumor associated fibroblasts (HNCAF) were cultured in DMEM supplemented with FBS 10% and Insulin-Transferrin-Selenium 1X (GIBCO).

Three-dimensional tissue culture was performed as previously described [Aranda, et al., 2006], with 2.5% collagen:matrigel (BD Biosciences) 1:1 mix as matrix. Cultured SCC cells or cells sorted from primary tumors were seeded onto 8-well chamber slides (Lab Tek-II system) and fresh media was added every 2 days. Morphology was assessed by phase microscopy. For immunofluorescence, spheres were fixed in PFA 4% for 30 min, and incubated with Glycine 20 mM in PBS for 10 min. Immunofluorescence was performed as described below.

12.1.3 Immunostaining

For direct fluorescence visualization tissue was fixed with 4% PFA for 2 hr at RT, equilibrated overnight at 4C in PBS-Sucrose 30%, embedded in OCT (Electron Microscopy Science) and frozen at −80°C. 7 μm frozen sections were dried at RT, fixed in PFA 4% for 10 min and permeabilized in PBS-Triton-X100 0.25% for 15 min.
Blocking was performed by incubation with PBS-Goat serum 10%. Primary antibodies were incubated overnight at 4C and secondary antibodies were incubated at RT for 2h. Incubation with the antibodies was performed in PBS-Goat Serum 1%. If needed, nuclei were stained with DAPI (Roche, 1:5000) and slides were mounted in Mowiol.
For immunofluorescence staining of paraffin embedded section, manual dehydration was performed, followed by antigen retrieval in 0.01 M Tricitric Acid pH6 for 12 min at 95 C. Permeabilization was done with PBS-Triton-X100 0.25% for 20 min. Blocking of not specific staining

was performed with PBS-BSA3%-GoatSerum 10%. Incubation with the primary and secondary antibodies was done overnight at 4C in DAKO Diluent (DAKO).

The primary antibodies were used at the following dilutions: 1:200 for CD44 (Abcam, ab 34485), 1:200 for K14, 1:100 for CD45 (eBioscience, Clone 30-F11), 1:100 for Mac1 (BD Bioscience BD 550282), 1:100 for Involucrin, 1:100 for Ki67 (BD Pharmingen, 550609), 1:100 for CD36 (Abcam, ab137320), 1:100 for CD44 (Abcam, ab119863), 1:200 for CD44 (BD Bioscience, BD560533), 1:100 for Runx2 (Santa Cruz, sc-101145), 1:200 for CD37 (Novus Biological NBP1-52428).

Hematoxilin-Heosin staining was done according to the standard protocols. Pictures were acquired using a LEICA DMI 6000B or a Leica TCS SP5 Confocal Microscope.

12.1.4 Tumor xenografts

SCID and SCID-Beige mice were purchased from JAX mice. Mice were housed in an AAALAC-I approved animal unit under 12h light/12h cycles, and SPF conditions, and all the procedures were approved by the CEEA (Ethical Committee for Animal Experimentation) of the Government of Catalunya.

For primary tumor formation, 2-4 10^6 SCC cell lines were mixed with tumor associated fibroblasts (HNCAF), primary human keratinocytes and used for transplantation in 8-week-old SCID female as previously described [Lichti, et al, 2008]. Grafts were biopsied after 8-12 weeks,

when tumors reached 1 cm of diameter. Tumors were used for FACS-sorting, immune-staining or serial transplantation.
For secondary and tertiary tumor formation, 100-1000 cells were sorted from primary or secondary tumors, mixed with 10^5 HNCAF in FAD-30% Matrigel (BD Bioscience, 356230) and subcutaneously transplanted in SCID-Beige mice.

For intraosseous xenograft experiments, 8-week old female SCID-beige mice (JAX) were anesthetized by intraperitoneal injection, and a small hole was drilled with a 30-gauge sterile needle of a Hamilton Syringe (Hamilton Co). Cells were filtered through a 40 mm strainer and resuspended in 30 μL of PBS-FBS 4% before inoculation in the bone marrow cavity. For tail vein injections, un-anesthetized mice were warmed with a heat lamp to allow for venous dilation. Mice were then placed into a plastic retraining apparatus, and 100 μL of cells were injected via the lateral tail vein.

For 5-Bromo-2-deoxyuridine (BrdU) labelling experiments, 100 mg/g BrdU (Invitrogen) was injected i.p. in the transplanted mice every 12h for 3 days before collecting the xenografts.

To evaluate response to chemotherapy, 2 mg/kg of Cisplatin (Sigma-Aldrich) was injected for 3 consecutive days in transplanted mice when tumor reached 0.5-1 cm. Tumors were collected after 2 days from the last administration and used for FACS analysis.

Development of metastasis was monitored by BLI with the IVIS 200 imaging system (Caliper Life Science) and analyzed with the Living image software as described [Minn, et al, 2005]. Briefly, mice were

anaesthetized, injected i.p with 200 μL of 5 mg/mL D-luciferin (Promega) and imaged for luciferase activity as previously described [Minn, et al, 2005]. Luciferase activity measured immediately after cell injection was used to exclude any mice that were not successfully xenografted and to normalize bioluminescence.

12.1.5 Tumor disaggregation from human biopsies and xenografts

Primary human SCC byopsies were sterilized by submerging in Betadine and Ethanol 70%, and then rinsed in PBS. Tumors were chopped with scissors and incubated in Collagenase/Hyaluronidase 1X (Stem Cell Technologies) for 2h at 37C. Single cell suspensions were obtained, diluted in PBS-FBS 2% and centrifuged to eliminate cellular debris and adipose tissue. For subcutaneous transplants or implantation of 2-4 mm^3 tumor pieces, cells were re-suspended in FAD-30%Matrigel. When the cells were used for FACS analysis, they were rinsed with PBS-FBS 2% and incubated with the selected antibodies as described.

For FACS analysis and FACS-sorting of the xenografts, tumors were harvested from transplanted mice, chopped with surgical bladder and incubated overnight at 4C (or 2h at 37C) in Collagenase/Hyaluronidase 1X (Stem Cell Technologies) in DMEM-F12 (GIBCO). Chopped tumors were rinsed with PBS-FBS 2%, minced and homogenized using an 18G needle. Cells were centrifuged for 10 min at 1500 rpm at 4C, re-suspended in PBS-FBS 2%, filtered through a 70 μm cell strainer and used for FACS-staining.

12.1.6 Flow cytometry

For flow-cytometric analysis, single cell suspensions from xenografts or human biopsies were passed trough a 70 μm filter and used for FACS. Cell suspensions were incubated for 45 min on ice with the selected antibodies. The antibodies used were: CD44-PeCy7 (1:100, BD Pharmingen, 560533), CD36-FITC (1:50, BD Pharmingen, 561820), Annexin-FITC (1:25, BD Pharmingen, 556419), CD37-FITC (1:20, BD Pharmingen, 555457), mouse Lineage cocktail (MACS Miltinyi Biotech, 120-003-582), CD36-PerCp (1:100, BD Pharmingen, 561533), CD37-PE (1:50, BD Pharmingen, 561546), Human Lineage Cocktail-APC (1:10, Ebioscience, 227776).
For ALDH activity assay, the ALDEFLUOR kit (Stem Cell Technologies) was used before staining of the surface markers. Briefly, cell suspensions were incubated with a buffer containing the ALDH substrate for 45 min at 37C. As a negative control, cells were incubated with a specific ALDH inhibitor provided in the kit (DEAB control). Tumor cells were visualized by their direct fluorescence. Slow-cycling cells were defined as the Vibram DID retaining cells inside the cancer stem cell population. DAPI staining was used to eliminate the dead cells.

For sorting of the slow-cycling and active cancer stem cells from transplanted tumors, dead cells and debris were eliminated by gating, tumor cells were purified from the mouse and human contaminants using their red direct fluorescence (RFP+), and cancer stem cell population was selected depending on the expression of CD44 and ALDH activity. Slow-cycling stem cells were defined as the Vibram DID retaining cells in this subpopulation, whereas the proliferative cells

were negative for Vibram DID. Not cancer stem cells used as a control were gated as RFP+CD44- cells. For serial transplantation, cells were sorted in 100 μL of FAD at 4C. For RNA-extraction, equal numbers of cells were sorted in 45 μL Lysis buffer [Gonzalez-Roca, 2010]. For metastatic assay, cells were sorted directly in cold PBS1X. For *in vivo* proliferation assay, BrdU staining was performed in cell suspension isolated from primary tumors using the FITC BrdU Flow kit (BD Bioscience, 559619).

Fluorescence activated cell sorting was performed using FACS Aria-II and FACSDiva software (BD Bioscience). FACS analysis was performed using LRSII FACS Analyzers (BD Bioscience) and FlowJo software.

12.1.7 MicroArray analysis and generation of CSC signatures

cDNA was amplified from sorted cells as described [Gonzalez-Roca, 2010]. Equal amount of cDNA isolated from the different stem cell populations by cells sorting was used to perform Agilent Human Arrays (Human Genome CGH).

12.1.8 Real-Time qPCR

Equal amount of amplified cDNA was used to perform Real Time PCR with SYBR Green Master Mix (Roche) and gene specific primers (Table1) in a Light Cycler 480 instrument (Roche). Relative expression levels were determined by normalization with RPL34, Actin-B and GUSB1 using the ΔΔCt method. The full list of the primers used for qPCR is reported in **Tab12.**

Gene	Fw Primer	Rev Primer
Ki67	AGCACCAGAGGAAATTGTGGAGG	ATGATGACCACGGGTTCGGATGA
PCNA	ATCCTCAAGAAGGTGTTGGAGGC	ACGAGTCCATGCTCTGCAGGTTT
p21	CCCAGTTGCATTGCACTTTGA	AAGCACTTCAGTGCCTCCAG
CD44	CAACAACACAAATGGCTGGT	CTGAGGTGTCTGTCTCTTTCATCT
GUSB1	AAGAGTGGTGCTGAGGATTGGCA	TTGATGGCGATAGTGATTCGGAG
GAPDH	GAGTCAACGGATTTGGTCGT	TTGATTTTGGAGGGATCTCG
NRCAM	CCCAAAACTTCTTGAAGACTTGGT	GTCAAAATGAGTCCCATTACGGG
Nfatc2	AAGCCACGGTGGATAAGGACAAGA	ACTGGGTGGTAGGTAAAGTGCTGA
Nfatc1	AGCCGAATTCTCTGGTGGTTGAGA	TTCGCTTTCTCTTCCCGTTGCAGA
B-catenin	CGCTGGGACCTTGCATAACCTTT	TTGATGTAATAAAAGGTTGTGGAGA
Zeb1	GGCAGATGAAGCAGGATGTACAG	CTGCCTCTGGTCCTCTTCAGGT
Zeb2	ATATGGTGACACACAAGCCAGGGA	ACGTTTCTTGCAGTTTGGGCACTC
RPL34	CCAAGAAGGTTGGGAAAGCACCAA	GGCCCTGCTGACATGTTTCTTTGT
CyclinB1	GTGAACAACTGCAGGCCAAAATG	TGGCACTGGCTCAGACACTGG
CTSK.2	ACCTGTGGTGAGCTTTGCTCTGTA	TGCTTCCTGTGGGTCTTCTTCCAT
CD36.2	AAATGTAACCCAGGACGCTGAGGA	TGCCACAGCCAGATTGAGAACTGT
HGF_2	CCGAGGCCATGGTGCTATAC	TCCTTGACCTTGGATGCATTC
Runx2_2	TGGACGAGGCAAGAGTTTCACCTT	ACTGAGGCGGTCAGAGAACAAACT
IGF1	CAGCAGTCTTCCAACCCAAT	CAAGAACTGAAGAGCATCCA
IGF1 Isoform4	AAGGTGAAGATGCACACCATGTCC	AACTGAAGAGCATCCACCAGCTCA
SFTPD	AAAGGGAGAAAGTGGGCTTCCAGA	ACACTTTGGCCATTTGGGAAGAGC
AQP5	CCTGTCCATTGGCCTGTCTGTCAC	GGCTCATACGTGCCTTTGATGATG
TGFB1	CGTGGAGCTGTACCAGAAATAC	CACAACTCCGGTGACATCAA
STAB1	TGGGATGCTATTGGGCTATG	CAGGGACGAAGAGTGTCTTATAC
CD36 Variant2	AGATGCAGCCTCATTTCCAC	GCCTTGGATGGAAGAACAAA
Runx2 Varant2	GCAGTTCCCAAGCATTTCAT	CACTCTGGCTTTGGGAAGAG
CD37 Variant2	GTGGCTGCACAACAACCTTA	AGACGTGGTCCAGGTTTCTG
CD37 Variant1	TTGACAAGACCAGCTTCGTG	CAGCAGCATCCCAAAATACA

Table12. List of primers used for qPCR.

12.1.9 Statistical analysis

Results are reported as mean + S.E.M. All the mouse experiment were repeated at least three times with pool of at least 4 mice. All the in vitro experiments were performed at least three times. Comparison between two groups was performed using an unpaired t-test. Survival curves were realized using the GraphPad Prism Software. $P<0.05$ was considered statistically significant. For TMAs results, the Pearson statistical analysis was used.

REFERENCES PART 2

13 REFERENCES PART 2

Aerts JG, Hegmans JP. *Tumor-specific cytotoxic T cells are crucial for efficacy of immunomodulatory antibodies in patients with lung cancer.* **Cancer Res, 2013, 73(8):2381-8**

Aguirre-Ghiso JA. *Model, mechanisms and clinical evidence for cancer dormancy*. **Nat Rev Cancer, 2007, 7:834-846**

Akech J, Wixted JJ, Bedard K, van der Deen M, Hussain S, Guise TA, van Wijnen AJ, Stein JL, Languino LR, Altieri DC, Pratap J, Keller E, Stein GS, Lian JB. *Runx2 association with progression of prostate cancer in patients: mechanisms mediating bone osteolysis and osteoblastic metastatic lesions.* **Oncogene, 2010; 29(6):811-21**

Al-Hajj M, Wicha MS, Benito-Hernandez A, Morrison SJ & Clarke MF. *Prospective identification of tumorigenic breast cancer cells.* **Proc Natl Acad Sci USA, 2003, 100(7), 3983–3988**

Aranda V, T. Haire T, Nolan ME, Calarco JP, Rosenberg AZ, Fawcett JP, Pawson T, Muthuswamy SK. *Par6-aPKC uncouples ErbB2 induced disruption of polarized epithelial organization from proliferation control.* **Nat Cell Biol, 2006, 8(11):1235–1245**

Argiris A, Karamouzis MV, Raben D, Ferris RL. *Head and neck cancer*. **Lancet, 2008, 371(9625):1695-709**

Baccelli I, Trumpp A. *The evolving concept of cancer and metastasis stem cells*. **J Cell Biol, 2012, 198(3):281-293**

Baccelli I, I, Schneeweiss A, Riethdorf S, Stenzinger A, Schillert A, Vogel V, Klein C, Saini M, Bauerle T, Wallwiener M, Holland-Letz T, Hofner T, Sprick M, Scharpff M, Marme' F, Sinn HP, Pantel K, Weichert W, Trumpp A. *Identification of a population of blood circulating tumor cells from breast cancer patients that initiates metastasis in a xenograft assay.* **Nat Biotechnol, 2013**

Bertolini G, Roz L, Perego P, Tortoreto M, Fontanella E, Gatti L, Pratesi G, Fabbri A, Andriani F, Tinelli S, Roz E, Caserini R, Lo Vullo S, Camerini T, Mariani L, Delia D, Calabrò E, Pastorino U, Sozzi G. *Highly tumorigenic lungcancer CD133+ cells display stem-like features and are sparedby cisplatin treatment.* **Proc Natl Acad Sci U S A, 2009,106(38):16281-6**

Bidard FC, Pierga JY, Vincent-Salomon A, Poupon MF. *A "class of action" against the microenvironment: do cancer cells cooperate in metastasis*? **Cancer Metastasis Rev, 2008, 27(1):5-10**

Biddle A, McKenzie IC. *Cancer stem cells and EMT in carcinoma.* **Cancer Metastasis Rev, 2012, Feb 3**

Bonnet D., and Dick JE. *Human acute myeloid leukemia is organized as a hierarchy that originates from a primitive hematopoietic cell*. **Nat Med, 1997, 3,(7)730–737**

Braun KM, Niemann C, Jensen UB, Sundberg JP, Silva-Vargas V, Watt FM. *Manipulation of stem cell proliferation and lineage commitment: visualisation of label-retaining cells in whole mounts of mouse epidermis.* **Development, 2003, 130(21):5241-55**

Cabarcas SM, Mathews LA, Farrar WL. *The cancer stem cells niche-there goes the neighbourhood?* **Int J Cancer, 2011, 129(10):2315-2327**

Chambers AF, Groom AC, MacDonald IC. *Dissemination and growth of cancer cells in metastatic sites.* **Nat Rev Cancer, 2002, 2(8):563-72.**

Chen J, Li Y, Yu TS, McKay RM, Burns DK, Kernie SG, Parada LF. *A restricted cell population propagates glioblastoma growth after chemotherapy.* **Nature, 2012, 488(7412):522-6**

Cheng L, Huang Z, Zhou W, Wu Q, Donnola S, Liu JK, Fang X, Sloan AE, Mao Y, Lathia JD, Min W, McLendon RE, Rich JN, Bao S. *Glioblastoma stem cells generate vascular pericytes to support vessel function and tumor growth.* **Cell, 2013; 153(1):139-52**

Chen Q, Zhang XH, Massague J. *Macrophage binding to receptor VCAM-1 transmits survival signals in breast cancer cells that invade the lungs.* **Cell, 2011, 20:538-549**

Chen YC, Chen YW, Hsu HS, Tseng LM, Huang PI, Lu KH, Chen DT, Tai LK, Yung MC, Chang SC, Ku HH, Chiou SH, Lo WL. *Aldheyde Dehydrogenase is a putativemarker for cancer stem cells in head and neck squamous cancer.* **Biochem Biophys Res Communication, 2009, 385(3): 307-313**

Clay MR, Tabor M, Owen JH, Carey TE, Bradford CR, Wolf GT, Wicha MS, Prince ME. *Single-marker identification of head and neck squamous cell carcinoma cancer stem cells with aldehyde dehydrogenase.* **Head Neck, 2010, 32(9):1195-201**

Clevers H. *The cancer stem cells, premises, promises, and challenges.* ***Nat Med, 2011, 17(3)313-319***

Cotsarelis G, Sun TT, and Lavker RM. *Label-retaining cells reside in the bulge area of pilosebaceous unit: implications for follicular stem cells, hair cycle, and skin carcinogenesis.* **Cell, 1990, 61(7): 1329–1337**

Dalerba P, Dylla SJ, Park IK, Liu R, Wang X, Cho RW, Hoey T, Gurney A,
Huang EH, Simeone DM, Shelton A, Parmiani G, Castelli C, Clarke M. *Phenotypic characterization of human colorectal cancer stem cells.* **Proc Natl Acad Sci USA, 2007, 104(24):10158–10163**

Dembinski JL, Krauss S. *Characterization and functional analysis of a slow cycling stem cell-like subpopulation in pancreas adenocarcinoma.* **Clin Exp Metastasis, 2009, 26(7):611–623**

Deng S, Yang X, Lassus H, Liang S, Kaur S, Ye Q, Li C, Wang LP, Roby KF, Orsulic S, Connolly DC, Zhang Y, Montone K, Bützow R, Coukos G, Zhang L. *Distinct expression levels and patterns of stem cell marker, aldehyde dehydrogenase isoform 1 (ALDH1), in human epithelial cancers.* **PLoS One, 2010, 5(4):102777**

Driessens G, Beck B, Caauwe A, Simons BD, Blanpain C. *Defining the model of tumor growth by clonal analysis.* **Nature, 2012, 488(7412):527-30**

Ferlito A, Shaha AR, Silver CE, Rinaldo A, Mondin V. *Incidence and sotes of distant metastasis from head and neck cancer.* J **Othorhinolaryngol Relat Spec, 2001, 63(4):202-207**

Firlej V, Mathieu JR, Gilbert C, Lemonnier L, Nakhlé J, Gallou-Kabani C, Guarmit B, Morin A, Prevarskaya N, Delongchamps NB, Cabon F. *Thrombospondin-1 triggers cell migration and development of advanced prostate tumors.* **Cancer Res, 2011;71(24):7649-58**

Fuchs E. *The tortoise and the hair: slow-cycling cells in the stem cell race.* **Cell, 2009, 137(5):811–819**

Gaggioli C, Hooper S, Hidalgo-Carcedo C, Grosse R, Marshall JF, Harrington K, Sahai E. *Fibroblast-led collective invasion of carcinoma cells with differing roles for RhoGTPases in leading and following cells.* **Nat Cell Biol,2007;9(12):1392-400**

Gandarillas A, Watt FM. *c-Myc promotes differentiation of human epidermal cells.* **Genes Dev, 1997, 11(21):2869-82**

Gao H, Chakraborty G, Lee-Lim AP, Mo Q, Decker M, Vomnica A, Shen R, Brogi E, Brivanlou AH, Giancotti FG. *The BMP inhibitor Coco reactivate breast cancer cells at lung metastatic sites.* **Cell, 2012, 150(4):764:779**

Gartlan KH, Janet LW, De Maria MC, Roza N, Chang TM, Jones EL, Apostolopoulos V, Pietersz GA, Hickey MJ, Van Spriel AB, Wright MD. *Tetraspanin CD37 contributes to the initiation of cellular immunity by promoting dendritic cell migration.* **Eur J Immunology, 2013, 43(5):1208-1219**

Ginestier C, Hur MH, Charafe-Jauffret E, Monville F, Dutcher J, Brown M, Jacquemier J, Viens P, Kleer CG, Liu S, Schott A, Hayes D, Birnbaum D, Wicha MS, Dontu G. *ALDH1 is a marker of normal and malignant human mammary stem cells and a predictor of poor clinical outcome.* **Cell Stem Cell, 2007;1(5):555-567**

Gonzalez-Roca E, Garcia-Albeniz X, Rodriguez-Mulero S, Gomis RR, Kornacker K, Auer H**.** *Accurate expression profiling of very small cell populations.* **PlosOne, 2010, 5(12):e14418**

Grivennikov S, Karin E, Terzic J, Mucida D, Yu GY, Vallabhapurapu S, J. Scheller, Rose-John S, Cheroutre H, Eckmann L, Karin M. *IL-6 and Stat3 are required for survival of intestinal epithelial cells and development of colitis-associated cancer.* **Cancer Cell, 2009, 15(2):103–113**

Guise TA, Mohammad KS, Clines G, Stebbins EG, Wong DH, Higgins LS, Vessella R, Corey E, Padalecki S, Suva L, Chirgwin JM. *Basic mechanisms mediating responsible for osteolytic and osteoblastic bone metastasis.* **Clin Cancer Res, 2006, 12(20):6213s-6216s**

Heider KH, Kiefer K, Zenz T, Volden M, Stilgenbauer S, Ostermann E, Baum A, Lamche H, Küpcü Z, Jacobi A, Müller S, Hirt U, Adolf GR, Borges E. *A novel Fc-engineered monoclonal antibody to CD37 with enhanced ADCC and high proapoptotic activity for treatment of B-cell malignancies.* **Blood, 2011, 118(15):4159-68**

Hermann, PC, Huber SL, T. Herrler T, Aicher A, Ellwart JW, Guba M, Bruns CJ, Heeschen C. *Distinct populations of cancer stem cells determine tumor growth and metastatic activity in human pancreatic cancer.* **Cell Stem Cell, 2007, 1(3):313–323**

Hynes NE, Lane HA. *ERBB receptors and cancer: the complexity of targeted inhibitors.* **Nat Rev Cancer, 2005, 5(5):341-54**

Ishizawa K, Rasheed ZA, Karisch R, Wang Q, Kowalski J, Susky E, Pereira K, Karamboulas C, Moghal N, Rajeshkumar NV, Hidalgo M, Tsao M, Ailles L, Waddell TK, Maitra A, Neel BG, Matsui W. *Tumor-initiating cells are rare in many human tumors*. **Cell Stem Cell, 2010 Sep 3;7(3):279-82**

Kang Y, Siegel PM, Shu W, Drobnjak M, Kanonen S, Cordon-Cardo C, Guise T, Massague' J.*A multigenic programme mediating breast cancer metastasis to the bone.* **Cancer Cell, 2003, 3:537-549**

Kang Y, Pantel K. *Tumor cell dissemination: emerging biological insights from animal models and cancer patients.* **Cell, 2013, 23(5):573-81**

Kaplan RN, Rafii S, Lyden D. *Preparing the "soil": the premetastatic niche.* **Cancer Res, 2006, 66(23):11089-11093**

Klein AC. *Framework model of tumor dormancy from patient derived observations.* **Curr Opi Gen and Dev, 2011, 21(1):42-49**

Lapalombella R, Yeh YY, Wang L, Ramanunni A, Rafiq S, Jha S, Staubli J, Lucas DM, Mani R, Herman SE, Johnson AJ, Lozanski A, Andritsos L, Jones J, Flynn JM, Lannutti B, Thompson P, Algate P, Stromatt S, Jarjoura D, Mo X, Wang D, Chen CS, Lozanski G, Heerema NA, Tridandapani S, Freitas MA, Muthusamy N, Byrd JC. *Tetraspanin CD37 directly mediates transduction of survival and apoptotic signals.* **Cancer Cell, 2012;21(5):694-708**

Lazarov M, Kubo Y, Cai T, Dajee M, Tarutani M, Lin Q, Fang M, Tao S, Green CL, Khavari PA. *CDK4 coexpression with Ras generates malignant human epidermal tumorigenesis.* **Nat Med, 2002, 8(10):1105-14**

Leemans CR, Braakhuis BJ, Brakenhoff RH. *The molecular biology of head and neck cancer.* **Nat Rev Cancer, 2011;11(1):9-22**

Li AG, Lu SL, Han G, Hoot KE, Wang XJ. *The role of TGFbeta in skin inflammation and carcinogesis.* **Mol Carcinog, 2006, 45(6):389-96**

Li C, Heidt DG, Dalerba P, Burant CF, Zhang L, Adsay V, Wicha M, Clarke MF, Simeone DM. *Identification of pancreatic cancer stem cells.* **Cancer Res, 2007, 67(3):1030-7**

Li F, Massague' J, Kang Y. *Beyond tumorigenesis: Cancer stem cells in metastasis.* **Cell Research, 2007, 17(1):3-14**

Li N, Yang H, Lu L. Duan C, Zhao C, Zhao H. *Comparison of the labeling efficiency of BrdU, DiI and FISH labeling techniques in bone marrow stromal cells*. **Brain Res, 2008, 1215:11–19**

Li Z, Bao S, Wu Q, Wang H, Eyler C, Sathornsumetee S, Q. Shi Q, Y. Cao Y, Lathia J, McLendon RE, Hjelmeland AB, Rich JN. *Hypoxia-inducible factors regulate tumorigenic capacity of glioma stem cells.* **Cancer Cell, 2009, 15(6):501–513**

Lichti U, Anders J, Yuspa SH. *Isolation and short-term culture of primary keratinocytes, hair follicle populations and dermal cells from newborn mice and keratinocytes from adult mice for in vitro analysis and for grafting to immunodeficient mice.* **Nat Protoc, 2008, 3(5):799-810**

Loebinger RM, Giangreco A, Groot KR, Prichard L, Allen K, Simpson C, Bazley L, Navani N, Tibrewal S, Davies D, Janes SM. *Squamous cell cancers contain a side population of stem-like cells that are made chemosensitive by ABC transporter blockade.* **British Journal of Cancer, 2008, 98(2):380–387**

Luis NM, Morey L, Mejetta S, Pascual G, Janich P, Kuebler B, Cozutto L, Roma G, Nascimento E, Frye M, Di Croce L, Benitah SA. *Regulation of human epidermal stem cell proliferation and senescence requires polycomb-dependent and -independent functions of Cbx4.* **Cell Stem Cell, 2011, 9(3):233-46**

Malanchi I, Peinado H, Kassen D, Hussenet T, Metzger D, Chambon P, Huber M, Hohl D, Cano A, Birchmeier W, Huelsken J. *Cutaneous cancer stem cell maintenence is dependent on b-catenin signaling.* **Nature, 2008, 452(7187):650-654**

Malanchi I, Martinez S, Susanto E, Peng H, Lehr HA, Delaloye F, Huelsken J. *Interactions between cancer stem cells and their niche govern metastatic colonization.* ***Nature, 2011, 481(7379):85-89***

Mani SA, Guo W, Liao MJ, Eaton EN, Ayyanan A, Zhou AY, Brooks M, Reinhard F, Zhang CC, Shipitsin M, Campbell LL, Polyak K, Brisken C, Yang J, Weinberg RA. *The epithelial-mesenchymal transition generates cells with properties of stem cells.* **Cell, 2008, 133(4):704– 715**

Minn AJ, Kang Y, Serganova I, Gupta GP, Giri DD, Doubrovin M, Ponomarev V, Gerald WL, Blasberg R, and Massague J. *Distinct organ-specific metastatic potential of individual breast cancer cells and primary tumors*. **J Clin Invest, 2005, 115(1), 44-55**

Monroe M, Anderson E, Clayburgh D, and Wong M. *Cancer Stem Cells in Head and Neck Squamous Cell Carcinoma.* **J Oncol, 2011, 2011:762780**

Moore N, Lyle S. *Quiescent, slow-cycling stem cell populations in cancer: a review of the evidence and discussion of significance.* **J Oncol, 2011, 2011:396076**

Morandi F, Scaruffi P, Gallo F, Stigliani S, Moretti S, Bonassi S, Gambini C, Mazzocco K, Fardin P, Haupt R, Arcamone G; Italian Cooperative Group for Neuroblastoma, Pistoia V, Tonini GP, Corrias MV. *Bone marrow-infiltrating human neuroblastoma cells express high levels of calprotectin and HLA-G proteins.* **PLoS One, 2012;7(1):e29922**

Nguyen DX, Bos PD, Massague J. *Metastasis: from dissemination to organ-specific colonization.* **Nat Rev Cancer, 2009, 9(4):274-28**

Nowell PC. *The clonal evolution of tumor cell populations.* **Science, 1976,194(4260):23-8**

Pang R, Law W, Chu AC, Poon JT, Lam C, Chow AK, Ng L, Cheung LW, Lan XR, Lan HY, Tan VP, Yau TC, Poon RT, Wong BC. *A subpopulation of CD26+ cancer stem cells with metastatic capacity in human colorectal cancer.* **Cell Stem Cell, 2010, 6(6):603-615**

Pece S, Tosoni D, Confalonieri S, Mazzarol G, Vecchi M, Ronzoni S, Bernard L, Viale G, Pelicci PG, Di Fiore PP. *Biological and molecular heterogeneity of breast cancers correlates with their cancer stem cell content.* **Cell, 2010, 140(1):62-72**

Pratap J, Lian JB, Javed A, Barnes GL, van Wijnen AJ, Stein JL, Stein GS. *Regulatory roles of Runx2 in in metastatic tumors and cancer cell interactions with bone.* **Cancer Metastasis Rev, 2006, 25(4):589-600**

Price KA, Cohen EE. *Current treatment options for metastatic head and neck cancer.* **Curr. Treat Options Oncol, 2012, 13(1):35-46**

Prince ME, Sivanandan R, Kaczorowski A, Wolf GT, Kaplan MJ, Dalerba P, Weissman IL, Clarke MF, Ailles LE. *Identification of a subpopulation of cells with cancer stem cell properties in head and neck squamous cell carcinoma.* **PNAS, 2007, 104(3):973–978**

Psaila B, and Lyden D. *The metastatic niche: adapting the foreign soil.* **Nature Rev Cancer, 2009, 9(4):285-293**

Qin J, Liu X, Laffin B, Chen X, Choy G, Jeter CR, Calhoun-Davis T, Li H, Palapattu GS, Pang S, Lin K, Huang J, Ivanov I, Li W, Suraneni MV, Tang DG. *The PSA(-/lo) prostate cancer cell population harbors self-renewing long-term tumor-propagating cells that resist castration.* **Cell Stem Cell, 2012 10(5):556-69**

Reya T, Morrison SJ, Clarke MF, Weissman IL. *Stem cells, cancer and cancer stem cells*. **Nature 2001, 414(6859):105-11**

Rhim AD, Mirek ET, Aiello NM, Maitra A, Bailey JM, Mc Allister F, Reichert M, Beatty JL, Rustgi AK, Vonderheide RH, Leach S, Stanger BZ. *EMT and dissemination precede pancreatic tumor formation.* **Cell, 2012, 148(1-2):349-361**

Ricci-Vitiani L, Lombardi DG, Signore M, Biffoni M, Pallini R, Parati E, Peschle C, De Maria R. *Identification and expansion of human colon-cancer-initiating cells.* **Nature, 2007, 445(7123):111-5**

Ricci-Vitiani L, Pallini R, Biffoni M, Todaro M, Invernici G, Cenci T, Maira G, Parati EA, Stassi G, Larocca LM, De Maria R. *Tumour vascularization via endothelial differentiation of glioblastoma stem-like cells.* **Nature, 2010, 468(7325):824-8**

Roesch A, Fugunaga-Kalabis M, Schmidt E, Zabierowski S, Brafford P, Vultur A, Basu D, Gimotti P, Vogt T, Herlyn M. *A temporarily distinct subpopulation of slow-cycling melanoma cells is required for continuous tumor growth*. **Cell, 2010, 141(4):583-594**

Schatton T, Murphy GF, Frank NY, Yamaura K, Waaga-Gasser AM, Gasser M, Zhan Q, Jordan S, Duncan LM, Weishaupt C, Fuhlbrigge RC, Kupper TS, Sayegh MH, Frank MH. *Identification of cell initiating human melanomas.* **Nature, 2008, 451(7176):345-9**

Schepers AG, Snippert HJ, Stange DE, van den Born M, van Es JH, van de Wetering M, Clevers H. *Lineage tracing reveals Lgr5+ stem cell activity in mouse intestinal adenomas.*
Science, 2012, 337(6095):730-5

Sethi N, Dai X, Winter CG, Kang Y. *Tumor-derived Jagged1 promotes osteolytic bone metastasis of breast cancer by engaging Notch signaling in bone cells.* **Cancer Cell, 2011, 19(2):192-205**

Straathof K, Pule' MA, Yotdna P, Dotti G, Vanin EF, Brenner MK, Heslop HE, Spencer DM, Rooney CM. *An inducible Caspase-9 switch for T-cell therapy.* **Blood, 2012, 105(11):4247-4254**

Sun A and Wang Z. *Head neck squamous cell carcinoma (HNSCC) c-Met(+) cells display cancer stem cell properties and are responsible for cisplatin-resistance and metastasis.* **Int Journ Cancer, 2010, 129(10):2337-48**

Tian H., Biehs B, Warming S, Leong KG, Rangell L, Klein OD, and de Sauvage FJ. *A reserve stem cell population in small intestine renders Lgr5-positive cells dispensable.* **Nature, 2011. 478(7383):255–259**

Van Houten VM, Tabor MP, van den Brekel MW, Kummer JA, Denkers F, Dijkstra J, Leemans R, van der Waal I, Snow GB, Brakenhoff RH. *Mutated p53 as a molecular marker for the diagnosis of head and neck cancer.* **J Pathol, 2002, 198(4),476–486**

Viale A, De Franco F, Orleth A, Cambiaghi V, Giuliani V, Bossi D, Ronchini C, Ronzoni S, Muradore I, Monestiroli S, Gobbi A, Alcalay M, Minucci S, Pelicci PG. *Cell-cycle restriction limits DNA damage and maintains self-renewal of leukaemia stem cells.* **Nature, 2009, 457(7225):51-6**

Visvader J, Lindeman GJ. *Cancer stem cells in solid tumors: accumulating evidence and unresolved questions.* **Nat Rev Cancer, 2008, 8(10):755-768**

Visvader J. *Cells of origin in cancer.* **Nature, 2011, 469(7330):314-322**

Wang R, Chadalavada K, Wilshire J, Kowalik U, Hovinga KE, Geber A, Fligelman B, Leversha M, Brennan C, Tabar V. *Glioblastoma stem-like cells give rise to tumour endothelium.* **Nature, 2010, 468(7325):829-33**

Weilbaecher K, Guise T, McCauley LK. *Cancer to bone: a fatal attraction.* **Nat Rev Cancer, 2011, 11, 411-425**

Weinberg AS, Ogle CA, Shim EK. *Metastatic cutaneous squamous cell: an update.* **Dermatol Surg, 2007; 33(8):885-99**

Yee K, Connolly CM, Mark Duquette M, Shideh Kazerounian S, Washington R, and Lawler J. *The effect of Thrombospondin-1 on breast cancer metastasis.* **Breast Cancer Res Treat, 2009, 114(1):85-96.**

Zhao X, La Palombella R, Trupti J, Cheney C, Gowda A, Hayden-Ledbetter MS, Baum PR, Lin TS, Jarjoura D, Lehman A, Kussewitt D, Lee RJ, Caliguri MA, Trndantapani S, Muthusamy N, Bird JC. *Targeting CD37-positive lymphoid malignancies with a novel engineered small moduar immunopharmaceutical.* **Blood, 2007, 100(4):254-67**

Zoller M. *Tetraspanins: push and pull in suppressing and promoting metastasis.* **Nat Rev Cancer, 2009, 9(1):40-55**

Zoller M. *CD44: can a cancer-initiating cell profit from an abundantly expressed molecule?* **Nat Rev Cancer, 2011, 11(4)254-267**

Zuber J, Radtke I, Pardee TS, Zhao Z, Rappaport AR, Luo W, McCurrach ME, Yang MM, Dolan ME, Kogan SC, Downing JR, Lowe S. *Mouse models of human AML accurately predict chemotherapy response.* **Genes Dev, 2009, 23(7): 877-889**

ACKNOWLEDGMENT

ACKNOWLEDGMENTS

First of all, I want to thank my parents and my sister for all the encouragement they gave me in these years, for the emotional support and for helping me in the difficult decisions I had to make in the last year.

I need to thank Salva for all the motivation, for the ideas and for the scientific discussion. I'm especially thankful to his optimism and to have always believed in this project from the beginning.

I also need to mention Agustin Toll from Hospital del Mar and Joan Antonio Hueto from Vall D'Hebron, without whom the human part would not been possible.

Special thanks go to Cristina, for all the help inside and outside the lab.

I want to thank also the other people of the lab, especially Alex for sharing her knowledge in the cancer field.

Outside the lab I want to give a special thank to Luciano, that has always been nice with me at personal and scientific level, and obviously my friends in his Lab, Livia and Andrea, I don't need to explain why.

I want to thanks Laura Batlle for her help with the intrafemural injections.

I also need to mention all the people I've met at conferences that gave me helpful advices, especially to Jason Gill, that help to set up bone metastatic assay.

I also need to thank Thomas Lab for all the FACS antibodies they lent me when he was here.

And then I want to thank Giorgio Iotti, that taught me first to stay in a lab and to enjoy research (or maybe I should damn him…).

Thanks also to all the collaborators for plasmids, antibodies…